

Statistics of avalanches with relaxation and Barkhausen noise: A solvable model

Alexander Dobrinevski,^{*} Pierre Le Doussal,[†] and Kay Jörg Wiese[‡]

CNRS-Laboratoire de Physique Théorique de l'Ecole Normale Supérieure, 24 rue Lhomond, 75005 Paris, France

(Received 26 April 2013; published 4 September 2013)

We study a generalization of the Alessandro-Beatrice-Bertotti-Montorsi (ABBM) model of a particle in a Brownian force landscape, including retardation effects. We show that under monotonous driving the particle moves forward at all times, as it does in absence of retardation (Middleton's theorem). This remarkable property allows us to develop an analytical treatment. The model with an exponentially decaying memory kernel is realized in Barkhausen experiments with eddy-current relaxation and has previously been shown numerically to account for the experimentally observed asymmetry of Barkhausen pulse shapes. We elucidate another qualitatively new feature: the breakup of each avalanche of the standard ABBM model into a cluster of subavalanches, sharply delimited for slow relaxation under quasistatic driving. These conditions are typical for earthquake dynamics. With relaxation and aftershock clustering, the present model includes important ingredients for an effective description of earthquakes. We analyze quantitatively the limits of slow and fast relaxation for stationary driving with velocity $v > 0$. The v -dependent power-law exponent for small velocities, and the critical driving velocity at which the particle velocity never vanishes, are modified. We also analyze nonstationary avalanches following a step in the driving magnetic field. Analytically, we obtain the mean avalanche shape at fixed size, the duration distribution of the first subavalanche, and the time dependence of the mean velocity. We propose to study these observables in experiments, allowing a direct measurement of the shape of the memory kernel and tracing eddy current relaxation in Barkhausen noise.

DOI: [10.1103/PhysRevE.88.032106](https://doi.org/10.1103/PhysRevE.88.032106)

PACS number(s): 02.50.Ey, 05.40.Jc, 75.60.Ej

I. INTRODUCTION AND MODEL

A. Barkhausen noise

The Barkhausen noise [1] is a characteristic magnetic signal emitted when a soft magnet is slowly magnetized. It can be measured and made audible as *crackling* through an induction coil: periods of quiescence followed by pulses, or *avalanches*, of random strength and duration. The statistics of the emitted signal depends on material properties and its state. By analyzing the Barkhausen signal, one can deduce, for example, residual stresses [2,3] or grain sizes [4,5] in metallic materials. Understanding how particular details of the Barkhausen noise statistics depend on microscopic material properties is important for such applications.

On the other hand, Barkhausen noise pulses are just one example for avalanches in disordered media. Such avalanches also occur in the propagation of cracks during fracture [6–8], in the motion of fluid contact lines on a rough surface [9–12], and as earthquakes driven by motion of tectonic plates [13–16]. Some features of the avalanche statistics, like size and duration distributions [17,18], are universal for many of these phenomena [19]. Barkhausen noise is easily measurable experimentally and provides a good way to study aspects of avalanche dynamics common to all these systems.

A first advance in the theoretical description of Barkhausen noise was the stochastic model postulated by Alessandro, Beatrice, Bertotti, and Montorsi [20,21] (the ABBM model). They proposed modeling the domain-wall position $u(t)$ through the stochastic differential equation (SDE),

$$\Gamma \dot{u}(t) = 2I_s [H(t) - ku(t) + F(u(t))]. \quad (1)$$

We follow here the conventions of Refs. [22] and [23]. I_s is the saturation magnetization and $H(t)$ the external field which drives the domain-wall motion. A typical choice is a constant ramp rate c , $H(t) = ct = kvt$, which leads to a constant average domain-wall velocity $v = c/k$ [20]. k is the demagnetizing factor characterizing the strength of the demagnetizing field $-ku$ generated by effective free magnetic charges on the sample boundary [20,24]. The domain-wall motion induces a voltage proportional to its velocity $\dot{u}(t)$, which is the measured Barkhausen noise signal. Here $F(u(t))$ is a random local pinning force. It is assumed to be a Brownian motion, i.e., Gaussian with correlations

$$\overline{[F(u) - F(u')]^2} = 2\sigma|u - u'|.$$

This choice may seem unnatural, since the physical disorder does not exhibit such long-range correlations. It is only recently that it has been shown [17,18,25] that the “ABBM guess” emerges as an effective disorder to describe the avalanche motion of the center of mass of the interface, denoted $u(t)$, in the mean-field limit of the field theory of an elastic interface with d internal dimensions. This correspondence holds both for interfaces driven quasistatically [18,25] and for static interfaces at zero temperature [17]. The mean-field description is accurate above a certain critical internal dimension d_c . For $d < d_c$, a systematic expansion in $\epsilon = d_c - d$ using the functional renormalization group yields universal corrections to the scaling exponents [26–28] and avalanche size [17,18] and duration [18,25,29] distributions.

For the particular case of magnetic domain walls, the predictions of the ABBM model are well verified experimentally in certain ferromagnetic materials, for example, FeSi alloys [21,30,31]. These are characterized by long-range dipolar forces decaying as $1/r^3$ between parts of the domain wall a distance r apart. This leads [32] to a critical dimension $d_c = 2$

^{*}alexander.dobrinevski@lpt.ens.fr

[†]ledou@lpt.ens.fr

[‡]Corresponding author: wiese@lpt.ens.fr

coinciding with the physical dimension of the domain wall. In this kind of system, as expected, the mean-field approximation is reasonably well satisfied. Measurements on other types of ferromagnets, for example, FeCoB alloys [31], indicate a universality class that differs from the mean-field ABBM model. This may be explained by short-range elasticity and a critical dimension $d_c > 2$. To describe even the center-of-mass mode in this class of domain walls, one needs to take into account the spatial structure of the domain wall. Predictions for roughness exponents [27,28] and avalanche statistics [17,18,25,29] for this non-mean-field universality class have been obtained using the functional renormalization group.

On the other hand, even for magnets in the mean-field universality class, a careful measurement of Barkhausen pulse shapes [19,22,33,34] shows that they differ from the simple symmetric shape predicted by the ABBM model [25,35]. This hints at a more complicated equation of motion than the first-order overdamped dynamics usually considered for elastic interfaces in disordered media.

In a physical interface, there may be additional degrees of freedom. One example was studied in Refs. [36,37]. Other examples include deformations of a plastic medium or eddy currents arising during the motion of a magnetic domain wall. For viscoelastic media, these can be modeled by a memory term which is nonlocal in time [38,39]. At the mean-field level, this is equivalent to a model with dynamical stress overshoots [40]. Such memory terms may lead to interesting new phenomena, like coexistence of pinned and moving states [38,39,41]. A similar memory term, nonlocal in time, is argued in Ref. [22] to describe the dissipation of eddy currents in magnetic domain-wall dynamics,

$$\frac{1}{\sqrt{2\pi}} \int_{-\infty}^t ds f(t-s) \dot{u}(s) = 2I_s [H(t) - ku(t) + F(u(t))]. \quad (2)$$

The response function f , derived by solving the Maxwell equations in a rectangular sample [22–24,42], is

$$f(t) = \sqrt{2\pi} \frac{64I_s^2}{ab^2\sigma\mu^2} \sum_{n,m=0}^{\infty} \frac{e^{-t/\tau_{m,n}}}{(2n+1)^2\omega_b}. \quad (3)$$

$\tau_{m,n}$ are relaxation times for the individual eddy current modes,

$$\begin{aligned} \tau_{m,n}^{-1} &= (2m+1)^2\omega_a + (2n+1)^2\omega_b \\ \omega_a &= \frac{\pi^2}{\sigma\mu a^2}, \quad \omega_b = \frac{\pi^2}{\sigma\mu b^2}. \end{aligned}$$

They depend on the sample width a , thickness b , permeability μ , and conductivity σ . Equations (2) and (3) correspond to Eqs. (13), (17), and (21) in Ref. [23]; we refer the reader there for details of the derivation.

Zapperi *et al.* [22] showed numerically that avalanche shapes in model (2) are asymmetric. They concluded that eddy-current relaxation may be one way of explaining the experimentally observed skewness of Barkhausen noise pulses. They also argue that similar relaxation effects may be relevant

for other physical situations where asymmetric pulse shapes are observed.¹

A simplification of Eq. (3) occurs when considering only the leading contributions for small and large relaxation times.² One then obtains [22] a natural generalization of the ABBM equation (1):

$$\begin{aligned} \Gamma \dot{u}(t) + \frac{\Gamma_0}{\tau} \int_{-\infty}^t ds e^{-(t-s)/\tau} \dot{u}(s) \\ = 2I_s [H(t) - ku(t) + F(u(t))]. \end{aligned} \quad (4)$$

Here τ is the longest relaxation time of the eddy-current modes, $\tau = \tau_{0,0} = \frac{\mu\sigma}{\pi^2} \left(\frac{1}{a^2} + \frac{1}{b^2}\right)^{-1}$. Γ and Γ_0 are damping coefficients given in Ref. [22].

B. The ABBM model with retardation

For the remainder of this work, we adopt the conventions used in the study of elastic interfaces. Let us introduce a more general model than (4),

$$\eta \dot{u}(t) + a \int_{-\infty}^t ds f(t-s) \dot{u}(s) = F(u(t)) + m^2 [w(t) - u(t)]. \quad (5)$$

which describes a particle driven in a force landscape $F(u)$, with retardation. At this stage $F(u)$ is arbitrary. Here $f(t)$ is a general memory kernel with the following properties:

- (1) $f(0) = 1$ (without loss of generality, since a constant may be absorbed into the parameter a).
- (2) $f(x) \rightarrow 0$ as $x \rightarrow \infty$.
- (3) $f'(x) \leq 0$ for all x , i.e., memory of the past trajectory always decays with time.

This model possesses a remarkable property for any such kernel $f(t)$ and any landscape $F(u)$. It has monotonicity, i.e., it satisfies the Middleton theorem: For non-negative driving $\dot{w} \geq 0$, after an initial transient period, one has $\dot{u} \geq 0$ at all times. A more precise statement and a proof are given in Appendix A. It has very important consequences both in the driven regime and in the limit of quasistatic driving, i.e., small $\dot{w} \rightarrow 0^+$. In that limit it converges to the quasistatic process $u(t) \rightarrow u(w(t))$, where $u(w)$ is the (forward) Middleton metastable state, defined as the smallest (leftmost) root of

$$m^2 u - F(u) = m^2 w \quad \Leftrightarrow \quad u = u(w). \quad (6)$$

It is independent of the precise form of the kernel $f(t)$. Hence, the domain-wall position $u(t)$ is uniquely determined by the value of the driving field $w(t)$, due to the monotonicity property [44]. This process $u(w)$ exhibits jumps at a set of individual points, the avalanche locations w_i , and the

¹For example, the authors of Ref. [22] mention slip velocity profiles during earthquakes [14,43]. However, it is not clear if there are physical reasons to expect a relaxation of the form (2).

²We have $f(0) \propto \sum_{m,n} \frac{1}{(2n+1)^2} = \infty$ and $\int_0^\infty f(t) dt \propto \sum_{m,n} \frac{1}{(2n+1)^2 [(2n+1)^2 + (2m+1)^2]} = \text{const.}$ Thus, for small times, $f(t)$ is well approximated by $\Gamma \delta(t)$ for some constant Γ . On the other hand, for long times, only the mode that relaxes slowest remains. Hence, for long times one can set $f(t) \approx \frac{\Gamma_0}{\tau_{0,0}} e^{-t/\tau_{0,0}}$.

quasistatic avalanche sizes

$$S_i = u(w_i^+) - u(w_i^-) \quad (7)$$

are, thus, independent of the retardation kernel. What depends on the kernel is the dynamics within these avalanches, and that is studied here. The quasistatic avalanche sizes S_i have a well-defined distribution $P(S)$ which has been computed for a particle in various force landscapes [45,46] and for the nontrivial case of a d -dimensional elastic interface using functional renormalization group (FRG) methods [29,47,48]. As long as the dynamics obeys the Middleton theorem, the *avalanche-size* distribution remains *independent* of the details of the dynamics [18].

While monotonicity holds for any $F(u)$, in this article we focus on the case of the Brownian force landscape which can be solved analytically. As in the standard ABBM model, we choose the effective random pinning force $F(u)$ to be a random walk, i.e., Gaussian with correlator given by (2).³ We call this the *ABBM model with retardation*. In view of the application to Barkhausen noise, the parameter $a > 0$ describes the overall strength of the force exerted by eddy currents on the domain wall. For $a = 0$, (5) reduces to the equation of the standard ABBM model in the conventions of Refs. [45,46].

The retarded ABBM model is particularly interesting in view of the monotonicity property. Other ways of generalizing the ABBM model to include inertia, e.g., by a second-order derivative [49], do not inherit this property from the standard ABBM model (see also Appendix A). This makes the ABBM model with retardation very special, and it will be important for its solution in Sec. III.

When considering the particularly interesting case of exponential relaxation motivated in [22], we set

$$f(t) = e^{-t/\tau}, \quad (8)$$

where τ is the longest time scale of eddy-current relaxation, as discussed above. In this approximation, (5) can be rewritten as two coupled, *local* equations for the domain-wall velocity $\dot{u}(t)$, and the eddy-current pressure $h(t)$,

$$h(t) = \frac{1}{\tau} \int_{-\infty}^t ds e^{-(t-s)/\tau} \dot{u}(s), \quad (9)$$

$$\eta \dot{u}(t) + a\tau h(t) = F(u(t)) + m^2[w(t) - u(t)], \quad (10)$$

$$\tau \partial_t h(t) = \dot{u}(t) - h(t). \quad (11)$$

Although most of our quantitative results will be derived for this special case only, most qualitative features carry over to more general kernels with sufficiently fast decay.

By rescaling u , w , and t in Eq. (5) (for details, see Sec. III A), one finds the characteristic time scale $\tau_m = \eta/m^2$ and length scale $S_m = \sigma/m^4$ of the standard ABBM model ($a = 0$). They set the scales for the durations and sizes of the largest avalanches. There are, of course, avalanches of smaller size (up to some microscopic cutoff if one defines it). The velocity scale is $v_m = \sigma/(\eta m^2)$ and one can define

³It can be realized as a stationary landscape, $\overline{F(u)F(u')} = \Delta_0 - \sigma|u - u'|$, with a cutoff at scale $u \sim \Delta_0/\sigma$, or by $\overline{F(u)F(u')} = 2\sigma \min(u, u')$ (nonstationary landscape with $F(0) = 0$). In both cases, $F'(u)$ is a white noise, and that is the important feature.

a renewal time for the large avalanches as $\tau_v = S_m/v$, the limit of quasistatic driving being $\tau_m \ll \tau_v$, equivalent to $v/v_m \ll 1$. In the retarded ABBM model (8) one introduces an additional memory time scale τ and various regimes will emerge depending on how τ compares with the other time scales (whose meaning will be changed).

Equation (11) then describes a depinning model with relaxation, i.e., one can think of the disorder landscape as relaxing via the additional degree of freedom $h(t)$. This is a feature of interest for earthquake models as discussed below. In this context one considers the limit of well separated time scales, $\tau_m \ll \tau \ll \tau_v$.

Other features of Barkhausen noise predicted for the ABBM model with retardation differ substantially from those of the standard ABBM model. Zapperi *et al.* [22] already realized that the inclusion of eddy currents leads to a skewness in the avalanche shape. In this article, we go further and discuss changes in the avalanche statistics. The relaxation of eddy currents introduces an additional slow time scale into the model. This leads to avalanches which stretch further in time. In particular, avalanches following a kick (or, more generally, an arbitrarily shaped pulse of the driving velocity which stops at some point in time) never terminate, in contrast to the standard ABBM model. This is because of the exponentially decaying retardation kernel, which never vanishes.⁴ Avalanche sizes, however, are not changed by retardation in the limit of quasistatic driving, as discussed above. In that limit, retardation leads to a breakup of avalanches into subavalanches, which can also be called aftershocks. Avalanches at continuous driving overlap stronger, and the velocity threshold for the infinite avalanche (i.e., the velocity \dot{u} no longer vanishes) is decreased. We now describe these effects in detail and formulate more precise statements.

C. Protocols

Let us, first, review qualitatively the main situations that we will study and define the terminology.

(i) Stationary driving: The driving velocity is constant, $w(t) = vt$, and the distributions of the domain-wall velocity \dot{u} and of the eddy-current pressure h reach a steady state, which we study. If v is large enough the velocity will never vanish and one has a single infinite avalanche, also called “continuous motion.” At smaller $v > 0$ the velocity will sometimes vanish. That defines steady-state avalanches. These are more properly called subavalanches of the infinite avalanche since at finite $v > 0$ they immediately restart. Only in the limit $v = 0^+$ do they become well separated in time and then can be called steady-state avalanches.

(ii) Avalanches following a kick: We consider an initial condition at $t = 0$ prepared to lie in the “Middleton attractor” at $u = u(w(t < 0))$, as discussed above. It can be obtained by driving the system monotonously in the far past with $\dot{w} > 0$, until memory of the initial condition is erased; then it is allowed to relax for a long time with $\dot{w} = 0$ until time $t = 0$. Hence, the initial condition is $\dot{u}(t = 0) = h(t = 0) = 0$. At $t = 0$, one

⁴For a model such that $f(t) = 0$ for $t > t_0$, avalanches would remain of finite duration.

changes the external magnetic field instantaneously by w_0 , i.e., sets $\dot{w}(t) = w_0\delta(t)$. For $t > 0$, the external field no longer changes; thus, a kick in the driving velocity corresponds to a step in the applied force. At $t = \infty$ the system has settled again into the Middleton attractor at $u(t = \infty) = u(w + w_0)$, because of the properties discussed above. One thus can consider the total motion to define a single avalanche following a kick, which is, thus, unambiguously defined. The total size $S = \int_0^\infty \dot{u}(t) dt$ is the same as in the absence of retardation. We will ask about the total duration (which becomes infinite) and whether the velocity has vanished at intermediate times, i.e., whether the avalanche has broken into subavalanches.

Avalanches following a kick are called *nonstationary avalanches* (since driving is nonstationary). However, in the limit of $w_0 \rightarrow 0^+$ they become identical to the steady-state avalanches obtained by stationary driving discussed above (conditioned to start at $t = 0$).

D. Organization of this article

The remainder of this article is structured as follows: In Sec. II, we discuss in more detail the phenomenology and the qualitative physics of the ABBM model with retardation. We discuss the splitting of a quasistatic avalanche into *subavalanches* and the effects of retardation on the stationary and the nonstationary dynamics.

In Sec. III we explain how the probability distribution of observables linear in the domain-wall velocity can be computed by solving a nonlinear, nonlocal “instanton” equation. By this, the stochastic model is mapped onto a purely deterministic problem of nonlinear dynamics. This is a generalization of the method developed in Refs. [25,46] for the standard ABBM model with arbitrary driving.

Section IV discusses how the explicit form of the memory kernel $f(t)$ can be extracted in an experiment from the response to a kick.

Section V is devoted to an analysis of the instanton equations in the limit $\frac{\eta}{m^2} \ll \tau$. This means that eddy currents relax much more slowly than the domain wall moves. In this limit, we obtain the stationary distributions of the eddy-current pressure and domain-wall velocity, as well as their behavior following an instantaneous kick in the driving field. The instanton solution reflects the two time scales in the problem: A short time scale, on which eddy currents build up but do not affect the dynamics, and a long time scale, on which they relax quasistatically. We prove that, even after the driving has stopped, the velocity never becomes zero permanently.

In Sec. VI we discuss the fast-relaxation limit $\frac{\eta}{m^2} \gg \tau$. In this limit, eddy currents relax much faster than the domain wall moves. The instanton solutions again exhibit two time scales, but now eddy currents are irrelevant for the long-time asymptotics. Qualitative results (like the fact that the domain-wall motion never stops entirely) are in agreement with those for the slow-relaxation limit, considered in Sec. V.

In Sec. VII we discuss nonstationary avalanches following an instantaneous kick in the driving. In particular, we compute their average shape at fixed size.

In Sec. VIII, we show how to include an absorbing boundary in the instanton solution of Sec. III. This is required for treating avalanches during stationary driving. We then

derive the distribution of avalanche durations in the standard ABBM model at finite driving velocity, $v > 0$, and the leading corrections for weak relaxation and $\tau = \tau_m$. We also show numerical results for more general situations and give some conjectures on the modification of size and duration exponents by retardation effects.

Last, in Sec. IX, we summarize our results. We discuss how they can be used to learn more about the dependence of Barkhausen noise on eddy current dissipation.

II. PHYSICS OF THE MODEL AND SUMMARY OF THE RESULTS

A. Quasistatic driving: Subavalanches and aftershocks

Consider the system either under stationary driving at $v = 0^+$ or following an infinitesimal kick $w_0 = 0^+$ as discussed above, and call $t = 0$ the starting time of the avalanche. The main physics can be understood from Fig. 1 and keeping in mind Eqs. (11).

In Fig. 1(a) we represent the usual construction for $u(w)$ in the standard ABBM as the leftmost solution of Eq. (6) (in the figure we set $m = 1$). Assuming $\tau_m \ll \tau_v$ this construction indicates the position of the domain wall as a function of $w = w(t)$ on time scales of order τ_v . At w_1 the solution jumps from $u_1 = u(w_1^-)$ to $u'_1 = u(w_1^+) = u_1 + S$, corresponding to an avalanche of size S ; the latter occurs on the much faster time scale τ_m . During the avalanche the velocity $\dot{u}(u)$ (setting $\eta = 1$) is given by the difference in height between the line $m^2 w = m^2 w_1$ and the landscape $m^2 u - F(u)$, providing a graphic representation of the motion. The velocity $\dot{u}(u)$ vanishes at $u = u_1$ and $u = u'_1$. For illustration we have represented a force landscape which is ABBM like at large scales but smooth at small scales. For the continuous ABBM model the construction is repeated at all scales and one has avalanches of all smaller sizes.

Let us now add retardation, setting $a > 0$, and varying the memory time τ . The graphical construction corresponding to Eq. (11) is represented in Figs. 1(b) to 1(d). The difference in height is now the sum of \dot{u} and $a\tau h$ (in the figure we chose $a = 1$), which evolves according to the second equation in Eq. (11). It can be rewritten as

$$\tau \partial_u h = 1 - \frac{h}{\dot{u}(u)}. \quad (12)$$

Hence, h increases from $h = 0$, initially as $h \approx (u - u_1)/\tau$ (since $\dot{u} \sim \sqrt{u - u_1}$). Thus, the curve $w - a\tau h$ versus u starts with a negative slope $-a$.

Another way to see this is to note that for $t \ll \tau$, the second equation of (11) gives

$$\tau h(t) = \int_0^t \dot{u}(t) + O(t/\tau) = u(t) - u_1 + O(t/\tau). \quad (13)$$

Inserting this into the first equation of (11), we obtain

$$\eta \dot{u}(t) = F(u(t)) + m^2[w(t) - u(t)] - a[u(t) - u_1] + \dots \quad (14)$$

Effectively, for short times the mass is modified from $m^2 \rightarrow m^2 + a$. Thus, while w is fixed, the end of the

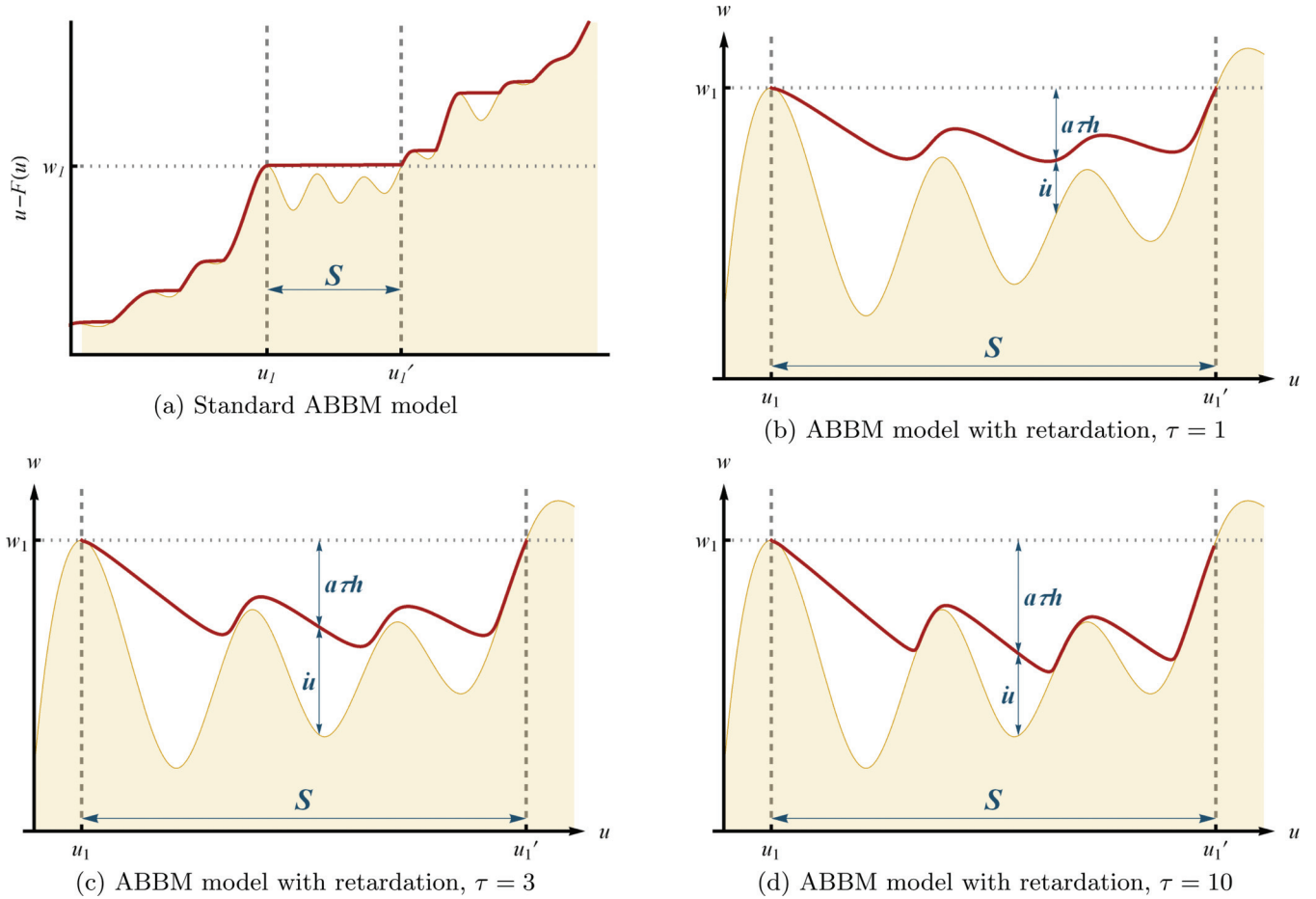


FIG. 1. (Color online) Splitting of an avalanche into subavalanches through the retardation mechanism. We have set $m^2 = 1$ and $a = 1$ and we vary the relaxation time τ .

first subavalanche is determined not by the roots of $m^2w = m^2u - F(u)$ but by the roots of $m^2w = (m^2 + a)u - au_1 - F(u)$. Equivalently, in the landscape $m^2u - F(u)$, instead of looking at intersections with the horizontal curve m^2w , we should look at intersections with $m^2w - a(u - u_1)$, a line with slope $-a$.

At the point where this curve intersects first the landscape $m^2u - F(u)$ we get a point $u_{s1} < u_1'$, where \dot{u} first vanishes. This defines the size $S_1 = u_{s1} - u_1$ of the first *subavalanche*. If τ is small this usually occurs near the end, but if τ is larger the original avalanche (called the main avalanche) is divided—in size—in a sequence of subavalanches $S = \sum_{\alpha} S_{\alpha}$. The number of subavalanches in the main avalanche is finite for a smooth landscape and infinite for the continuous Brownian landscape. The total size $S = u_1' - u_1$ is, however, the same as for $a = 0$, due to the Middleton theorem. For instance, in the landscape of Fig. 1(d), the main avalanche is divided into three large subavalanches, and for the continuous Brownian landscape the intermediate segments are also divided into smaller subavalanches *ad infinitum*. Figure 1 illustrates the correlation between the subavalanche structure (in u) and the realization of the random landscape, where larger hills favor the breakup into subavalanches. Note also that in intermediate regions where \dot{u} is very small, τh starts decreasing again (it decreases whenever $\dot{u} < h$). The effective

driving seen by the particle then becomes $m^2w - a\tau h$ and increases. This mechanism triggers a new subavalanche, and so on.

To obtain the dynamics one must solve Eqs. (11), which we do below. For the standard ABBM model [46], and in the mean-field theory of the elastic interface [18,25], it was seen that an avalanche terminates with probability 1, i.e., $\dot{u}(t) = 0$ for $t > T$. This allows us to define and compute the distribution of avalanche durations [25,46] and their average shape [25,35,46].

In presence of retardation, and for an exponential kernel, the avalanche duration defined in the same way becomes infinite. Inside one avalanche, the velocity $\dot{u}(t)$ becomes zero infinitely often but is then pushed forward again by the relaxation of the eddy-current pressure. Thus, an avalanche in the ABBM model with retardation splits into an infinite number of subavalanches, delimited by zeros of \dot{u} . Each subavalanche has a finite size S_i and duration T_i with $S = \sum_i S_i$ (the same size as in the standard ABBM model), but $\sum_i T_i = \infty$.

We study in detail two limits as follows:

(1) In the slow-relaxation limit $\tau \gg \tau_m$ the duration of the largest subavalanches remains of order τ_m , while the total duration is of order τ . This leads to the estimate that the main avalanche breaks into $\sim \tau/\tau_m$ significant (i.e., nonmicroscopic) subavalanches.

(2) For the fast-relaxation limit $\tau \ll \tau_m$ ($=1$ here) $h \approx \dot{u}$. The correction to the domain-wall velocity $\dot{u}(u)$ is small in this limit and vanishes as $\tau/\tau_m \rightarrow 0$ (in contrast to the limit $\tau/\tau_m \rightarrow \infty$ discussed above). In fact, the correction due to retardation amounts to a rescaling of the velocity as $\dot{u} \rightarrow (1 + a\tau)\dot{u}$.

Of course, in presence of driving, the total duration is not strictly infinite since at some time scale the driving will kick in again and lead to another main avalanche, itself again divided in subavalanches and so on. We can call that scale again τ_v but its precise value may differ from the estimate for the case $a = 0$.

Thus, one main property of the retarded ABBM model is that it leads to *aftershocks*, a feature not contained in the standard ABBM model. The main avalanche is divided into a series of aftershocks (the subavalanches) which can be unambiguously defined and attributed to a main avalanche (which basically contains all of them) in the limit of small driving. This sequence of subavalanches is also called an avalanche cluster. The aftershocks are triggered by the relaxation of the additional degree of freedom h . That in turn changes the force acting on the elastic system. Relaxation and aftershock clustering have been recognized as important ingredients of an effective description of earthquakes; the present model is a solvable case in this class. In some earthquake models considered previously, relaxation was implemented in the disorder landscape itself [50–52]. Here the relaxation mechanism is simpler, which makes it amenable to an analytic treatment. Note, of course, that at this stage it is still rudimentary. First, it is not clear how to identify the “main shock” among the sequence of subavalanches; and while there is indeed some tendency, see, e.g., Fig. 1(d), that the earliest subavalanche is the largest, this is not necessarily true. Second, to account for features such as the decay of activity in time as a power law (Omori law [53]), one needs to go beyond the exponential kernel to a power-law one. Finally, more ingredients are needed if one wants to account for other features of realistic earthquakes, such as quasiperiodicity.

B. Stationary motion

In the case where the driving velocity is constant, $w(t) = vt$, the distributions of the domain-wall velocity \dot{u} and of the eddy current pressure h become stationary. The distribution of \dot{u} for small \dot{u} has a power-law form with an exponent depending on v ,

$$P(\dot{u}) \sim \dot{u}^{-1 + \frac{v}{v_c}}. \quad (15)$$

There is no contribution $\sim \delta(\dot{u})$. v_c is a critical driving velocity, which separates several different regimes:

(1) For $v > v_c$, the velocity \dot{u} never becomes zero. It is not possible to identify individual avalanches; therefore, one can say that there is a single infinite avalanche.

(2) For $0 < v < v_c$, the velocity \dot{u} vanishes infinitely often. The times $\{t_i | \dot{u}(t_i) = 0\}$ delimit individual (sub-)avalanches.⁵

⁵Note that there are no finite-time intervals where the velocity \dot{u} is identically zero, since otherwise the probability distribution (15) would have a $\delta(\dot{u})$ part. Thus, the times t_i are single points, which

Their durations $T_i := t_{i+1} - t_i$ and sizes $S_i = \int_{t_i}^{t_{i+1}} dt' \dot{u}(t')$ have distributions $P_v(T)$ and $P_v(S)$ depending on the driving velocity v . In Sec. VIII we compute $P_v(T)$ for the standard ABBM model and for a special case of the ABBM model with retardation. For subavalanches, starting at $\dot{u}_i = 0$, and a fixed value of the eddy-current pressure h_i , in the limit of small a and $\tau = \tau_m$, we show that

$$P_v(T) \sim T^{-2+v+ah_i} \quad \text{for } T \rightarrow 0.$$

In particular, the pure ABBM power-law exponent $P_v(T) \sim T^{-2+v}$ is not modified for the first subavalanche, starting at $h_i = 0$. Since the typical h_i goes to zero as $v \rightarrow 0$, we conjecture that the quasistatic exponents are still given by the mean-field values $P(S) \sim S^{-3/2}$, $P(T) \sim T^{-2}$.

In Secs. VC and VI, we compute v_c in several limiting regimes. For $\tau \gg \tau_m$, i.e., when eddy-current relaxation is slow with respect to the domain-wall motion, we obtain, in Sec. VC,

$$v_c = \frac{\sigma}{\eta(m^2 + a)} + O(\tau_m/\tau).$$

This means that slow eddy-current relaxation decreases the critical velocity. The stronger the eddy-current pressure a , the smaller v_c becomes. On the other hand, for $\tau \ll \tau_m$, i.e., fast eddy-current relaxation, we obtain, in Sec. VI,

$$v_c = \frac{\sigma}{\eta m^2} \left[1 - a \frac{\tau}{\eta} + O(\tau/\tau_m)^2 \right].$$

Hence, fast eddy-current relaxation also decreases the critical velocity. However, the correction in this case is small and vanishes as the time-scale separation between τ_m and τ becomes stronger.

The above regimes 1 and 2 do not change qualitatively compared to the standard ABBM model. This means that features like the power-law behavior of $P(\dot{u})$ around $\dot{u} = 0$ are robust towards changes in the dynamics, as long as it remains monotonous.

C. Nonstationary driving: Response to a finite kick

Instead of continuous driving, let us now perform a kick as defined in Sec. IC. In the standard ABBM model, like for the quasistatic driving discussed above, this leads to an avalanche on a time scale of order τ_m , which terminates with probability 1. At some time T , the domain-wall velocity \dot{u} becomes zero. The domain wall then stops completely, so $\dot{u}(t) = 0$ for all $t \geq T$. This gives an unambiguous definition for the size and duration of the nonstationary avalanche following a kick [46]. Formally, this behavior is seen by computing the probability $p_{\dot{u}(t)=0}$. It turns out that $p_{\dot{u}(t)=0} > 0$ for any $t > 0$ and tends to 1 as $t \rightarrow \infty$. The distribution $P(\dot{u}_t)$ [with $\dot{u}_t \equiv \dot{u}(t)$] for $t > 0$ has a continuous part and a δ -function part: $P(\dot{u}_t) = p_{\dot{u}_t=0} \delta(\dot{u}_t) + \mathcal{P}(\dot{u}_t)$ [46].

In the ABBM model with retardation, the situation differs. We show in Sec. VD that $p_{\dot{u}_t=0} = 0$ following a kick, so

may, however, be spaced arbitrarily close. Scaling arguments suggest that the set of points $\{t_i\}$ has a fractal dimension of $\frac{v}{v_c}$.

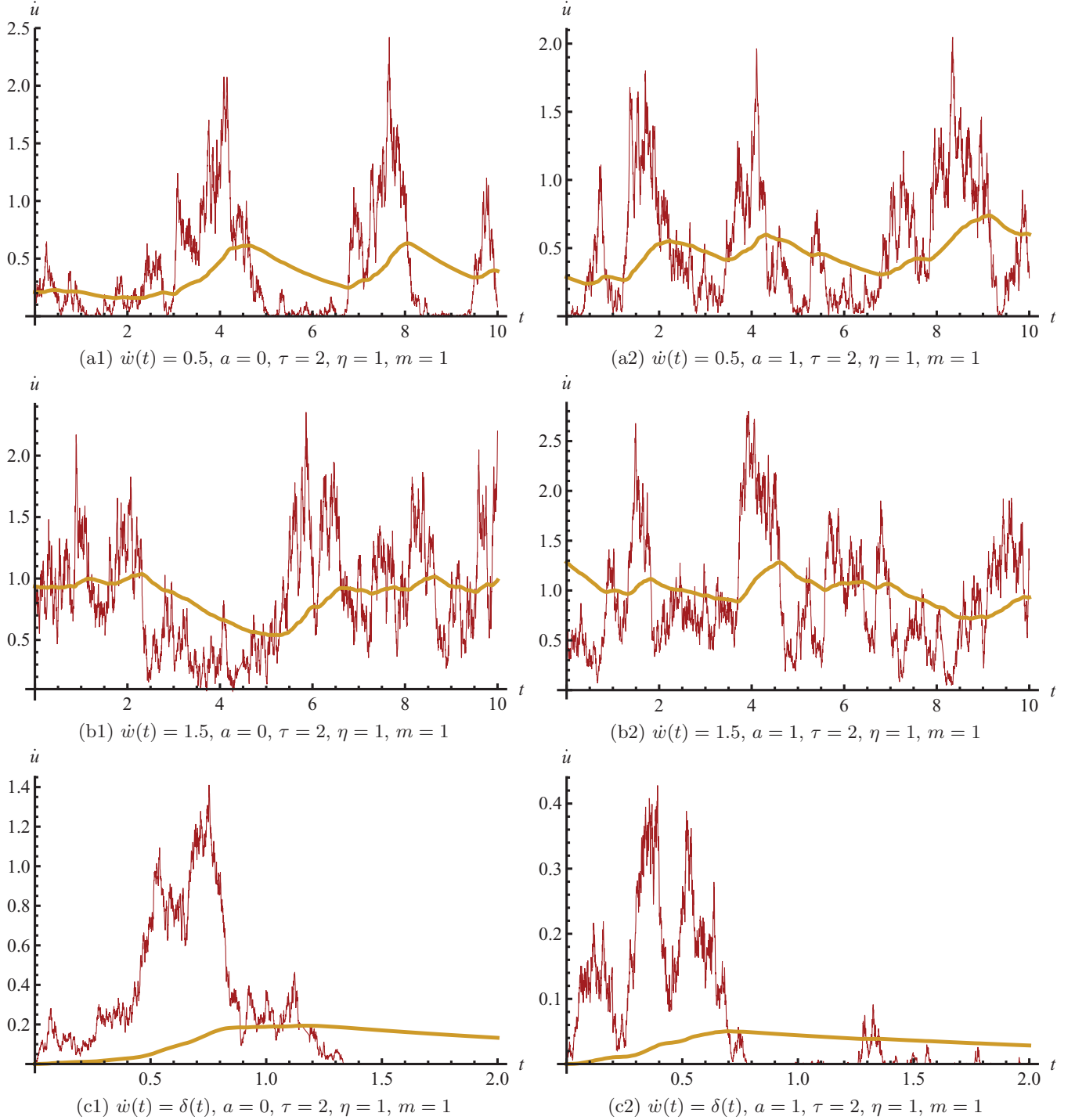


FIG. 2. (Color online) Example trajectories for $\dot{u}(t)$ (thin red lines) and $h(t)$ (thick yellow lines) for various parameter values. The left column [(a1), (b1), and (c1)] corresponds to the standard ABBM model ($a = 0$) and the right column to the model with retardation (here $a = 1$). Panels (a) and (b) correspond to stationary driving with a constant velocity, whereas the driving in (c) has a kick at $t = 0$. Observe that after a kick, $\dot{u}(t)$ in the standard ABBM model becomes zero permanently after a certain time, see panel (c1), whereas in the ABBM model with retardation [panel (c2)] subavalanches restart infinitely often.

the dynamics never terminates completely. If one defines the avalanche duration T as $T = \min\{t | \dot{u}_s = 0 \text{ for } s \geq t\}$, T is infinite. This is also seen from the example trajectories in Fig. 2(b). However, the velocity intermittently becomes zero an infinite number of times. Thus, the avalanche following a

kick is split into an infinite number of *subavalanches*, just like a quasistatic avalanche discussed above.

On the other hand, the subavalanches become smaller and smaller with time. In Sec. VII A, we show that the total avalanche size $S := \int_0^\infty dt \dot{u}_t$ following a kick of size w_0

is finite and distributed according to the same law as in the standard ABBM model [45],

$$P_{w_0}(S) = \frac{w_0}{2\sqrt{\pi}\sigma S^{\frac{3}{2}}} e^{-\frac{(w_0 - m^2 S)^2}{4\sigma S}}. \quad (16)$$

This result holds independently of the memory kernel f . For infinitesimal kicks, $w_0 \rightarrow 0$, $P_{w_0}(S)$ becomes the distribution of quasistatic avalanche sizes discussed above.

The disorder-averaged velocity \bar{u}_t following the kick decays smoothly. In the standard ABBM model, the decay is exponential [46]. With retardation, we show in Sec. IV that the dependence of \bar{u}_t on t is directly related to the form of the memory kernel f .

Another interesting observable is the mean avalanche shape. Conventionally, it is defined at stationary driving for a *subavalanche*: One takes two neighboring zeros $\dot{u}(0) = 0$ and $\dot{u}(T) = 0$ which delimit a (*sub*-)avalanche of duration T . The mean avalanche shape is then the average of the domain-wall velocity $\dot{u}(t)$ as a function of time in the ensemble of all such (*sub*-)avalanches of duration T . It has been realized [22] that the skewness of this shape provides information on the relaxation of eddy currents.

However, this definition is hard to treat analytically. Instead of considering the mean (*sub*-)avalanche shape at a constant duration, we discuss the mean shape of a complete avalanche (consisting of infinitely many subavalanches, with infinite total duration) of a fixed size S , triggered by a step in the force at $t = 0$. In Sec. VII B we give an explicit expression for this shape at fixed size, for exponential eddy-current relaxation. We show how it reflects the time scale of eddy-current relaxation.

The phenomenology discussed here is expected to be similar if, instead of a kick at $t = 0$, one takes some arbitrary driving w_t for $t < 0$, which stops at $t = 0$ so $\dot{w}_{t>0} = 0$.

We see that the nonstationary relaxation properties of the retarded ABBM model differ qualitatively from those of the standard ABBM model. They provide a more sensitive way of distinguishing experimentally the effect of eddy currents than stationary observables at finite velocity and allow one to identify the form of the memory kernel f . In the following sections, we provide quantitative details underlying this picture.

III. SOLUTION OF THE RETARDED ABBM MODEL

In this section, we apply the methods developed in Refs. [18,25,46,49] to obtain the following exact formula for the generating functional of domain-wall velocities,

$$\overline{e^{\int_t \lambda_t \dot{u}_t dt}} = e^{m^2 \int_t \dot{w}_t \bar{u}_t dt}. \quad (17)$$

It is valid for an arbitrary monotonous driving $\dot{w}_t \geq 0$, where \bar{u}_t is the solution of the following nonlocal instanton equation,

$$\begin{aligned} \eta \partial_t \bar{u}(t) - (m^2 + a)\bar{u}(t) + \sigma \bar{u}(t)^2 - a \int_t^\infty ds f'(s-t)\bar{u}(s) \\ = -\lambda(t), \end{aligned} \quad (18)$$

with boundary condition $\bar{u}(\infty) = 0$. The important observation that allows such an exact formula is that for monotonous driving, the motion in the ABBM model with retardation

is still monotonous, as in the standard ABBM model (see Appendix A) as discussed above.

To prove (17) we apply the same series of arguments as in the absence of retardation [18,25,46]. Taking one derivative of Eq. (5) gives a closed equation of motion for $\dot{u}(t)$, instead of $u(t)$,

$$\begin{aligned} \eta \partial_t \dot{u}(t) + a\dot{u}(t) + a \int_{-\infty}^t ds f'(t-s)\dot{u}(s) \\ = \sqrt{\dot{u}(t)}\xi(t) + m^2[\dot{w}(t) - \dot{u}(t)]. \end{aligned} \quad (19)$$

$\xi(t)$ is a Gaussian white noise, with $\overline{\xi(t)\xi(t')} = 2\sigma\delta(t-t')$. The term $\sqrt{\dot{u}(t)}$ comes from rewriting the *position-dependent* white noise in terms of a *time-dependent* white noise,

$$\begin{aligned} \overline{\xi(u(t))\xi(u(t'))} &= 2\sigma\delta(u(t) - u(t')) = \frac{2\sigma}{\dot{u}(t)}\delta(t - t') \\ \Rightarrow \xi(u(t)) &= \frac{1}{\sqrt{\dot{u}(t)}}\xi(t) \\ \Rightarrow \partial_t F(u(t)) &= \dot{u}(t)\xi(u(t)) = \sqrt{\dot{u}(t)}\xi(t). \end{aligned} \quad (20)$$

This uses crucially the monotonicity of each trajectory. For our model, this is assured by the Middleton property discussed in Appendix A. This breaks down when, e.g., inertia is included via a second-order derivative in (5), even for monotonous driving (see Appendix A and Ref. [49]). Then, even for the case of Brownian disorder, the correlations of the pinning force are nonlocal in time [unlike in Eq. (20)], due to trajectories returning to the same point (and, hence, the same pinning force) at different times. Although some limiting cases can be analyzed with simplifying approximations (for a detailed analysis of the inertial case see Ref. [49]), the monotonous motion considered here is much simpler.

Using the Martin-Siggia-Rose method, we express the generating functional for solutions of (19) as a path integral,

$$\begin{aligned} \overline{e^{\int_t \lambda_t \dot{u}_t}} &= \int \mathcal{D}[\dot{u}, \bar{u}] e^{-S[\dot{u}, \bar{u}] + \int_t \lambda_t \dot{u}_t} \\ S[\dot{u}, \bar{u}] &= \int_t \bar{u}_t \left[\eta \partial_t \dot{u}_t + a\dot{u}_t + a \int_{-\infty}^t ds f'(t-s)\dot{u}_s \right. \\ &\quad \left. - m^2(\dot{w}_t - \dot{u}_t) \right] - \sigma \int_t \bar{u}_t^2 \dot{u}_t. \end{aligned} \quad (21)$$

For compactness, we have noted time arguments via subscripts. We will use this notation from now on when convenient.

As in the standard ABBM model, the action (21) is linear in \dot{u} . Thus, the path integral over \dot{u} can be evaluated exactly. It gives a δ functional enforcing the instanton equation (18). The only term not involving \dot{u} in the action is $m^2 \int_t \bar{u}_t \dot{w}_t$, which yields the result (17) for the generating functional. For more details, see Sec. II in Ref. [46] and Secs. II B–II E in Ref. [18].

Similarly to the discussion in Refs. [18,46], the solution (17) generalizes to an elastic interface with d internal dimensions in a Brownian force landscape (i.e., elastically coupled ABBM models). There is indeed a simple way to introduce retardation in that model to satisfy the monotonicity property. We will not study this extension here.

For the case of exponential relaxation, $f(x) = e^{-x/\tau}$, Eq. (19) can be simplified to a set of two local Langevin

equations for the velocity \dot{u} and the eddy-current pressure h ,

$$\eta \partial_t \dot{u}_t = \sqrt{\dot{u}_t} \xi_t + m^2 [\dot{w}_t - \dot{u}_t] - a(\dot{u}_t - h_t), \quad (22)$$

$$\tau \partial_t h_t = \dot{u}_t - h_t. \quad (23)$$

The action for this coupled system of equations is

$$S[\dot{u}, \tilde{u}] = \int_t \left\{ \tilde{u}_t [\eta \partial_t \dot{u}_t + a(\dot{u}_t - h_t) + m^2(\dot{u}_t - \dot{w}_t)] - \sigma \tilde{u}_t^2 \dot{u}_t + \tilde{h}_t (\tau \partial_t h_t + h_t - \dot{u}_t) \right\}.$$

This action is linear in \dot{u}_t and h_t . Thus, integrating over these fields gives δ functionals enforcing a set of two local instanton equations for \tilde{u}_t and \tilde{h}_t ,

$$\eta \partial_t \tilde{u}_t - (m^2 + a)\tilde{u}_t + \sigma \tilde{u}_t^2 + \tilde{h}_t = -\lambda_t, \quad (24)$$

$$\tau \partial_t \tilde{h}_t - \tilde{h}_t + a\tilde{u}_t = -\mu_t. \quad (25)$$

We then obtain the generating functional for the joint distribution of velocity \dot{u} and eddy-current pressure h ,

$$e^{\int_t (\lambda_t \dot{u}_t + \mu_t h_t) dt} = e^{m^2 \int_t \dot{w}_t \tilde{u}_t dt}, \quad (26)$$

in terms of the solution to these two instanton equations. It reduces to (17) for $\mu_t = 0$.

Now the remaining difficulty for arbitrary observables is to obtain sufficient information on the solutions of (24) and (25) with the corresponding source terms. We shall see that this is more difficult than in the standard ABBM model but can be done for certain observables and certain parameter values.

A. Dimensions and scaling

Before we proceed to compute observables, let us discuss the scaling behavior of our model and determine the number of free parameters. The mass m can be eliminated by dividing both sides of (19) by m^2 ,

$$\begin{aligned} \frac{\eta}{m^2} \partial_t \dot{u}(t) + \frac{a}{m^2} \dot{u}(t) + \frac{a}{m^2} \int_{-\infty}^t ds \partial_t f(t-s) \dot{u}(s) \\ = \frac{1}{m^2} \sqrt{\dot{u}(t)} \xi(t) + \dot{w}(t) - \dot{u}(t). \end{aligned} \quad (27)$$

The time derivative $\frac{\eta}{m^2} \partial_t \dot{u}(t)$ shows that there is a natural time scale $\tau_m = \eta/m^2$ so $t = t' \tau_m$, where t' is dimensionless. The nonlinear term $\frac{1}{m^2} \sqrt{\dot{u}(t)} \xi(t)$ shows that there is a natural length scale $S_m = \frac{\sigma}{m^4}$, so $u = S_m u'$, where u' is dimensionless. We thus rescale velocities as

$$\dot{u}(t) = \frac{\sigma}{\eta m^2} \dot{u}'(t'), \quad \dot{w}(t) = \frac{\sigma}{\eta m^2} \dot{w}'(t'), \quad (28)$$

using the natural unit of velocity $v_m = S_m/\tau_m$. Multiplying with $m^2 \eta/\sigma$, we get the equation

$$\begin{aligned} \partial_{t'} \dot{u}'(t') + \frac{a}{m^2} \dot{u}'(t') + \frac{a}{m^2} \int_{-\infty}^{t'} ds' \partial_{t'} f(t' - s') \dot{u}'(s') \\ = \sqrt{\dot{u}'(t')} \xi'(t') + \dot{w}'(t') - \dot{u}'(t'), \end{aligned} \quad (29)$$

where the noise is now $\langle \xi'(t_1) \xi'(t_2) \rangle = 2\delta(t_1 - t_2)$. Effectively, for the dynamics in terms of the primed variables we have $m = \sigma = \eta = 1$ (i.e., we have fixed the units of time and space so $\tau_m = S_m = 1$).

For the standard ABBM model, $a = 0$, and Eq. (29) is a dimensionless equation without any free parameters. To describe a signal $\dot{u}(t)$ produced by the standard ABBM model, it thus suffices to fix the velocity (amplitude) scale $v_m = \frac{\sigma}{\eta m^2}$ and the time scale $\tau_m = \frac{\eta}{m^2}$.

For the ABBM model with retardation, we have an additional time scale τ , on which the memory kernel $f(t-s)$ in (19) changes. The ratio of τ to the time scale of domain-wall motion $\tau_m = \frac{\eta}{m^2}$ is a dimensionless parameter $\tau' := \tau/\tau_m$. Equation (29) also contains a second dimensionless parameter $a' := \frac{a}{m^2}$, which gives the strength of the eddy-current pressure, as compared to the driving \dot{w} by the external magnetic field. We thus remain with *two* dimensionless parameters τ' and a' , which cannot be scaled away.

From now on, we will use the rescaled (primed) variables only. To simplify the notation, we drop all primes; we thus remain with the dimensionless equation of motion,

$$\begin{aligned} \partial_t \dot{u}(t) + a \dot{u}(t) + a \int_{-\infty}^t ds \partial_t f(t-s) \dot{u}(s) \\ = \sqrt{\dot{u}(t)} \xi(t) + \dot{w}(t) - \dot{u}(t). \end{aligned} \quad (30)$$

This amounts to setting $m = \sigma = \eta = 1$ in the original equation of motion, i.e., to working in the natural units for the ABBM model without retardation.

IV. MEASURING THE MEMORY KERNEL f

First, we discuss how the function f in Eq. (5) can be measured in an experiment or in a simulation. This permits verifying the validity of the exponential approximation (4). We consider the mean velocity $\dot{u}(t)$ at $t > 0$ following a kick by the driving field $w(t)$ at $t = 0$, i.e., $\dot{w}(t) = w_0 \delta(t)$. Our claim is that its Fourier transform and the Fourier transform of the memory kernel f are related via

$$u_\omega := \int_0^\infty dt e^{-i\omega t} \overline{\dot{u}(t)} = \frac{w_0}{m^2 + i\omega[\eta + af(\omega)]}, \quad (31)$$

where $f(\omega) := \int_0^\infty dt e^{-i\omega t} f(t)$.

To show this, we apply (17) to express the mean velocity at time $t_0 > 0$ as

$$\begin{aligned} \overline{\dot{u}(t_0)} &= \partial_\lambda |_{\lambda=0} \overline{e^{\lambda \dot{u}(t_0)}} = \partial_\lambda |_{\lambda=0} e^{\int_t dt \tilde{u}(t) \dot{w}(t)} \\ &= \partial_\lambda |_{\lambda=0} e^{w_0 \tilde{u}(t=0; t_0)}. \end{aligned} \quad (32)$$

The function $\tilde{u}(t)$ is the solution of (18) with $\lambda(t) = \lambda \delta(t - t_0)$. Since above we only need the term of order λ , and $\tilde{u}(t; t_0)$ is of order λ itself, the nonlinear term in (18) can be neglected. In other words, the disorder does not influence the mean velocity $\overline{\dot{u}(t_0)}$, and to obtain $\tilde{u}(t; t_0)$, it suffices to solve the linear equation

$$\begin{aligned} \eta \partial_t \tilde{u}(t; t_0) - (m^2 + a)\tilde{u}(t; t_0) - a \int_t^\infty ds f'(s-t) \tilde{u}(s; t_0) \\ = -\lambda \delta(t - t_0). \end{aligned} \quad (33)$$

Its solution is a function of the time difference $t - t_0$ only, $\tilde{u}(t; t_0) = \tilde{u}(t - t_0)$, which can be obtained by taking the

Fourier transform $\tilde{u}(\omega) := \int_{-\infty}^{\infty} d\tau e^{-i\omega\tau} \tilde{u}(\tau)$ as

$$(i\omega\eta - m^2 - a)\tilde{u}(\omega) - a\tilde{u}(\omega)[-i\omega f(-\omega) - 1] = -\lambda$$

$$\Rightarrow \tilde{u}(\omega) = \frac{\lambda}{-i\omega\eta + m^2 - ai\omega f(-\omega)}. \quad (34)$$

Here $f(\omega) = \int_0^{\infty} dt e^{-i\omega t} f(t)$ is the Fourier transform of the memory kernel. Inserting this relation into (32), the Fourier transform of the mean velocity after a kick is

$$\int_0^{\infty} dt_0 e^{-i\omega t_0} \overline{\tilde{u}(t_0)} = w_0 \int_{-\infty}^{\infty} dt_0 e^{-i\omega t_0} \tilde{u}(0 - t_0)$$

$$= w_0 \tilde{u}(-\omega), \quad (35)$$

which then gives (31), as claimed. In fact, it is easy to see from (32) that a more general relation holds for a kick of arbitrary shape,

$$\overline{\tilde{u}_\omega} := \int_0^{\infty} dt e^{-i\omega t} \overline{\tilde{u}_t} = \frac{w_0(\omega)}{m^2 + i\omega[\eta + af(\omega)]}, \quad (36)$$

where $w_0(\omega) := \int_0^{\infty} dt e^{-i\omega t} \dot{w}(t)$.

This relation allows one to obtain, at least in principle, the memory kernel $f(t)$ by measuring $\overline{\tilde{u}(t)}$ following a kick. This permits verifying the validity of the exponential approximation (11) experimentally. It also allows to test the validity of the ABBM model. Indeed, while (36) at small $w_0(\omega)$ is simply a linear response, the fact that it holds for a kick of arbitrary amplitude is a very distinctive property of the ABBM model. Alternatively, it may allow to determine the frequency range in which the model provides a good description of the experiment.

V. THE SLOW-RELAXATION LIMIT $\frac{\eta}{m^2} \ll \tau$

In order to go beyond the mean velocity and see the influence of disorder, one needs to solve the instanton equation (18) including the nonlinear term. Even in the special case of exponential relaxation, where (18) reduces to the local equations (24) and (25), their solution is complicated. However, we can analyze the latter in the slow-relaxation limit $\tau_m = \eta/m^2 \ll \tau$. In this limit, the relaxation of the domain wall to the next (zero force) metastable state, occurring on a time scale τ_m , is much faster than the relaxation of eddy currents (occurring on a time scale τ).⁶ Using the expressions for the relaxation times derived in Ref. [22], one sees that this is the case for very thick or very permeable samples. To simplify the expressions, we rescale \dot{u} as discussed in Sec. III A. This amounts to setting $m = \sigma = \eta = 1$. Thus, the time scale of domain-wall motion becomes $\tau \gg 1$.

In the following sections, we will compute stationary distributions of the eddy-current pressure h_t and domain-wall velocity \dot{u}_t at constant driving $w_t = vt$, as well as their behavior following a kick. A similar calculation for position differences at constant driving velocity is relegated to Appendix B.

⁶In the pure ABBM model, the small-dissipation limit $\eta \rightarrow 0$, i.e., $\tau_m \rightarrow 0$, is equivalent—up to a choice of time scale—to the limit of quasistatic driving $v \rightarrow 0^+$. However, these two limits differ for the retarded ABBM model which we discuss here.

A. Stationary distribution of eddy-current pressure

Using (26), the generating functional for the eddy-current pressure $h = h(t = 0)$ at constant driving $w_t = vt$ is

$$\overline{e^{\mu h}} = e^{v \int_t \tilde{u}(t)}. \quad (37)$$

$\tilde{u}(t)$ is obtained from the instanton equations (24) and (25) with the sources $\mu(t) = \mu\delta(t)$ and $\lambda(t) = 0$. From (25), one sees that $\tilde{h}(t)$ evolves on a time scale $s = t/\tau$. On this scale, both $\tilde{h}(t)$ and $\tilde{u}(t)$ have a finite limit for $\frac{\eta}{m^2\tau} \rightarrow 0$. In this limit they are related via

$$\tilde{h}(s) = -\tilde{u}(s)^2 + (1+a)\tilde{u}(s), \quad (38)$$

$$\tilde{u}(s) = \frac{1}{2}[a+1 - \sqrt{(a+1)^2 - 4\tilde{h}(s)}]. \quad (39)$$

Equation (25) for $\partial_s \tilde{h}(s)$ reads

$$\partial_s \tilde{h}(s) = \tilde{h}(s) - a\tilde{u}(s). \quad (40)$$

Replacing $\tilde{h}(s)$ on both sides of this equation using Eq. (38) yields a closed equation for $\tilde{u}(s)$,

$$[1+a-2\tilde{u}(s)]\partial_s \tilde{u}(s) = \tilde{u}(s) - \tilde{u}(s)^2. \quad (41)$$

The boundary condition at $s = 0$ is fixed by the source, $\mu(s) = \mu\delta(s) = \frac{\mu}{\tau}\delta(s) =: \mu_r\delta(s)$ [note $\tilde{u}(s > 0) = \tilde{h}(s > 0) = 0$ by causality]:

$$\tilde{h}(0) = \mu_r \Rightarrow \tilde{u}(0) = \frac{1}{2}[a+1 - \sqrt{(a+1)^2 - 4\mu_r}]. \quad (42)$$

Using Eq. (41), we can now compute the generating functional (37),

$$\int_{-\infty}^0 \tilde{u}(t) dt = \tau \int_{-\infty}^0 \tilde{u}(s) ds = \tau \int_0^{\tilde{u}(0)} \frac{\tilde{u} d\tilde{u}}{\partial_s \tilde{u}(\tilde{u})}$$

$$= \tau \int_0^{\tilde{u}(0)} \frac{(1+a-2\tilde{u}(s))d\tilde{u}}{1-\tilde{u}}$$

$$= \tau[2\tilde{u}(0) + (1-a)\ln(1-\tilde{u}(0))]. \quad (43)$$

Inserting this result into Eq. (37) we get

$$\overline{e^{\mu h_0}} = e^{2v_r \tilde{u}_0(\mu_r)} [1 - \tilde{u}_0(\mu_r)]^{(1-a)v_r}, \quad (44)$$

where $\tilde{u}_0(\mu_r) \equiv \tilde{u}(0)$ is given by (42) and we have defined a rescaled velocity $v_r := v\tau$ (i.e., the driving length during the relaxation time).

The stationary distribution of $h_r := \tau h$, obtained by inverting the Laplace transform, is

$$P(h_r) = \frac{v_r}{\sqrt{\pi}} 2^{\frac{1}{2}(a-1)v_r - 1} h_r^{\frac{1}{2}[(a-1)v_r - 3]}$$

$$\times \exp\left\{h_r - \frac{[2v_r - (3+a)h_r]^2}{8h}\right\}$$

$$\times \left\{(a-1)\sqrt{2h_r} D_{(1-a)v_r - 1}\left[\frac{(1-a)h_r + 2v_r}{\sqrt{2h_r}}\right]\right.$$

$$\left. + 2D_{(1-a)v_r}\left[\frac{(1-a)h_r + 2v_r}{\sqrt{2h_r}}\right]\right\}. \quad (45)$$

D is a parabolic cylinder function [54].

For small h_r , the distribution (45) behaves as

$$P(h_r) = \frac{1}{\sqrt{\pi}} e^{-\frac{(1+a)h_r - 2v_r}{4h_r}} v_r h_r^{-\frac{3}{2}} \left(\frac{h_r}{v_r}\right)^{(a-1)v_r} (1 + O(\sqrt{h_r})). \quad (46)$$

Thus, there is a small- h cutoff (due to the exponential term) and a power-law regime with a nontrivial exponent, $h_r^{-\frac{3}{2}+v_r(a-1)}$. Note that the above results hold in the double limit $v \rightarrow 0$ and $\tau \rightarrow \infty$ with $v_r = v\tau$ fixed. Restoring units this is $v_r = v\tau/S_m = \tau/\tau_v$ fixed, with both $\tau, \tau_v \gg \tau_m$, hence, v_r compares the two longest time scales, the driving time scale and the eddy-relaxation time scale.

In the limit where the driving is slow compared to the eddy-relaxation time scale, $v_r \rightarrow 0^+$, the stationary distribution (45) takes the form of a limiting (un-normalized) density $\rho(h_r)$ proportional to

$$\partial_{v_r}|_{v_r=0} P(h_r) = \frac{e^{-ah_r}}{2h_r} (a-1) \left\{ \operatorname{erf} \left[\frac{1}{2}(a-1)\sqrt{h_r} \right] + 1 \right\} + \frac{e^{-\frac{1}{4}(a+1)^2 h_r}}{\sqrt{\pi} h_r^{3/2}}.$$

In this limit, the small- h_r behavior is a pure power law,

$$\partial_{v_r}|_{v_r=0} P(h_r) = \frac{1}{\sqrt{\pi} h_r^{3/2}} + \frac{a-1}{2h_r} + O(h_r^{-\frac{1}{2}}). \quad (47)$$

We note the resemblance of the tail of the distribution of h and the one of the size S in the usual ABBM model with the $3/2$ exponent in both cases. If we assume that during avalanches (subavalanches) \dot{u} varies much faster than the relaxation time τ (i.e., on scales $\tau_m \ll \tau$) we can rewrite $h(t) \sim \sum_{\alpha, t_\alpha < t} S_\alpha e^{-(t-t_\alpha)/\tau}$ where subavalanche α occurs at t_α . Schematically $h(t)$ integrates avalanche sizes occurring in a time window of order τ , which could account for the similarity.

B. Eddy-current pressure following a kick

Still in the limit $\frac{\eta}{m^2} \rightarrow 0$, let us now discuss a nonstationary situation: The dynamics following a kick of size w_0 at $t = t_0 < 0$, $\dot{w}_t = w_0 \delta(t - t_0)$. Using (26), the generating function for the eddy-current pressure at time 0 is given by

$$\overline{e^{\mu h_0}} = e^{w_0 \tilde{u}_0}, \quad (48)$$

where \tilde{u}_t is the solution of (24) and (25) with the sources $\lambda(t) = 0$, $\mu(t) = \mu \delta(t)$, as in the previous section. Now we need its time dependence and not just the total integral. An implicit solution for $\tilde{u}(t)$ at $t < 0$ is obtained from Eq. (41),

$$\begin{aligned} \frac{t}{\tau} &= \int_{\tilde{u}_0}^{\tilde{u}_t} \frac{d\tilde{u}}{\tau \partial_t \tilde{u}(\tilde{u})} \\ &= (1+a) \ln \frac{\tilde{u}_t}{\tilde{u}_0} + (1-a) \ln \frac{1-\tilde{u}_t}{1-\tilde{u}_0}. \end{aligned} \quad (49)$$

\tilde{u}_0 is fixed by (42). As in the previous section, we define a rescaled time $s := \frac{t}{\tau}$. There is no expression in closed form for \tilde{u}_s for general a , but for specific values one obtains simple expressions (see Table I). In the case $a = 1$, the solution is particularly simple. Equation (48) gives

$$\overline{e^{\mu h(0)}} = e^{w_0 e^{0/(2\tau)(1-\sqrt{1-\mu_r})}}. \quad (50)$$

Taking the inverse Laplace transform, one obtains the distribution of eddy-current pressure $h_r := \tau h(0)$ after a kick of size

TABLE I. Some particular solutions of the implicit equation (49) describing the eddy-current pressure following a kick, in the limit $\frac{\eta}{m^2\tau} = 0$.

$a = 0$	$\tilde{u}_s = \frac{1}{2}(1 - \sqrt{1 - 4e^s \tilde{u}_0(1 - \tilde{u}_0)})$
$a = 1$	$\tilde{u}_s = e^{\frac{s}{2}} \tilde{u}_0$
$a = 3$	$\tilde{u}_s = \frac{\tilde{u}_0^2 e^{s/2} - \tilde{u}_0 e^{s/4} \sqrt{\tilde{u}_0^2 e^{s/2} - 4\tilde{u}_0 + 4}}{2(\tilde{u}_0 - 1)}$

w_0 at time $t_0 < 0$,

$$P(h_r) = \frac{w_0}{2\sqrt{\pi} h_r^{3/2}} \exp \left(\frac{t_0}{2\tau} - \frac{[e^{t_0/(2\tau)} w_0 - 2h_r]^2}{4h_r} \right). \quad (51)$$

The average pressure $\overline{h_r} = e^{t_0/(2\tau)} w_0/2$ decays exponentially with time. Note that the limit $t_0 = 0^-$ leads to a nontrivial $P(h_r)$ which should hold within the entire matching region $\tau_m \ll |t_0| \ll \tau$.

For $a \neq 1$, we did not obtain an exact solution. However, for any a , taking the limit $\mu \rightarrow -\infty$, or equivalently $\tilde{u}_0 \rightarrow -\infty$, Eq. (49) shows that $\tilde{u}_t \rightarrow -\infty$. This implies that the probability to find zero pressure, $p_{h=0} = \lim_{\lambda \rightarrow -\infty} e^{w_0 \tilde{u}_0} = 0$. Thus, after a kick at $t = t_0$, there is no time $T > 0$ such that $h_t = 0$ for all $t > T$; the eddy current pressure never stops. A similar discussion for the domain-wall velocity follows in Sec. V D.

Another interesting statement can be made regarding the time integral of the eddy-current pressure following a kick. From Eq. (11) it must equal the total avalanche size [integrating this equation and using that for a kick $h(0) = h(\infty) = 0$], i.e., $\int_0^\infty h(t) dt = S$.

C. Distribution of instantaneous velocities

The distribution of instantaneous velocities $P(\dot{u})$ at stationary driving is one of the simplest observables that can be determined from an experimental Barkhausen signal. For the standard ABBM model, it has been obtained in Ref. [20]. For a d -dimensional elastic interface driven quasistatically through short-range correlated disorder, this form is modified by universal corrections below the critical dimension d_c . These corrections have been computed using the functional renormalization group to one loop in $\epsilon = d_c - d$ in Refs. [18,25]. Using (26), the generating function of the instantaneous velocity, for constant driving $w_t = vt$, is

$$\overline{e^{\lambda \dot{u}}} = e^{v \int_t \tilde{u}_t}. \quad (52)$$

Now \tilde{u}_t is the solution of the instanton equations (24) and (25) with the sources $\lambda(t) = \lambda \delta(t)$, $\mu(t) = 0$.

To obtain the leading-order velocity distribution for $\tau \gg 1$, we need to solve (24) to order τ^{-1} . The solution \tilde{u}_t, \tilde{h}_t has two time scales, which are well separated in the $\tau \rightarrow \infty$ limit: $t \propto 1$ and $t \propto \tau$. We thus introduce

$$s := t/\tau \quad (53)$$

and assume the scaling

$$\tilde{u}(t) =: \tilde{u}^{(b)}(t) + \tau^{-1} \tilde{u}_1^{(b)}(t) + O(\tau^{-2}), \quad |t| \propto 1, \quad (54)$$

$$\tilde{h}(t) =: \tau^{-1} \tilde{h}^{(b)}(t) + O(\tau^{-2}), \quad |t| \propto 1, \quad (55)$$

$$\tilde{u}(t) =: \tau^{-1} \tilde{u}^{(a)}(s) + O(\tau^{-2}), \quad |t| \propto \tau, \quad (56)$$

$$\tilde{h}(t) =: \tau^{-1} \tilde{h}^{(a)}(s) + O(\tau^{-2}), \quad |t| \propto \tau. \quad (57)$$

Physically, the first regime $|t| \propto 1$ is the regime where the eddy currents have not yet built up ($\tilde{h} \ll \tilde{u}$) and are negligible. Hence the instanton is, up to a parameter change, identical to that of the standard ABBM model. The second regime is the regime of quasistatic relaxation of the eddy currents built up during the first stage. In that regime the instanton will be related to the instanton for the eddy-current relaxation discussed in the previous section.

The source terms enforce the boundary conditions $\tilde{u}^{(b)}(0) = -\lambda$, $\tilde{h}^{(b)}(0) = 0$. We now construct $\tilde{u}^{(a,b)}$ and $\tilde{h}^{(a,b)}$ in turn.

1. Boundary layer: $|t| \propto 1$

Let us first compute the leading term $\tilde{u}^{(b)}$, which is of order 1. For $-\tau \ll t < 0$, inserting Eq. (54) into Eq. (25), the term \tilde{h}_t is subdominant compared to $\tau \partial_t \tilde{h}_t$ and \tilde{u}_t . We therefore obtain

$$\tilde{h}^{(b)}(t) = a \int_t^0 dt' \tilde{u}^{(b)}(t') + O(\tau^{-1}). \quad (58)$$

$$\begin{aligned} \tilde{u}_1^{(b)}(t) = & \frac{a}{(1+a)[1+a+(1-e^{-(1+a)t})\lambda]^2} \left\{ -\lambda e^{(a+1)t} \left[2(1+a-\lambda) \left(\text{Li}_2\left(-\frac{e^{(a+1)t}\lambda}{1+a-\lambda}\right) - \text{Li}_2\left(-\frac{\lambda}{1+a-\lambda}\right) \right) \right. \right. \\ & \left. \left. - (1+a)t(1+a-\lambda) + \lambda(e^{(a+1)t} - 1) \right] - [(1+a-\lambda)^2 - \lambda^2 e^{2(a+1)t}] \ln\left(1 + \frac{\lambda(e^{(a+1)t} - 1)}{a+1}\right) \right. \\ & \left. + 2(a+1)\lambda t e^{(a+1)t} (1+a-\lambda) \ln\left(1 - \frac{\lambda}{a+1}\right) \right\}. \end{aligned} \quad (63)$$

For $t \rightarrow -\infty$, this tends to a constant,

$$\lim_{t \rightarrow -\infty} \tilde{u}_1^{(b)}(t) = -\frac{a}{1+a} \ln\left(1 - \frac{\lambda}{1+a}\right). \quad (64)$$

Since $\tilde{u}^{(b)}(-\infty) = 0$, see Eq. (60), this is the dominant contribution of the boundary-layer solution for \tilde{u} in the limit $t \rightarrow -\infty$.

2. Long-time regime: $|t| \propto \tau$

Now let us consider the regime $t \lesssim -\tau$. Inserting the rescaled time $s := t/\tau$ into Eq. (24), we see that the term $\partial_t \tilde{u}(t) = \tau^{-1} \partial_s \tilde{u}(s)$ is subdominant in τ^{-1} . The instanton in this regime is, thus, a special case of the instanton discussed in Sec. V A. Applying Eq. (56) we see that $\tilde{u}(t) \propto \tau^{-1}$ is small. Thus, we can also neglect the nonlinear term $\tilde{u}(t)^2$ in (24). This gives the simple relation

$$\tilde{u}^{(a)}(s) = \frac{1}{1+a} \tilde{h}^{(a)}(s).$$

Consequently, Eq. (25) reduces to

$$\partial_s \tilde{h}^{(a)}(s) = \frac{1}{1+a} \tilde{h}^{(a)}(s).$$

Thus, the term $\tilde{h}(t)$ in Eq. (24) is of order τ^{-1} and negligible in this regime. This is consistent with the interpretation of the boundary layer as the regime where the eddy currents have not yet built up. Equation (24) reduces to

$$\partial_t \tilde{u}_t^{(b)} - (1+a)\tilde{u}_t^{(b)} + \sigma(\tilde{u}_t^{(b)})^2 = -\lambda_t. \quad (59)$$

This is just the instanton equation (Eq. (13) of Ref. [25]) of the standard ABBM model but with a modified mass, $m^2 = 1 \rightarrow 1+a$. We obtain the known solution [25,46]

$$\tilde{u}^{(b)}(t) = \frac{(a+1)\lambda e^{(a+1)t}}{a+1+\lambda(e^{(a+1)t}-1)}. \quad (60)$$

Consequently, for $t \rightarrow -\infty$, $\tilde{h}^{(b)}(t)$ is given by

$$\tilde{h}^{(b)}(-\infty) = a \int_{-\infty}^0 dt \tilde{u}^{(b)}(t) = -a \ln\left(1 - \frac{\lambda}{a+1}\right). \quad (61)$$

To compute the correction $\tilde{u}_1^{(b)}$ of order τ^{-1} , we need to expand (24) to the next order. We get the linear equation

$$\partial_t \tilde{u}_1^{(b)}(t) - (1+a)\tilde{u}_1^{(b)}(t) + 2\tilde{u}^{(b)}(t)\tilde{u}_1^{(b)}(t) + \tilde{h}^{(b)}(t) = 0. \quad (62)$$

Using the expressions (58) and (60) for $\tilde{h}^{(b)}(t)$, its solution is given by

The boundary condition at $s = 0$ is now nontrivial and given not by the sources but by the asymptotics of the boundary layer as $t \rightarrow -\infty$,

$$\tilde{h}^{(a)}(0) = \tilde{h}^{(b)}(-\infty) = -a \ln\left(1 - \frac{\lambda}{a+1}\right). \quad (65)$$

The resulting solution of Eq. (24) is

$$\tilde{h}^{(a)}(s) = \tilde{h}^{(a)}(0) e^{\frac{s}{1+a}} = -a \ln\left(1 - \frac{\lambda}{a+1}\right) e^{\frac{s}{1+a}}, \quad (66)$$

$$\Rightarrow \tilde{u}^{(a)}(s) = -\frac{a}{1+a} e^{\frac{s}{1+a}} \ln\left(1 - \frac{\lambda}{a+1}\right). \quad (67)$$

A nontrivial consistency check is that this expression matches the $O(\tau^{-1})$ term of the $t \rightarrow -\infty$ asymptotics of the boundary layer given in Eq. (64),

$$\tilde{u}^{(a)}(0) = \tilde{u}_1^{(b)}(-\infty). \quad (68)$$

The boundary-layer solution (60) for $t \propto 1$ and the long-time asymptotics (66) for $t \propto \tau$ compare well to a direct numerical solution of (24) and (25) in the corresponding regimes; see Fig. 3.

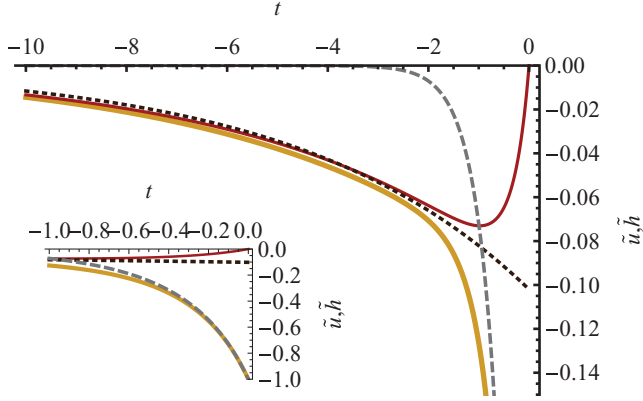


FIG. 3. (Color online) Instanton solution \tilde{u}_t, \tilde{h}_t of (24) and (25) with sources $\lambda(t) = -\delta(t)$, $\mu(t) = 0$ in the slow-relaxation limit $\tau \gg 1$. Parameters are $a = 1.3$, $\tau = 2$. Yellow (thick) curve: \tilde{u}_t ; red (thin) curve: $\frac{1}{1+a}\tilde{h}_t$; black dotted curve: long-time asymptotics (66); gray dashed curve: short-time asymptotics (60). The inset shows details of the boundary layer $|t| \propto 1$.

3. The velocity distribution

From the combined knowledge of the previous sections, we can extract the generating function for the velocity distribution (52). We have

$$\begin{aligned} \int_t \tilde{u}_t &= \left[\int_{-\infty}^0 dt \tilde{u}^{(b)}(t) + \int_{-\infty}^0 ds \tilde{u}^{(a)}(s) \right] \\ &= \left[-\ln \left(1 - \frac{\lambda}{a+1} \right) - a \ln \left(1 - \frac{\lambda}{a+1} \right) \right] \\ &= -(1+a) \ln \left(1 - \frac{\lambda}{a+1} \right). \end{aligned} \quad (69)$$

Thus, the generating function for the velocity distribution (52) is

$$\overline{e^{\lambda \tilde{u}}} = \left(1 - \frac{\lambda}{a+1} \right)^{-(1+a)v} [1 + O(\tau)^{-1}]. \quad (70)$$

The Laplace inversion is easy to do, giving the distribution of instantaneous velocities to leading order in τ^{-1} (but without any approximation in v). Restoring units, this is

$$P(\dot{u}) = \frac{e^{-\frac{\eta}{\sigma}(m^2+a)\dot{u}}}{\Gamma\left[\frac{\eta}{\sigma}(m^2+a)v\right]} \frac{1}{\dot{u}} \left[\dot{u} \frac{\eta}{\sigma}(m^2+a) \right]^{\frac{\eta}{\sigma}(m^2+a)v}. \quad (71)$$

We can compare this to the distribution of the standard ABBM model,

$$P(\dot{u}) = \frac{e^{-\frac{\eta}{\sigma}m^2\dot{u}}}{\Gamma\left(\frac{\eta}{\sigma}m^2v\right)} \frac{1}{\dot{u}} \left(\dot{u} \frac{\eta}{\sigma}m^2 \right)^{\frac{\eta}{\sigma}m^2v}. \quad (72)$$

We see that the effect of eddy currents on the instantaneous velocity distribution, in the limit of $\tau \rightarrow \infty$, is the same as if the mass in the standard ABBM model were increased from m^2 to $m^2 + a$. In particular, this means that the transition between intermittent avalanches and continuous motion happens for driving velocities v reduced by a factor of $(1 + a/m^2)$. In dimensionful units

$$v_c = \frac{\sigma}{\eta(m^2 + a)}. \quad (73)$$

D. Velocity following a kick

Let us now assume that the driving velocity undergoes a kick at time $t < 0$, i.e., $\dot{w}(t') = w_0\delta(t' - t)$. As discussed in Sec. IC, we consider an initial condition at $t = 0$ prepared in the ‘‘Middleton attractor’’ $u(w)$ with $\dot{u}(0) = h(0) = 0$. The kick gives deterministically $\dot{u}(t^+) = m^2w_0 =: \dot{u}_i$, so the distribution of velocities $\dot{u}_t := \dot{u}_0$ is the propagator $\mathcal{P}(\dot{u}_t, 0 | \dot{u}_i, t)$ at zero driving velocity.⁷ Applying (17), the generating function for the velocity \dot{u}_0 at time $t = 0$ is given by

$$\overline{e^{\lambda \dot{u}_0}} = e^{w_0 \tilde{u}_t}. \quad (74)$$

One can obtain the probability distribution of \dot{u}_0 in the slow-relaxation limit $\tau \gg 1$ by inverse Laplace transformation as follows. There are two time regimes as follows:

(i) For $|t| \sim 1$ we need to insert $\tilde{u}_t = \tilde{u}^{(b)}(t) + \tau^{-1}\tilde{u}_1^{(b)}(t)$ in (74) as given by (60) and (63). For small t we need to use only (60) and we recover the velocity distribution and propagator of the standard ABBM model at zero driving velocity but with modified parameters. The propagator of the standard ABBM model has been discussed, among others, in Refs. [24,25,46]. Here we use the result from Eq. (24) in Ref. [25], or, equivalently, (19) in Ref. [46], with $v = 0$ and $m^2 \rightarrow m^2 + a$ as follows:

$$\begin{aligned} P(\dot{u}) &= P(\dot{u}; 0 | m^2w_0; t) \\ &= \frac{m^2\sqrt{w_0/\dot{u}}}{2 \sinh\left[\frac{1}{2}t(a+m^2)\right]} \\ &\quad \times \exp\left\{ -\frac{(a+m^2)[\dot{u} + w_0e^{(a+m^2)t}]}{1 - e^{(a+m^2)t}} \right\} \\ &\quad \times I_1\left[\frac{(m^2+a)\sqrt{\dot{u}w_0}}{\sinh\left(\frac{1}{2}(m^2+a)t\right)} \right]. \end{aligned} \quad (75)$$

This distribution is not normalized; formally, there is an additional δ -function term as in Eq. (24) in Ref. [25]. This indicates that this formula is valid for $\dot{u} \sim 1$ only; there is another regime $\dot{u} \sim 1/\tau \ll 1$ which requires a more careful treatment but will not be considered here.

At later times there is a complicated crossover to regime (ii), which requires keeping the $1/\tau$ correction, which we will not detail here.

(ii) For long times $|t| \sim \tau$, \tilde{u}_t is given by (56) and (67). This gives

$$\overline{e^{\lambda \dot{u}_0}} = \left(1 - \frac{\lambda}{a+1} \right)^{-\frac{aw_0}{(a+1)\tau} \exp\left(\frac{t}{\tau(a+1)}\right)}. \quad (76)$$

Inverting the Laplace transform, one obtains the velocity distribution and propagator,

$$P(\dot{u}) \simeq \frac{(a+1)^{\epsilon_t} e^{-\dot{u}(1+a)}}{\Gamma(\epsilon_t)\dot{u}^{1-\epsilon_t}}, \quad \epsilon_t := \frac{aw_0}{(a+1)\tau} e^{\frac{t}{\tau(a+1)}}. \quad (77)$$

It approaches rather quickly a (normalized and regularized) power-law distribution proportional to $1/\dot{u}$. Note that for an infinitesimal kick we recover the limiting density obtained from the stationary motion $\rho(\dot{u}) = \partial_{w_0}|_{w_0=0}P(\dot{u}) =$

⁷In this section, we still keep $\eta = 1$ but restore units of m^2 in some places for clarity.

$\tau_{\text{typ}}^{-1} \partial_v|_{v=0} P^{\text{stat}}(\dot{u}) \sim \dot{u}^{-1} e^{-(1+a)\dot{u}}$, where $P^{\text{stat}}(\dot{u})$ was obtained in (71) and τ_{typ} is a typical time scale.

In general, the velocity distribution $P(\dot{u})$ following a kick can be decomposed as

$$P(\dot{u}) = p_{\dot{u}=0} \delta(\dot{u}) + \mathcal{P}_{\text{reg}}(\dot{u}), \quad (78)$$

where $p_{\dot{u}=0}$ is the probability that the domain wall has come to a complete halt. From (77) one sees that in the ABBM model with retardation, $p_{\dot{u}=0} = 0$ and the domain-wall motion following a kick never stops completely. This is in contrast to the standard ABBM model, where one has (cf. Ref. [46], Eq. (28))

$$p_{\dot{u}=0} = \exp\left(-\frac{w_0}{e^{-t} - 1}\right).$$

This can also be seen directly from the instanton solution \bar{u} : The decomposition (78) implies

$$\overline{e^{\lambda \bar{u}}} = \int_{\dot{u}} e^{\lambda \dot{u}} P(\dot{u}) \xrightarrow{\lambda \rightarrow -\infty} p_{\dot{u}=0}. \quad (79)$$

Since $\overline{e^{\lambda \bar{u}}} = e^{w_0 \bar{u}_t}$, we can conclude that $p_{\dot{u}=0}$ is zero if and only if $\lim_{\lambda \rightarrow -\infty} \bar{u}_t = -\infty$. This is the case in the retarded ABBM model, where (67) shows that $\bar{u}_t \propto -\ln(1 - \frac{\lambda}{1+a}) \xrightarrow{\lambda \rightarrow -\infty} -\infty$. However, it is not the case in the standard ABBM model, where $\lim_{\lambda \rightarrow -\infty} \bar{u}_t = \frac{1}{1-e^{-\tau}}$ is finite (cf. Ref. [46], Eq. (14)).

We conclude that in the ABBM model with retardation, the velocity following a kick never becomes zero permanently, even though its mean decays exponentially in time over time scales of order τ , with, for $t \lesssim -\tau$,

$$\langle \dot{u}_0 \rangle = \frac{aw_0}{(a+1)^2 \tau} e^{-\frac{|t|}{(a+1)\tau}}. \quad (80)$$

Although the calculation above was done at leading order in τ^{-1} , we expect the phenomenology to be similar for arbitrary τ . To make this explicit, we now consider the opposite limit of fast relaxation, $\tau \ll \frac{\eta}{m^2}$, in which analytical progress is also possible.

VI. THE FAST-RELAXATION LIMIT $\tau \ll \frac{\eta}{m^2}$

We can also consider the limit $\tau \ll \tau_m = \eta/m^2$, where the eddy currents relax much faster than the domain-wall motion. Experimentally, this limit is even more relevant than the slow-relaxation limit discussed in Sec. V: As a function of sample thickness b , the eddy-current relaxation time $\tau \propto b^2$, whereas the domain-wall motion occurs on a time scale $\frac{\eta}{m^2} \propto ab$. For typical experimental setups [22,55] $a \gg b$ and, hence, $\tau \ll \eta/m^2$.

We now discuss the stationary velocity distribution, and the velocity following a kick in the driving velocity, in the fast-relaxation limit. As in Sec. V C, we need to construct the instanton \bar{u} , \bar{h} solving Eqs. (24) and (25) with sources $\lambda(t) = \lambda \delta(t)$, $\mu(t) = 0$. Now, however, τ and not τ^{-1} is a small parameter. We expect a two-scale solution: A boundary layer for $|t| \propto \tau$ around $t = 0$ and an asymptotic regime for $|t| \propto 1$. We

thus introduce the rescaled time $s := t/\tau$ and make the ansatz

$$\bar{u}(t) =: \bar{u}_0^{(b)}(t) + \tau \bar{u}_1^{(b)}(t) + O(\tau)^2, \quad |t| \propto 1, \quad (81)$$

$$\bar{h}(t) =: \bar{h}_0^{(b)}(t) + O(\tau), \quad |t| \propto 1, \quad (82)$$

$$\bar{u}(t) =: \bar{u}_0^{(a)}(s) + \tau \bar{u}_1^{(a)}(s) + O(\tau)^2, \quad |t| \propto \tau, \quad (83)$$

$$\bar{h}(t) =: \bar{h}_0^{(a)}(s) + O(\tau), \quad |t| \propto \tau. \quad (84)$$

A. Leading order

At order τ^0 , the instanton equations (25) and (24) reduce in the asymptotic regime to

$$\begin{aligned} \partial_t \bar{u}_0^{(b)}(t) - (1+a) \bar{u}_0^{(b)}(t) + [\bar{u}_0^{(b)}(t)]^2 + \bar{h}_0^{(b)}(t) &= 0 \\ -\bar{h}_0^{(b)}(t) + a \bar{u}_0^{(b)}(t) &= 0, \end{aligned}$$

with boundary condition $\bar{u}_0(0) = \lambda$. This gives the leading-order solution

$$\bar{u}_0^{(b)}(t) = \frac{\lambda}{\lambda + (1-\lambda)e^{-t}}, \quad \bar{h}_0^{(b)}(t) = a \bar{u}_0^{(b)}(t). \quad (85)$$

In the boundary layer, the corresponding solution is $\bar{u}_0^{(a)}(s) = \bar{u}_0^{(b)}(0) = \lambda$, and Eq. (24) gives

$$\partial_s \bar{h}_0^{(a)}(s) - \bar{h}_0^{(a)}(s) + a\lambda = 0, \quad \Rightarrow \bar{h}_0^{(a)}(s) = a\lambda(1 - e^s).$$

B. Next-to-leading order

We obtained in Eq. (85) the leading-order solution $\bar{u}_0(t)$, valid in both regimes. Expanding around it, setting $\bar{u}(t) = \bar{u}_0(t) + \tau \bar{u}_1(t) + O(\tau)^2$, we get an equation for $\bar{u}_1(t)$

$$\partial_t \bar{u}_1(t) - (1+a) \bar{u}_1(t) + 2\bar{u}_0(t) \bar{u}_1(t) + \frac{1}{\tau} [\bar{h}(t) - a \bar{u}_0(t)] = 0.$$

In the boundary layer, $\partial_t \bar{u}_1(t) = \frac{1}{\tau} \partial_s \bar{u}_1^{(a)}(s)$, and

$$\bar{h}_0(s) - a \bar{u}_0(s) = a\lambda(1 - e^s) - a\lambda = -a\lambda e^s.$$

Hence, the next-to-leading-order contribution $\bar{u}_1^{(a)}(s)$ in the boundary layer satisfies

$$\partial_s \bar{u}_1^{(a)}(s) = a\lambda e^s \Rightarrow \bar{u}_1^{(a)}(s) = -a\lambda(1 - e^s). \quad (86)$$

On the other hand, Eq. (25) gives in the asymptotic regime

$$\partial_t \bar{h}_0^{(b)}(t) = \bar{h}_1^{(b)}(t) - a \bar{u}_1^{(b)}(t). \quad (87)$$

Inserting this relation into Eq. (24) gives

$$\begin{aligned} \partial_t \bar{u}_1^{(b)}(t) - \bar{u}_1^{(b)}(t) + 2\bar{u}_0^{(b)}(t) \bar{u}_1^{(b)}(t) + a \partial_t \bar{u}_1^{(b)}(t) &= 0 \\ \Rightarrow \bar{u}_1^{(b)}(t) &= \frac{a\lambda e^t (\lambda t - t - 1)}{(\lambda e^t - \lambda + 1)^2}. \end{aligned} \quad (88)$$

Here we used the matching condition $\bar{u}_1^{(b)}(0) = \bar{u}_1^{(a)}(-\infty) = -a\lambda$, as given by Eq. (86).

The next-to-leading order corrections (86) and (88) compare well to a direct numerical solution of Eqs. (24) and (25); see Fig. 4.

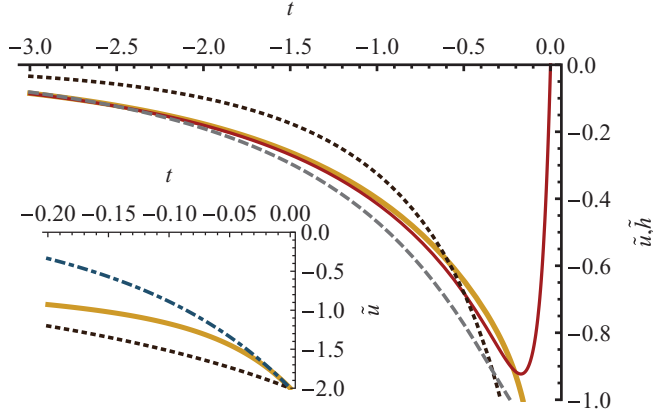


FIG. 4. (Color online) Instanton solution \tilde{u}, \tilde{h} of Eqs. (24) and (25) with sources $\lambda(t) = -\delta(t)$, $\mu(t) = 0$ for fast eddy-current relaxation, $\tau \ll \eta/m^2$. Parameters are $a = 5$, $\tau = 0.1$. Yellow (thick) curve: $\tilde{u}(t)$; red (thin) curve: $\frac{1}{a}\tilde{h}(t)$. Black dotted curve: Leading-order result (85), corresponding to the standard ABBM model. Gray dashed curve: Solution (85) plus next-to-leading order correction (88) in the long-time regime $|t| \propto 1$. The inset shows details of the boundary layer $|t| \propto \tau$. Blue dot-dashed curve (inset only): Solution (85) plus next-to-leading order correction (86) in the boundary layer.

C. Stationary velocity distribution

With the above analysis, we can obtain some results on the velocity distribution. The integral over the instanton solution gives

$$\begin{aligned} \int_t \tilde{u}(t) dt &= \int_{-\infty}^0 dt \tilde{u}_0^{(b)}(t) + \tau \int_{-\infty}^0 dt \tilde{u}_1^{(b)}(t) + O(\tau)^2 \\ &= -\ln(1 - \lambda) + a\tau \left[\frac{\lambda}{\lambda - 1} - \ln(1 - \lambda) \right] + O(\tau)^2. \end{aligned} \quad (89)$$

Inserting this result into Eq. (52) for the generating functional of instantaneous velocities gives

$$\overline{e^{\lambda \tilde{u}}} = (1 - \lambda)^{-v(1+a\tau)} e^{av\tau \frac{\lambda}{\lambda-1} + O(\tau)^2}. \quad (90)$$

To the same order in τ , this can also be rewritten as

$$\begin{aligned} \int_t \tilde{u}(t) dt &= -(1 + a\tau) \ln \left[1 - \frac{\lambda}{1 + a\tau} \right] + O(\tau)^2 \\ \Rightarrow \overline{e^{\lambda \tilde{u}}} &= \left[1 - \frac{\lambda}{1 + a\tau} \right]^{-v(1+a\tau)} + O(\tau)^2. \end{aligned} \quad (91)$$

This makes it clearer that, to leading order, the form of the velocity distribution is not modified; only the parameters entering it are rescaled. The only change is the replacement of the typical velocity scale $v_m = \frac{\sigma}{\eta m^2}$ of the standard ABBM model (in units of which the instantaneous velocity \dot{u} and the driving velocity v are measured, cf. Sec. III A) by

$$\begin{aligned} v_c &= \frac{\sigma}{\eta m^2} \left[1 - a \frac{\tau}{\eta} + O\left(\frac{\tau}{\eta/m^2}\right)^2 \right] \\ &= \frac{\sigma}{m^2(\eta + a\tau)} + O\left(\frac{\tau}{\eta/m^2}\right)^2. \end{aligned} \quad (92)$$

In particular, (91) indicates that, in the fast-relaxation limit, the instantaneous velocity distribution $P(\dot{u})$ has a power-law behavior for small \dot{u}

$$P(\dot{u}) \sim \dot{u}^{-1+v(1+a\tau+O(\tau)^2)} \sim \dot{u}^{-1+v/v_c}, \quad (93)$$

with v_c given in (92).

In a typical experimental measurement of Barkhausen noise, the saturation magnetization I_s , the demagnetizing factor k , the distribution of the random pinning forces F , and the retardation kernel which enter (4) are not known. The velocity scale v_c is, hence, usually obtained by fitting $P(\dot{u})$ to a histogram of the experimentally obtained Barkhausen signal. With the velocity scale v_c as a fit parameter, (91) shows that no difference between the predictions of the standard ABBM model, and the ABBM model with retardation, can be observed to this order in τ for the stationary velocity distribution.⁸ On the other hand, nonstationary observables, such as the response to a kick discussed in Sec. IV and the average avalanche shape at fixed avalanche size discussed in Sec. VII B, show the influence of retardation much more clearly.

Equation (92) shows that fast eddy-current relaxation decreases the velocity scale v_c , just as in Eq. (71) for slow eddy-current relaxation. Both formulas have the form $v_c = \frac{\sigma}{m^2(\eta+a\tau)}$, where τ_f is the fastest time scale in the problem, $\tau_f = \eta/m^2$ for the slow-relaxation limit, and $\tau_f = \tau$ for the fast-relaxation limit. In contrast to Eq. (71), however, the correction we obtain here is perturbative: It vanishes as $\tau \rightarrow 0$. In the limit $\tau \rightarrow 0$ we recover the standard ABBM model.

D. Velocity following a kick

The generating functional for the distribution of velocities $\dot{u}(0)$ following a kick of size w at $t < 0$ can also be expressed in terms of the instanton solution (81),

$$\overline{e^{\lambda \dot{u}_0}} = e^{w\tilde{u}(t)} = \exp[w\tilde{u}_0^{(b)}(t) + w\tau\tilde{u}_1^{(b)}(t) + O(\tau)^2]. \quad (94)$$

$\tilde{u}_0^{(b)}$ and $\tilde{u}_1^{(b)}$ are given by Eqs. (85) and (88) above. They have a finite limit as $\lambda \rightarrow -\infty$:

$$\lim_{\lambda \rightarrow -\infty} \tilde{u}^{(b)} = \frac{1}{1 - e^{-t}}, \quad (95)$$

$$\lim_{\lambda \rightarrow -\infty} \tilde{u}_1^{(b)} = \frac{ate^{-t}}{(1 - e^{-t})^2}. \quad (96)$$

This would suggest that the velocity distribution contains a term $\sim \delta(\dot{u})$. However, for large negative λ , the expansion above breaks down, and higher orders in τ become non-negligible. By solving the complete instanton equations numerically one obtains Fig. 5. One observes that the leading-order (standard ABBM) instanton (85) goes to a fixed value for $\lambda \rightarrow -\infty$. The next-to-leading order correction (88) coincides better with the numerical solution but still breaks down around $\lambda \approx -10$ and goes to a fixed value, too. However, the true (numerically obtained) solution of the instanton equations goes to $-\infty$ as $\lambda \rightarrow -\infty$. Hence, $\lim_{\lambda \rightarrow -\infty} \overline{e^{\lambda \dot{u}_0}} =$

⁸The only exception would be if τ and a could be tuned without modifying the other sample parameters, but this does not seem realistic.

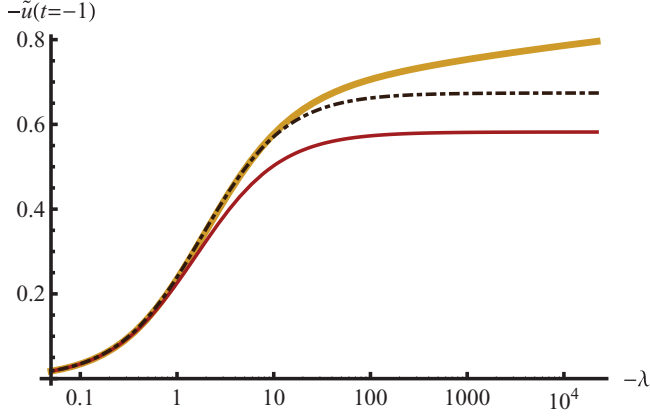


FIG. 5. (Color online) Instanton $\tilde{u}(t)$ at a fixed time $t = -1$, as a function of λ , for $\tau = 0.1$ and $a = 1$. Thick yellow line: Numerical solution of (24) and (25). Thin red line: Leading-order ABBM solution (85), corresponding to $a = 0$. Dot-dashed black line: Next-to-leading order correction (88).

$\lim_{\lambda \rightarrow -\infty} e^{w\tilde{u}(t)} = 0$, and the distribution $P(\dot{u}_0)$ does not have a $\delta(\dot{u}_0)$ piece, consistent with the results obtained above in Sec. VD in the $\tau \rightarrow \infty$ limit.

From the instanton expansion (85) and (88), valid for $\lambda \propto 1$, we can obtain the velocity distribution $P(\dot{u}_0)$ following a kick at $t < 0$ in the regime $\dot{u}_0 \propto 1$. Using Eq. (94), we write its generating function to order τ as

$$\overline{e^{\lambda \dot{u}_0}} = \exp\left(wA - \frac{wB}{\lambda - q} + \frac{wC}{(\lambda - q)^2}\right), \quad (97)$$

with

$$\begin{aligned} q &= \frac{1}{1 - e^t} \\ A &= \frac{e^t}{e^t - 1} + \tau \frac{ae^t t}{(e^t - 1)^2} \\ B &= \frac{e^t}{(e^t - 1)^2} + \tau \frac{ae^t [e^t(t+1) + t - 1]}{(e^t - 1)^3} \\ C &= \tau \frac{ae^t [e^t(t+1) - 1]}{(e^t - 1)^4}. \end{aligned}$$

The inverse Laplace transform of $\overline{e^{\lambda \dot{u}_0}}$ can be written as

$$\begin{aligned} P(\dot{u}) &= e^{wA - q\dot{u}} \int_0^{2\pi} \frac{d\phi}{2\pi} r e^{i\phi} \\ &\times \exp\left(w \left[\frac{C e^{-2i\phi}}{r^2} + \frac{B e^{-i\phi}}{r} \right] - \dot{u} r e^{i\phi}\right). \quad (98) \end{aligned}$$

We have set $\lambda = q + r e^{i\phi}$ to arrive at the above formula. We numerically checked that the integral is independent of r . One can evaluate it analytically, if either $B = 0$ or $C = 0$, by expanding in powers of r and retaining only terms which scale as r^0 (note $r^n \sim e^{i\phi n}$). The final result can be written as a convolution of the two:

$$P(\dot{u}) = e^{wA - q\dot{u}} \int_0^{\dot{u}} d\dot{u}_1 P_1(\dot{u}_1) P_2(\dot{u} - \dot{u}_1), \quad (99)$$

$$P_1(\dot{u}) = \delta(\dot{u}) + \sqrt{\frac{Bw}{\dot{u}}} I_1(2\sqrt{Bw\dot{u}}), \quad (100)$$

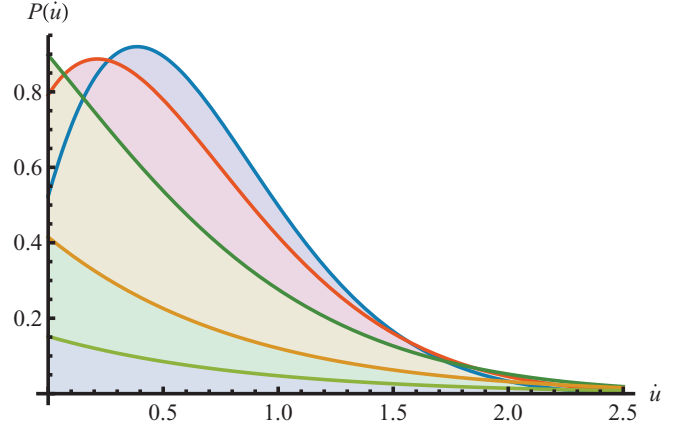


FIG. 6. (Color online) Velocity distribution $P(\dot{u}_0)$ given by (99) (without the δ part) after a kick at time $t < 0$. The parameters were chosen to be $w = 1$, $a = 1$, $\tau = 0.2$. The time of the kick varies from right to left as $t = -0.3, -0.4, -0.7, -1.5, -2.5$.

$$P_2(\dot{u}) = \delta(\dot{u}) + Cuw_0 F_2\left(\frac{3}{2}, 2 \middle| \frac{1}{4} Cu^2 w\right). \quad (101)$$

Note again that formally the δ -function parts are an artifact of our expansion, which is not valid as $\lambda \rightarrow -\infty$ or $\dot{u} \rightarrow 0$. We expect them to be smeared out on a scale $e^{t/\tau}$, which goes to 0 as $t \rightarrow -\infty$. However, physically, these velocities are extremely small and unlikely to be observable. Thus, the δ -function term is physically sensible and can be interpreted as the probability that all *significant* avalanche activity has stopped.

Numerically, the convolution can easily be computed. An example of the distributions for various times is shown in Fig. 6. We see that for small times the distribution is peaked around the value w imposed by the step in the force. Later on the typical value of the velocity approaches 0, and the distribution becomes monotonous. Its area decreases since part of the probability is absorbed by the (smoothened) δ function near $\dot{u} = 0$ ($\lambda = -\infty$), which we are unable to analyze here in more detail.

VII. AVALANCHE STATISTICS AT FIXED SIZE

In the previous section we saw, at least in the two limits $\eta/m^2 \ll \tau$ and $\eta/m^2 \gg \tau$, that avalanches following even an infinitesimal kick never completely stop. Computing observables conditioned to their duration of first return to $\dot{u} = 0$, i.e., the subavalanche duration, requires introducing an artificial “absorbing boundary” at $\dot{u} = 0$ which will terminate the avalanche once \dot{u} becomes zero.⁹ This task is deferred to Sec. VIII. However, the mean velocity following a (finite or infinitesimal) kick still decreases, and the total avalanche size remains finite. We will now compute its distribution, and other observables conditioned on the total avalanche size.

⁹The natural boundary at $\dot{u} = 0$ would be reflecting, since, if \dot{u}_t becomes zero at some instant of time, it immediately restarts to positive velocities due to the decrease of the eddy current pressure in the next time step.

A. Avalanche sizes

We define the size S of a nonstationary avalanche following a kick of size w_0 at $t = 0$ as $S = \int_{-\infty}^{\infty} \dot{u}(t) dt$. The Laplace transform of the probability distribution of S is given by Eq. (17),

$$\overline{e^{\lambda S}} = \overline{e^{\lambda \int_{-\infty}^{\infty} \dot{u}(t) dt}} = e^{w_0 \tilde{u}_0}. \quad (102)$$

Here \tilde{u}_t is the solution of (18) with a time-independent source $\lambda(t) = \lambda$. This means that $\tilde{u}_t = \tilde{u}$ is also time independent. Then, using $f(0) = 1$ and $f(\infty) = 0$, the terms proportional to a drop out from Eq. (18) and we get

$$-m^2 \tilde{u} + \sigma \tilde{u}^2 = -\lambda. \quad (103)$$

Choosing the solution which tends to 0 as $\lambda \rightarrow 0$, we get

$$\tilde{u} = \frac{m^2 - \sqrt{m^4 - 4\lambda\sigma}}{2\sigma} \quad (104)$$

and

$$\overline{e^{\lambda S}} = e^{w_0 \frac{m^2 - \sqrt{m^4 - 4\lambda\sigma}}{2\sigma}}. \quad (105)$$

Inverting the Laplace transform gives

$$P(S) = \frac{w_0}{2\sqrt{\pi\sigma} S^{\frac{3}{2}}} e^{-\frac{(w_0 - m^2 S)^2}{4\sigma S}}. \quad (106)$$

with $\bar{S} = w_0$. Note that this extends to any finite kick of arbitrary shape replacing $w_0 = \int_0^\infty dt \dot{w}(t)$ [18]. This is precisely the distribution obtained for the standard ABBM model and the mean-field theory of interfaces in Refs. [18,45,46]. Of course, this can already be seen from the fact that the terms proportional to a drop out from (18) when \tilde{u} is time independent. Note that this result is *independent* of the shape of the memory kernel f in (5). This is a consequence of the monotonicity of the model, as discussed in the Introduction. In the limit of an infinitesimal kick, i.e., small w_0 , one recovers the stationary avalanche-size density.

Universal corrections to the distribution (106) are expected when one goes beyond the mean-field limit and considers d -dimensional elastic interfaces. Without retardation effects, the universal corrections at slow driving were obtained to one loop in an expansion around the critical dimension [18]. We expect them to remain unchanged by retardation effects, as seen in this section for the mean-field case.

B. Avalanche shape at fixed size

The avalanche shape is usually obtained by computing the mean velocity as a function of time, in the ensemble of all avalanches of a fixed duration [19,22,35,56]. Here we shall instead consider the ensemble of all avalanches of a fixed size S . In a numerical simulation or in an experiment, the shape at fixed size is just as easily measurable as the shape at fixed duration. However, it is easier to obtain theoretically with our methods, and it can be defined without a microscopic cutoff. We will thus compute the shape function defined via

$$\mathfrak{s}(t, S) := \int_0^\infty d\dot{u}_t \dot{u}_t P(\dot{u}_t | S) = \frac{\int_0^\infty d\dot{u}_t \dot{u}_t P(\dot{u}_t, S)}{P(S)}. \quad (107)$$

$P(S)$ is the avalanche size distribution (106).

We follow the approach used in Refs. [18,45,46] to obtain the avalanche shape in the standard ABBM model from the Martin-Siggia-Rose field theory. The driving w_t performs a kick at $t = 0$, i.e., we set $\dot{w}_t = w_0 \delta(t)$. We then consider the observable

$$\hat{\mathfrak{s}}(t_0, \lambda) := \overline{\dot{u}_{t_0} e^{\lambda S}} = \partial_\mu |_{\mu=0} \overline{e^{\lambda S + \mu \dot{u}_{t_0}}}. \quad (108)$$

$\hat{\mathfrak{s}}$ is related to the shape function \mathfrak{s} via a Laplace transform,

$$\hat{\mathfrak{s}}(t_0, \lambda) = \int_0^\infty dS \mathfrak{s}(t, S) P(S) e^{\lambda S}. \quad (109)$$

$\hat{\mathfrak{s}}$ as defined in (108) can be evaluated using (17),

$$\hat{\mathfrak{s}}(t_0, \lambda) = \partial_\mu |_{\mu=0} e^{w_0 \tilde{u}_0(\mu)}, \quad (110)$$

where $\tilde{u}_0(\mu)$ is the solution of (18) with the source $\lambda_t = \lambda + \mu \delta(t - t_0)$. To compute (110), we need to solve the instanton equation (18) to first order in μ . The solution for $\mu = 0$ is the constant $\tilde{u}(\lambda)$, obtained previously in Eq. (104) for the size distribution. The correction of order μ , $\tilde{u}^{(1)}$ has to satisfy the linear (but still nonlocal) equation

$$\begin{aligned} \partial_t \tilde{u}_t^{(1)} - (1 + a - 2\tilde{u}) \tilde{u}_t^{(1)} - a \int_t^\infty ds f'(s - t) \tilde{u}_s^{(1)} \\ = -\mu \delta(t - t_0). \end{aligned} \quad (111)$$

We now restrict ourselves to the case of an exponentially decaying memory term, $f(t) = e^{-t/\tau}$. Through the substitution $\tilde{u}_t^{(1)} = \mu(1 - \tau \partial_t) g_t$, Eq. (111) is transformed into a linear second-order differential equation,

$$(\partial_t - 1 - a + 2\tilde{u})(1 - \tau \partial_t) g_t + a g_t = -\delta(t - t_0). \quad (112)$$

The right-hand side yields the boundary conditions $g(t_0) = 0$, $g'(t_0) = -1/\tau$. The resulting solution for g_t is

$$g_t = \frac{2r e^{(t-t_0)/\tau} \left[e^{-\frac{2a(t-t_0)}{r}} - e^{-\frac{r(t-t_0)}{2\tau}} \right]}{4a\tau + r^2},$$

where we defined r via

$$\frac{(2+r)(r-2a\tau)}{2r\tau} = \sqrt{1-4\lambda}. \quad (113)$$

The shape function (110) is then

$$\begin{aligned} \hat{\mathfrak{s}}(t_0, \lambda) &= e^{w_0 \tilde{u}_0(\mu=0)} w_0 \tilde{u}^{(1)}(0) \\ &= e^{\frac{w_0}{2}(1-\sqrt{1-4\lambda})} w_0 [g(0) - \tau g'(0)] \\ &= e^{\frac{w_0}{2}(1-\sqrt{1-4\lambda})} w_0 \frac{4a e^{\frac{2a t_0}{r}} + r^2 e^{-\frac{r}{2} t_0/\tau}}{4a\tau + r^2} e^{-t_0/\tau}. \end{aligned} \quad (114)$$

The shape at fixed size S is finally obtained by inverting the Laplace transform. This is best done using the coordinate r

introduced in Eq. (113):

$$\begin{aligned}
& \int d\dot{u}_t \dot{u}_t P(\dot{u}_t, S) \\
&= - \int_{r_0-i\infty}^{r_0+i\infty} \frac{dr}{2\pi i} \hat{s}(t, \lambda(r)) e^{-\lambda(r)S} \frac{d\lambda}{dr} \\
&= \int_{r_0-i\infty}^{r_0+i\infty} \frac{dr}{2\pi i} \frac{(r-2a\tau)(r+2)(4a\tau e^{\frac{2at}{r}} + r^2 e^{-\frac{r}{2\tau}})}{8\tau^2 r^3} \\
&\quad \times \exp \left[\frac{S(r+2)^2(r-2a\tau)^2}{16r^2\tau^2} - \frac{S}{4} - \frac{t}{\tau} \right] \\
&\quad \times w_0 \exp \left[\frac{w_0}{2} \left(1 - \frac{(2+r)(r-2a\tau)}{2r\tau} \right) \right]. \quad (115)
\end{aligned}$$

r_0 fixes the location of the integration contour; it can be chosen arbitrarily, as long as $r_0 \neq 0$.¹⁰

Our final result for the avalanche shape at fixed size (following a kick of arbitrary strength w_0) is, thus, obtained by inserting this result into

$$s(t, S) = 2\sqrt{\pi} S^{3/2} e^{\frac{(w_0-S)^2}{4S}} \frac{1}{w_0} \int_0^\infty d\dot{u}_t \dot{u}_t P(\dot{u}_t, S),$$

where we have used (106). On this expression the limit of $w_0 \rightarrow 0$ is easy to take and provides the result for the stationary avalanches.

One nontrivial check of this formula is that the resulting shape is properly normalized,

$$\begin{aligned}
& \int_0^\infty dt s(t, S) \\
&= \int_0^\infty dt \int d\dot{u}_t \dot{u}_t \frac{P(\dot{u}_t, S)}{P(S)} \\
&= \int_{r_0-i\infty}^{r_0+i\infty} \frac{dr}{4i\sqrt{\pi}} \frac{(r^2 + 4a\tau)}{r^2\tau} \\
&\quad \times \exp \left[\frac{S(r+2)^2(r-2a\tau)^2}{16r^2\tau^2} - \frac{S}{4} \right] \\
&\quad \times S^{\frac{3}{2}} e^{\frac{(w_0-S)^2}{4S}} \exp \left[\frac{w_0}{2} \left(1 - \frac{(2+r)(r-2a\tau)}{2r\tau} \right) \right] \\
&= \int_{-i\infty}^{i\infty} \frac{dp}{4i\sqrt{\pi}} S^{\frac{3}{2}} e^{\frac{(w_0-S)^2}{4S}} e^{\frac{Sp^2}{16} + \frac{w_0}{2}(1-\frac{p}{2}) - \frac{S}{4}} = S,
\end{aligned}$$

where in the second line we used the substitution $p = \frac{(r+2)(r-2a\tau)}{r\tau}$.

The integral (115) could be calculated in closed form in the case $a = 0$ of the standard ABBM model. There one finds

$$\int d\dot{u}_t \dot{u}_t P(\dot{u}_t, S) = \frac{(2t + w_0)w_0 e^{-\frac{S^2 - 2Sw_0 + (2t+w_0)^2}{4S}}}{2\sqrt{\pi} S^{3/2}},$$

¹⁰This is in order to avoid the singularity of the integrand at $r = 0$. We checked that the result of the (numerical) integration of (115) is independent of the value and the sign of r_0 .

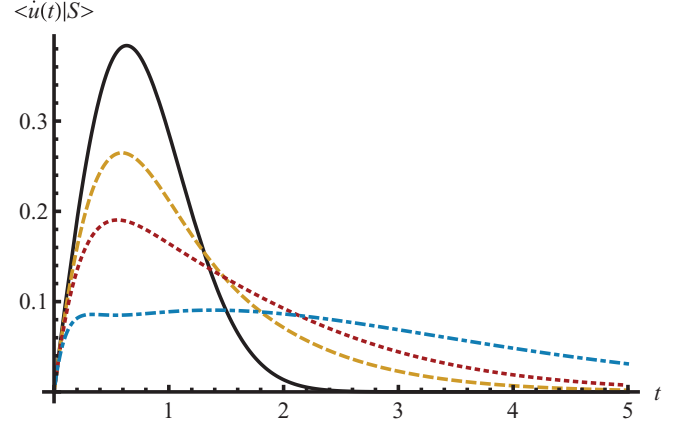


FIG. 7. (Color online) Avalanche shape at fixed size $S = 0.8$, $\tau = 0.5$, and $w_0 = 0$. Curves are, from top (black solid line) to bottom (blue dot-dashed line), $a = 0$ [standard ABBM model, as given by Eq. (116)], $a = 1$, $a = 2$, $a = 5$.

and the result for the shape,

$$s(t, S) = (2t + w_0)e^{-t(t+w_0)/S}. \quad (116)$$

In the limit of an infinitesimal kick $w_0 \rightarrow 0$ we thus obtain the shape at fixed size for the standard ABBM model ($a = 0$) for stationary avalanches as

$$s(t, S) = 2te^{-t^2/S}. \quad (117)$$

For $a > 0$ we could not find a closed expression; however, the integral (115) is easily evaluated numerically. Some example curves are shown in Fig. 7 in the limit of small w_0 . Observe that especially for large values of a , the additional time scale introduced by the eddy-current relaxation is clearly visible. Overall the shape stretches longer in time, and becomes nonmonotonous, as a is increased.

1. Tail of the shape function

The behavior of the avalanche shape for long times can also be understood analytically from Eq. (115). For simplicity, we consider the case $w_0 = 0$ in the following. For large t , the integral is dominated by its saddle point. Since we have $e^{\frac{2at}{r}} \gg e^{-\frac{r}{2\tau}}$ for all times, the dominant exponential factor is

$$e^{H(r)} := \exp \left(\frac{S(r+2)^2(r-2a\tau)^2}{16r^2\tau^2} - \frac{S}{4} - \frac{t}{\tau} + \frac{2at}{r} \right).$$

Its maximum for large t is obtained by solving $H'(r) = 0$,

$$r_m \approx 2\sqrt[3]{\frac{2at\tau^2}{S}} + \frac{2}{3}(a\tau - 1) + O(t)^{-1/3}.$$

Determining the location of the saddle point to higher order in t is more complicated. The terms of $O(t)^{-1/3}$ depend on whether the subexponential terms in (115) are included in the maximization procedure. However, to the order given here, r_m is independent of such choices.

Since the integral (115) does not depend on r_0 as discussed above, we can choose $r_0 = r_m$. Setting $r = u + iv$, we have $\partial_v^2 H(r) = -\partial_u^2 H(r)$ due to the Cauchy-Riemann equations. Thus, we can approximate the integral (115) for large t and

fixed S by

$$\begin{aligned} \mathfrak{s}(t, S) &\approx \sqrt{\frac{2\pi}{H''(r_m)}} \frac{(r_m - 2a\tau)(r_m + 2)a e^{H(r_m)}}{4\pi\tau r_m^3 P(S)} \\ &\approx \exp \left[-\frac{t}{\tau} + \frac{3}{2} \left(\frac{at}{\tau} \right)^{2/3} \left(\frac{S}{2} \right)^{1/3} \right. \\ &\quad \left. + \left(\frac{at}{\tau} \right)^{1/3} \frac{1 - a\tau}{\tau} \left(\frac{S}{2} \right)^{2/3} \right. \\ &\quad \left. + \frac{S(a^2\tau^2 - 5a\tau + 1)}{6\tau^2} + O(t)^{-1/3} \right] \\ &\quad \times \left[\frac{S^{4/3} a^{2/3}}{\sqrt{3}(2t)^{1/3} \tau^{2/3}} + O(t)^{-2/3} \right]. \end{aligned} \quad (118)$$

Again, note that to this order both the exponent and the prefactor are independent of whether the subexponential terms are included in the maximization. In particular, the term of order $O(t)^0$ in the exponent is independent of the term of order $O(t)^{-1/3}$ in r_m . We thus see that the Gaussian tail of the shape in the standard ABBM model is replaced by an exponential tail, decaying on a time scale τ . This is confirmed by numerical Laplace inversion of Eq. (115); see Fig. 8. We also observe good agreement between the asymptotic expansion and the numerical result.

Using a similar method one can try to determine the tail of $\mathfrak{s}(t, S)$ for fixed t at large S . In this limit, the maximum obtained by solving $H'(r) = 0$ is

$$r_m \approx 2a\tau + O(S)^{-1}.$$

One finds

$$H(r_m) = -\frac{S}{4} + O(S)^{-1}, \quad H''(r_m) = \frac{(1 + a\tau)^2}{8a^2\tau^4} S + O(S)^0.$$

Noting that $P(S) \sim e^{-S/4}$, this means that the exponential factor in the saddle-point contribution to $\mathfrak{s}(t, S) \sim e^{H(r_m)}/P(S)$ vanishes to leading order. This indicates that $\mathfrak{s}(t, S)$ will scale

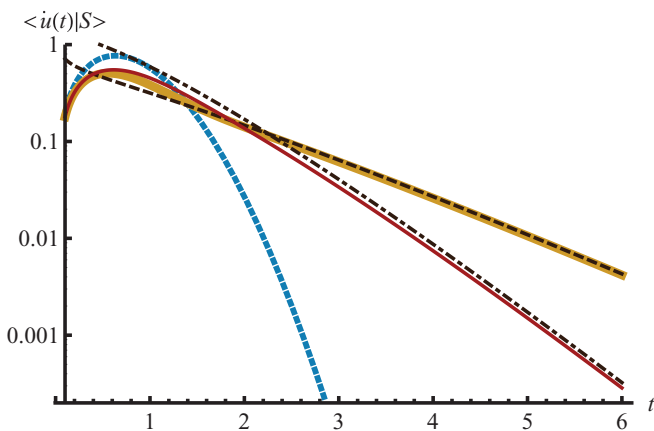


FIG. 8. (Color online) Tail of the avalanche shape at fixed size $S = 0.8$. Blue dotted line: Gaussian ABBM tail (116). Red (thin) and yellow (thick) lines: numerical Laplace inversion of (115) for $\tau = 0.7$ and $\tau = 0.4$, respectively. Black dot-dashed and dashed lines: Asymptotics (118) for the corresponding values. $a = 1$ in all cases.

as a power law for fixed t at large S . However, since the pre-exponential factors in (115) also vanish at $r_m = 2a\tau$, obtaining a quantitative result requires a more controlled approximation.

VIII. SUBAVALANCHE STATISTICS

As we saw in Sec. VD, an avalanche in the ABBM model with exponential retardation never strictly terminates, even after the driving has stopped. It thus is interesting to explore the “sub”-avalanches, or *aftershocks*, inside an avalanche, and their durations T_i , $i = 1, \dots$. T_i is defined as the time it takes \dot{u} to start from $\dot{u} = 0$ at time $t_{i-1} = \sum_{j=1}^{i-1} T_j$ and go to positive values $\dot{u} > 0$ and back to $\dot{u} = 0$ at time $t_i = \sum_{j=1}^i T_j$ without touching $\dot{u} = 0$ in the interval $0]t_{i-1}, t_i[$. In other words, it is the separation in time between successive passages of \dot{u} at zero. The same question can be asked for avalanches at nonzero driving velocity $v > 0$ in the standard ABBM model, which can also be seen as subavalanches of an infinite avalanche (there, too, \dot{u} never vanishes on a finite time interval).¹¹ We will obtain detailed results in that case.

A convenient setting to study this problem is the Fokker-Planck approach, introducing an *artificial* absorbing boundary at $\dot{u} = 0$. It can be implemented in the case of the simple exponential relaxation (8) which reduces to two coupled Langevin equations for \dot{u} and h (11). We will discover that, with such an absorbing boundary, Eqs. (17) and (26) for the generating functional of domain-wall velocities, as well as some details of the instanton method, need to be modified.

A. Subavalanches in the standard ABBM model at finite driving velocity

In order to present our approach on a simple example, let us consider, first, the standard ABBM model with monotonous, but otherwise arbitrary driving $\dot{w}(t) \geq 0$. The equation of motion (19) with $a = 0$ is, due to its Markovian nature, completely characterized by the *propagator*

$$\mathcal{P}(\dot{u}_f; t_f | \dot{u}_i; t_i) := E[\delta(\dot{u}_{t_f} - \dot{u}_f) | \dot{u}_{t_i} = \dot{u}_i]. \quad (119)$$

Here E means “expectation”, i.e. the average over the disorder. As a function of the final velocity \dot{u}_f , $P_t(\dot{u}) = \mathcal{P}(\dot{u}_f = \dot{u}; t_f = t | \dot{u}_i; t_i)$ satisfies the forward Fokker-Planck equation

$$\partial_t P_t(\dot{u}) = \partial_{\dot{u}}^2 \dot{u} P_t(\dot{u}) + \partial_{\dot{u}}(\dot{u} - \dot{w}_t) P_t(\dot{u}) = \partial_{\dot{u}} J_t(\dot{u}), \quad (120)$$

where

$$J_t(\dot{u}) := \partial_{\dot{u}} \dot{u} P_t(\dot{u}) + (\dot{u} - \dot{w}_t) P_t(\dot{u}) \quad (121)$$

is (minus) the probability current. As a function of the initial condition \dot{u}_i , $Q_t(\dot{u}) = \mathcal{P}(\dot{u}_f; t_f | \dot{u}_i = \dot{u}; t_i = t)$ satisfies the backward Fokker-Planck equation

$$\begin{aligned} -\partial_t Q_t(\dot{u}) &= \dot{u} \partial_{\dot{u}}^2 Q_t(\dot{u}) - (\dot{u} - \dot{w}_t) \partial_{\dot{u}} Q_t(\dot{u}) \\ &= \partial_{\dot{u}}^2 \dot{u} Q_t(\dot{u}) + \partial_{\dot{u}}(\dot{w}_t - 2 - \dot{u}) Q_t(\dot{u}) + Q_t(\dot{u}). \end{aligned} \quad (122)$$

¹¹In the context of the standard ABBM models, these subavalanches are also called pulses [57].

The propagator also satisfies the initial condition

$$\mathcal{P}(\dot{u}_f; t_f | \dot{u}_i; t_i) = \mathcal{P}(\dot{u}_f; t_f | \dot{u}_i; t_f) = \delta(\dot{u}_f - \dot{u}_i). \quad (123)$$

In order to obtain the solution of the forward or backward FPEs, one needs to complement them with a boundary condition at $\dot{u} = 0$. We consider two cases:

(i) Propagator with *reflecting boundary* $\mathcal{P}_{\text{refl}}$. This is the case we studied so far in this article and in Ref. [46]. It is defined by a *vanishing probability current*: $J_t(\dot{u} = 0^+) = 0$ or

$$\lim_{\dot{u} \rightarrow 0} \partial_{\dot{u}} \dot{u} P_t(\dot{u}) + (\dot{u} - \dot{w}_t) P_t(\dot{u}) = 0. \quad (124)$$

Typically, this is satisfied by a power-law-like behavior $P(\dot{u}) \sim \dot{u}^{-1+\dot{w}_t}$ for $\dot{u} \rightarrow 0$ (see the examples in Refs. [20,24,46]).

(ii) Propagator with *absorbing boundary* \mathcal{P}_{abs} . This is the relevant case for subavalanches. The problem is characterized by a *vanishing propagator*, when starting from $\dot{u} = 0^+$, i.e., $Q_t(\dot{u} = 0^+) = 0$. This implies (except for pathological cases) that the “current” for the backwards FPE vanishes,

$$\lim_{\dot{u} \rightarrow 0} \partial_{\dot{u}} \dot{u} Q_t(\dot{u}) + (\dot{w}_t - 2 - \dot{u}) Q_t(\dot{u}) = 0. \quad (125)$$

On the other hand, for the forward Fokker-Planck equation, $P_t(\dot{u} = 0^+) = \mathcal{P}_{\text{refl}}(\dot{u}_f = 0^+, t_f = t | \dot{u}_i; t_i)$ will typically be a nonvanishing, nontrivial function of time, and the current J_t will not vanish (as expected from physical intuition, since trajectories touching $\dot{u} = 0$ are “absorbed”). This is why treating the absorbing boundary using the forward Fokker-Planck equation is inconvenient; instead, the backward equation is natural here.¹²

Let us now define Laplace transforms with respect to the final velocity for \hat{P} and with respect to the initial velocity for \hat{Q} ,

$$\hat{P}_t(\lambda | \dot{u}_i, t_i) := \int_0^\infty d\dot{u}_f e^{\lambda \dot{u}_f} \mathcal{P}(\dot{u}_f; t_f = t | \dot{u}_i; t_i), \quad (126)$$

$$\hat{Q}_t(\lambda | \dot{u}_f, t_f) := \int_0^\infty d\dot{u}_i e^{\lambda \dot{u}_i} \mathcal{P}(\dot{u}_f; t_f | \dot{u}_i; t_i = t). \quad (127)$$

Laplace-transforming the forward Fokker-Planck equation (120), with the reflecting boundary condition (124), we obtain a first-order PDE for $\hat{P}_t(\lambda)$,

$$\partial_t \hat{P}_t^{\text{refl}}(\lambda) = (\lambda^2 - \lambda) \partial_\lambda \hat{P}_t^{\text{refl}}(\lambda) + \dot{w}_t \lambda \hat{P}_t^{\text{refl}}(\lambda). \quad (128)$$

Note that while boundary terms would arise in general, the reflecting boundary condition (124) ensures that they vanish. Similarly, Laplace-transforming the backward Fokker-Planck equation (122) with the absorbing boundary condition (125), we obtain a first-order PDE for $\hat{Q}_t(\lambda)$,

$$-\partial_t \hat{Q}_t^{\text{abs}}(\lambda) = (\lambda^2 + \lambda) \partial_\lambda \hat{Q}_t^{\text{abs}}(\lambda) + [(2 - \dot{w}_t) \lambda + 1] \hat{Q}_t^{\text{abs}}(\lambda). \quad (129)$$

¹²Similarly, for the reflecting boundary, $Q_t(\dot{u} = 0^+) = \mathcal{P}_{\text{refl}}(\dot{u}_f, t_f | \dot{u}_i = 0^+; t_i = t)$ will typically be a nonvanishing, nontrivial function of time. So, for the reflecting boundary, the backward equation is inconvenient and the forward equation is natural. For the absorbing boundary it is the other way around. This peculiar behavior is due to the nature of the ABBM noise term, which vanishes for $\dot{u} = 0$. For a standard Brownian motion, the absorbing boundary can be treated equally well using the forward or the backward Fokker-Planck equation: There we have $\mathcal{P}_{\text{abs}}(\dot{u}_f = 0) = \mathcal{P}_{\text{abs}}(\dot{u}_i = 0) = 0$.

Again, vanishing of boundary terms for the Laplace transformation is ensured by the absorbing boundary condition (125). On the other hand, the Laplace-transformed equations for \hat{P}_t^{abs} and \hat{Q}_t^{refl} are more complicated: There, the boundary terms at $\dot{u} = 0$ do not vanish and are undetermined functions of time. Thus, in the following, we will always use the propagator in terms of the final condition P or its Laplace-transform \hat{P} when discussing a reflecting boundary and the propagator in terms of the initial condition Q or its Laplace-transform \hat{Q} when discussing an absorbing boundary.

Now Eqs. (128) and (129) can be solved using the method of characteristics. In the forward (reflecting boundary) case this method was shown to provide a general connection between the Fokker-Planck approach to the ABBM model and the dynamical path integral (instanton equation) approach [18,49]. In the following we take a first step towards generalizing this to the case of an absorbing boundary. The solution of (129) is

$$\hat{Q}_t(\hat{u}(t_i)) = e^{\int_{t_i}^{t_f} [(2 - \dot{w}_s) \hat{u}_s + 1] ds} \hat{Q}_{t_f}(\hat{u}(t_f)), \quad (130)$$

where \hat{u} satisfies the backward instanton equation

$$-\partial_t \hat{u}_t + \hat{u}_t + \hat{u}_t^2 = 0, \quad (131)$$

with the boundary condition $\hat{u}(t_i) = \lambda$.¹³

The initial condition (123) for the propagator gives $\hat{Q}_{t_f}(\lambda_f) = e^{\lambda_f \dot{u}_f}$. Inserting this into (130), we obtain

$$\int_0^\infty d\dot{u}_i e^{\lambda \dot{u}_i} \mathcal{P}_{\text{abs}}(\dot{u}_f; t_f | \dot{u}_i; t_i) = \hat{Q}_{t_i}(\lambda) = \exp \left\{ \int_{t_i}^{t_f} [(2 - \dot{w}_s) \hat{u}_s + 1] ds + \dot{u}_f \hat{u}_f \right\}. \quad (132)$$

It is useful to recall that the fact that this solves the problem with an *absorbing boundary* is an indirect consequence of our chain of arguments: It stems from the fact that we use the backward instanton equation (131) which encodes the solution (via the method of characteristics) of the Laplace-transformed backward FPE, which itself contains *no boundary term* precisely in the case of an absorbing boundary. For the case of a reflecting boundary, the analogous formula is

$$\int_0^\infty d\dot{u}_f e^{\lambda \dot{u}_f} \mathcal{P}_{\text{refl}}(\dot{u}_f; t_f | \dot{u}_i; t_i) = \hat{P}_t(\lambda) = \exp \left[\int_{t_i}^{t_f} \dot{w}_s \tilde{u}(s) ds + \dot{u}_i \tilde{u}(t_i) \right]. \quad (133)$$

As discussed in Ref. [49], this is equivalent to solving (19) as above using the MSR field theory and the instanton equations. For details, see Ref. [49], Sec. V C, and, in the present article, Sec. VIII D, where we discuss this in general for the ABBM model with retardation.

1. Propagator at constant driving

Let us now apply (132) in order to determine the propagator of the standard ABBM model with an absorbing boundary, at a constant driving velocity $0 < v < 1$.

¹³Note that this equation is causal—solved by increasing the time—in contrast to the forward instanton.

The solution of Eq. (131) is

$$\hat{u}(t) = \frac{\lambda \theta(t - t_i)}{e^{t-t_i}(\lambda + 1) - \lambda}. \quad (134)$$

Inserting this into (132), we obtain the Laplace transform (with respect to the initial condition) of the propagator with an absorbing boundary, at a constant driving velocity v ,

$$\begin{aligned} & \int d\dot{u}_i e^{\lambda \dot{u}_i} \mathcal{P}_{\text{abs}}(\dot{u}_f; t_f | \dot{u}_i; t_i) \\ &= \hat{Q}_t(\lambda) = \exp \left[\int_{t_i}^{t_f} [(2-v)\hat{u}(t) + 1] dt + \hat{u}(t_f)\dot{u}_f \right] \\ &= \exp \left[(2-v) \int_{t_i}^{t_f} \hat{u}(t) dt + (t_f - t_i) + \hat{u}(t_f)\dot{u}_f \right] \\ &= \exp \left[\frac{\lambda e^{t_f-t_i} \dot{u}_f}{1 - \lambda(e^{t_f-t_i} - 1)} + t_f - t_i \right] [1 - \lambda(e^{t_f-t_i} - 1)]^{v-2}. \end{aligned} \quad (135)$$

Inverting the Laplace transform from λ to \dot{u}_i yields the propagator of the ABBM model with an absorbing boundary at $\dot{u} = 0$,

$$\begin{aligned} & \mathcal{P}_{\text{abs}}(\dot{u}_f; t_f | \dot{u}_i; 0) \\ &= \exp \left(\frac{v}{2} t_f - \frac{\dot{u}_f e^{t_f} + \dot{u}_i}{e^{t_f} - 1} \right) \frac{(\dot{u}_f/\dot{u}_i)^{\frac{v-1}{2}}}{2 \sinh \frac{t_f}{2}} I_{1-v} \left(\frac{\sqrt{\dot{u}_f \dot{u}_i}}{\sinh \frac{t_f}{2}} \right). \end{aligned} \quad (136)$$

Here we set $t_i = 0$ for simplicity since the result depends only on $t_f - t_i$.

Our result is identical to Eq. (37) in the recent calculation [58], there obtained using completely different methods (decomposition in eigenfunctions of the Fokker-Planck operator). The advantage of our approach is that it makes the connection to field theory clearer and that it is easily generalizable to situations with a nonconstant driving velocity (where the eigenfunction method is not applicable).

It is straightforward to check explicitly that (136) satisfies the backward FPE (122). Near $\dot{u}_i = 0$ we have $\mathcal{P}_{\text{abs}}(\dot{u}_f; t_f | \dot{u}_i; 0) \sim \dot{u}_i^{1-v}$. For $0 \leq v \leq 1$, it satisfies the absorbing boundary condition $\mathcal{P}_{\text{abs}}(\dot{u}_f; t_f | \dot{u}_i = 0; t_i) = 0$ and (125). On the other hand, near $\dot{u}_f = 0$, \mathcal{P}_{abs} is a nonvanishing constant, so the ‘‘forward’’ current (121) does not vanish. For velocities $v > 1$, our assumption on the absorbing boundary condition, $\mathcal{P}_{\text{abs}}(\dot{u}_f; t_f | \dot{u}_i = 0; t_i) = 0$ and (125), seems to break down. In fact, the absorbing boundary becomes equal to the reflecting one since $\dot{u} = 0$ is unreachable.¹⁴

2. Subavalanche durations in the standard ABBM model

Another simple example is the ‘‘survival probability,’’ i.e., the probability never to touch the absorbing boundary $\dot{u} = 0$ until time t_f , starting at some initial \dot{u}_i at time t_i ,

$$P_{\text{surv}}(t_f | \dot{u}_i; t_i) := \int d\dot{u}_f \mathcal{P}_{\text{abs}}(\dot{u}_f; t_f | \dot{u}_i; t_i).$$

¹⁴In fact, for $v > 1$, one can still formally define avalanche-size distributions conditioned to \dot{u} being close to 0 instead of precisely 0 as for $0 \leq v < 1$; see the appendix in Ref. [45].

Its leading behavior as $\dot{u}_i \rightarrow 0$ corresponds to the probability of an avalanche duration $T > t_f - t_i$.

It can be obtained using (130) as in the previous section but with the initial condition

$$\hat{Q}_t(\lambda_f) = \int_0^\infty d\dot{u} e^{\lambda_f \dot{u}} = -\frac{1}{\lambda_f} \quad (137)$$

for $\lambda_f < 0$.

As above, inserting the solution (134) for $\hat{u}(t)$, we obtain for the survival probability at time t_f

$$\begin{aligned} & \int d\dot{u}_i e^{\lambda \dot{u}_i} P_{\text{surv}}(t_f | \dot{u}_i; t_i) \\ &= \exp \left\{ \int_{t_i}^{t_f} [(2-v_s)\dot{u}_s + 1] ds \right\} \left[-\frac{1}{\hat{u}(t_f)} \right] \\ &= -[1 + \lambda - \lambda e^{t_f-t_i}]^{v-2} \frac{(\lambda + 1) - \lambda e^{t_f-t_i}}{\lambda} \\ &= -\frac{[1 + \lambda - \lambda e^{t_f-t_i}]^{v-1}}{\lambda}. \end{aligned} \quad (138)$$

This is, of course, identical to the integral of (135) over \dot{u}_f . Inverting the Laplace transform, we obtain the survival probability at time $t_f > t_i$ when starting from \dot{u}_i at t_i . It is a function of $t_f - t_i$ only. For $v < 1$ it reads

$$P_{\text{surv}}(t_f - t_i | \dot{u}_i) = 1 - \frac{\Gamma(1-v, \frac{\dot{u}_i}{e^{t_f-t_i}-1})}{\Gamma(1-v)}. \quad (139)$$

It increases from 0 to 1 as \dot{u} increases from 0 to ∞ , while for $v \geq 1$ it is equal to unity for all $\dot{u} > 0$, i.e., there are no zeros of the velocity. Note that this result was obtained independently in Refs. [58,59] by completely different methods. It can also be obtained by integrating the propagator (136) over \dot{u}_f from 0 to ∞ .

The case $v < 1$ is considered from now on. Taking a derivative with respect to the final time gives the probability density of first-passage times T_0 for \dot{u} to become zero, given an initial velocity \dot{u}_i ,

$$P_{\text{first}}(T_0 | \dot{u}_i) = \frac{\dot{u}_i^{1-v}}{\Gamma(1-v)(e^{T_0} - 1)^{2-v}} e^{-\frac{\dot{u}_i}{e^{T_0}-1} + T_0}. \quad (140)$$

Since an avalanche always starts at $\dot{u} = 0^+$, we can extract from the leading term in small \dot{u}_i a density of durations T_0 ,

$$v \rho_{\text{duration}}(T_0) = e^{T_0} (1-v)(e^{T_0} - 1)^{v-2} \frac{\sin(\pi v)}{\pi}. \quad (141)$$

In the limit $v \rightarrow 0$, density means units of $1/u \equiv 1/w$. Since $\rho_{\text{duration}}(T_0)$ diverges like $1/T_0^{v-2}$, hence is not normalizable for $v < 1$, we have chosen to normalize it as $\langle v T_0 \rangle_\rho = 1$. Note that ρ has a finite limit at $v = 0^+$ which agrees with the avalanche-duration density obtained in Ref. [25].

The probability density for an avalanche to continue a time T_0 beyond an arbitrary chosen time t_i is obtained by integrating over the distribution of \dot{u}_0 in the stationary state $P_{\text{stat}}(\dot{u}_0) = \dot{u}_0^{-1+v} \frac{e^{-\dot{u}_0}}{\Gamma(v)}$,

$$\begin{aligned} P_{\text{beyond}}(T_0) &= \int_0^\infty d\dot{u}_i P_{\text{stat}}(\dot{u}_i) P_{\text{first}}(T_0 | \dot{u}_i) \\ &= (e^{T_0} - 1)^{v-1} \frac{\sin(\pi v)}{\pi}. \end{aligned} \quad (142)$$

Note that this is a bona-fide probability distribution (normalized to unity).

Finally, we obtain again the density of avalanche durations by taking a derivative,

$$\begin{aligned} v\rho(T) &= -\partial_{T_0}|_{T=T_0} P_{\text{beyond}}(T) \\ &= \frac{e^T}{(e^T - 1)^{2-v}} (1-v) \frac{\sin(\pi v)}{\pi}. \end{aligned} \quad (143)$$

This density can be interpreted as a probability $v\rho(T) \equiv P(T)$ in the following sense: Take a random time $t = 0$. The velocity \dot{u}_0 is positive with probability 1. Thus, there is a first-passage time $-t_1$ at zero velocity on the left of $t = 0$ and a first-passage time $+t_2$ at zero velocity on the right of $t = 0$. The duration $T = t_2 - (-t_1) = t_2 + t_1$ is the distance between the two. It thus is normalized not by $\int_0^\infty P(T)dT = 1$ but rather by

$$\int_0^\infty dt_1 \int_0^\infty dt_2 P(T = t_2 + t_1) = 1.$$

In terms of units, $P(T)$ is not a probability density (which would give a dimensionless number when multiplied by a time interval dT) but a “double”-probability density which gives a dimensionless number when multiplied by *two* time intervals dt_1, dt_2 . In other words, $\int T P(T)dT = 1$ since the probability that a randomly chosen time belongs to an avalanche is proportional to its duration T .

Note that for $v \rightarrow 0$ Eq. (143) reduces to the result known from Refs. [24,25,46]. The velocity-dependent power law for small T , $P(T) \propto T^{-2+v}$, was already predicted in Ref. [24]. A similar result for the distribution of avalanche sizes at finite velocity in the standard ABBM model is discussed in Appendix E.

B. Fokker-Planck equations and propagator including retardation

Now let us go back to the more general ABBM model with retardation.

The equations of motion (23) are equivalent to a Fokker-Planck equation¹⁵ generalizing (144) for the joint probability distribution $P(\dot{u}, h)$,

$$\begin{aligned} \partial_t P_t(\dot{u}, h) &= \partial_{\dot{u}}^2 \dot{u} P_t(\dot{u}, h) + \partial_{\dot{u}}(\dot{u} - \dot{w}_t + a\dot{u} - ah) P_t(\dot{u}, h) \\ &\quad + \tau^{-1} \partial_h(h - \dot{u}) P_t(\dot{u}, h). \end{aligned} \quad (144)$$

¹⁵To derive the forward Fokker-Planck equation (144), we set

$$P_t(\dot{u}, h) = \langle \delta(\dot{u} - \dot{u}_t) \delta(h - h_t) \rangle.$$

Then we apply Itô calculus to

$$P_{t+dt}(\dot{u}, h) = \langle \delta(\dot{u} - [\dot{u}_t + d\dot{u}_t]) \delta(h - [h_t + dh_t]) \rangle,$$

with

$$\begin{aligned} d\dot{u}_t &= \sqrt{\dot{u}_t} dB_t + [(\dot{w}_t - \dot{u}_t) - a\dot{u}_t + ah_t] dt, \\ \tau dh_t &= [\dot{u}_t - h_t] dt \\ \langle dB_t dB_{t'} \rangle &= 2\delta(t - t') dt. \end{aligned}$$

For the backward equation (145), apply Itô calculus to

$$Q_{t+dt}(\dot{u}_{t+dt}, h_{t+dt}) = Q_t(\dot{u}_t, h_t).$$

As discussed in Ref. [49], this forward Fokker-Planck equation provides an alternative derivation for the generating function (26). The instanton equations (24) and (25) are equivalent to the equations for the characteristics of the linear PDE (144), see Ref. [49], Sec. VC, for details. The transformation between the “real space” \dot{u}, h and the “Laplace space” \tilde{u}, \tilde{h} of the characteristics, i.e., instantons is a very useful tool whenever boundary terms are absent. This is the case for a zero probability current at $\dot{u} = 0$, i.e., for a reflecting boundary condition.

To study the case of an absorbing boundary, as noted above for the pure ABBM model, it is useful to consider the flow of the probability density as a function of the initial condition \dot{u}, h at time $t_i = t$, which satisfies the *backward* Fokker-Planck equation¹⁵ [60]

$$\begin{aligned} -\partial_t Q_t(\dot{u}, h) &= \dot{u} \partial_{\dot{u}}^2 Q_t(\dot{u}, h) - (\dot{u} - \dot{w}_t + a\dot{u} - ah) \partial_{\dot{u}} Q_t(\dot{u}, h) \\ &\quad - \tau^{-1} (h - \dot{u}) \partial_h Q_t(\dot{u}, h) \\ &= \partial_{\dot{u}}^2 \dot{u} Q_t(\dot{u}, h) - \partial_{\dot{u}}(\dot{u} + 2 - \dot{w}_t + a\dot{u} - ah) Q_t(\dot{u}, h) \\ &\quad - \tau^{-1} \partial_h (h - \dot{u}) Q_t(\dot{u}, h) + (1 + a + \tau^{-1}) Q_t(\dot{u}, h). \end{aligned}$$

Both (144) and (145) are linear in the probability density P or Q . Hence, they are completely characterized by the Green function or *propagator* $\mathcal{P}(\dot{u}_f, h_f; t | \dot{u}_i, h_i, 0)$, the probability to go from \dot{u}_i, h_i at t_i to \dot{u}_f, h_f at $t_f > t_i$. It satisfies (144) as a function of $t = t_f, \dot{u} = \dot{u}_f, h = h_f$ and (145) as a function of $t = t_f, \dot{u} = \dot{u}_i, h = h_i$; it has the initial condition $\mathcal{P}(\dot{u}_f, h_f; t_i | \dot{u}_i, h_i, t_i) = \delta(\dot{u}_f - \dot{u}_i) \delta(h_f - h_i)$.

C. Monotonicity, domains of definition, and boundaries

It is important to note that \dot{u} and h satisfy together a monotonicity property: If $\dot{w} \geq 0$ and both $\dot{u}(t=0) \geq 0$ and $h(t=0) \geq 0$, then they remain so at all times. Although the quadrant $\dot{u} \geq 0, h \geq 0$ is the more physical one, as we see below it is convenient to solve the FP equations in the half-space $\dot{u} \geq 0$ and then at the end restrict to the quadrant $h \geq 0$. The reason for this is simple: No matter whether we impose an absorbing or a reflecting boundary at $\dot{u} = 0$, one has a finite probability of reaching $\dot{u}_f > 0, h_f > 0$ starting from $\dot{u}_i > 0, h_i < 0$. So, as a function of the initial value h_i , $\mathcal{P}(\dot{u}_f, h_f; t_i | \dot{u}_i, h_i, t_i)$ is smooth around $h_i = 0$, and has a finite value there. Its natural boundary is at $h_i \rightarrow -\infty$, where $\mathcal{P} \rightarrow 0$. Thus, when considering the backward equation, we will work on the half-space $\dot{u}_i \geq 0, h_i \in \mathbb{R}$ in the following in order to avoid undetermined boundary terms.

Due to the aforementioned monotonicity property, we know that the restriction to $h_i > 0$ of the half-space propagator obtained in this way will actually be equal to the propagator restricted to the physical quadrant from the beginning.

By taking linear functionals of the propagator, one obtains other observables. We give a few examples:

(i) Starting not from a fixed point, but from a distribution of initial values $P_i(\dot{u}_i, h_i)$, the probability density of final values

$$P_t(\dot{u}, h) = \int_0^\infty d\dot{u}_i \int_{-\infty}^\infty dh_i P_i(\dot{u}_i, h_i) \mathcal{P}(\dot{u}, h; t | \dot{u}_i, h_i; t_i) \quad (146)$$

still satisfies the forward FPE (144). The initial condition is, naturally, $P_{t_i} = P_i$.

(ii) One may be interested not in the probability density of the final point at \dot{u}_f, h_f (given by the propagator), but the actual probability to land in a domain D , starting from an arbitrary initial condition \dot{u}, h . This is given by

$$Q_t(\dot{u}, h) = \int_0^\infty d\dot{u}_f \int_{-\infty}^\infty dh_f Q_i(\dot{u}_f, h_f) \mathcal{P}(\dot{u}_f, h_f; t | \dot{u}, h; t_i), \quad (147)$$

where $Q_i(\dot{u}_f, h_f) = \mathbb{1}_D$ is 1 inside D and 0 outside. $Q_t(\dot{u}, h)$ satisfies the backward FPE (145), with the initial condition $Q_{t_i} = Q_i = \mathbb{1}_D$. This can be used to determine the distribution of avalanche durations, starting from an initial value $\dot{u}_i > 0, h_i$. Choosing D to be the set $\{\dot{u}_f > 0\}$, one obtains the probability to have any positive domain-wall velocity at t_f , i.e., the probability not to have touched the boundary $\dot{u} = 0$ between t_i and t_f .

As mentioned above, our instanton solution (26) is equivalent to the forward propagator $\mathcal{P}(\dot{u}_f, h_f; t_f | \dot{u}_i, h_i, t_i)$ from a given initial condition $\dot{u}_i = 0, h_i = 0$ to some final point $\dot{u}_f > 0, h_f > 0$, with a *reflecting* boundary at $\dot{u} = 0$ (the boundary at $h = 0$ is unreachable when propagating forward). Imposing an *absorbing* boundary at $\dot{u} = 0$, as required for analyzing subavalanche durations, is less trivial. In contrast to the case of, e.g., a standard Brownian motion, the probability current at the final point $\dot{u}_f = 0$ vanishes as soon as one sets $\mathcal{P}_{\text{abs}}(\dot{u}_f = 0, h_f; t | \dot{u}_i, h_i; t_i) = 0$. The correct propagator with an absorbing boundary should, thus, have $\mathcal{P}_{\text{abs}}(\dot{u}_f = 0, h_f; t | \dot{u}_i, h_i; t_i) > 0$, an undetermined function of time, as confirmed by the explicit calculation in Sec. VIII A1 (see also the discussion in Appendix D of Ref. [18]). Hence, obtaining it from the forward FPE (144) is not easy. However, in terms of the initial condition, as motivated for the pure ABBM model above, we expect $\mathcal{P}_{\text{abs}}(\dot{u}_f, h_f; t | \dot{u}_i = 0, h_i, t_i) = 0$. The backward FPE (145) then is easy to analyze using Laplace transforms, since the boundary term $Q(\dot{u} = 0, h_i)$ vanishes.

D. Characteristics and instantons

To solve the backward FPE, we define the Laplace transform \hat{Q} via

$$\hat{Q}_t(\lambda, \mu) := \int_0^\infty d\dot{u} \int_{-\infty}^\infty dh e^{\lambda\dot{u} + \mu h} Q_t(\dot{u}, h). \quad (148)$$

Equation (145) then gives

$$\begin{aligned} -\partial_t \hat{Q}_t(\lambda, \mu) &= [\lambda^2 + (1+a)\lambda - \tau^{-1}\mu] \partial_\lambda \hat{Q}_t(\lambda, \mu) \\ &\quad \times [-a\lambda + \tau^{-1}\mu] \partial_\mu \hat{Q}_t(\lambda, \mu) \\ &\quad + [(2 - \dot{w}_t)\lambda + (1+a + \tau^{-1})] \hat{Q}_t(\lambda, \mu). \end{aligned} \quad (149)$$

Note that to obtain this equation (with vanishing boundary terms) we used $Q_t(\dot{u} = 0, h) = 0$, and the fact that the noise vanishes at $\dot{u} = 0$ (which is a special property of the ABBM model).¹⁶

¹⁶Equation (149) is valid for the Laplace transform (LT) (148) defined on the half-space $\dot{u} \geq 0, h \in \mathbb{R}$. If one wishes to define the LT on the

We now define the characteristics \tilde{u}, \hat{h} via the *backward* instanton equations

$$-\partial_t \tilde{u}(t) + (1+a)\tilde{u}(t) + \tilde{u}(t)^2 - \hat{h}(t) = 0, \quad (150)$$

$$-\tau \partial_t \hat{h}(t) + \hat{h}(t) - a\tilde{u}(t) = 0, \quad (151)$$

$$-\partial_t \hat{q}(t) = [(2 - \dot{w}_t)\tilde{u}(t) + (1+a + \tau^{-1})] \hat{q}(t). \quad (152)$$

The boundary conditions are $\tilde{u}(t_i) = \lambda, \hat{h}(t_i) = \mu/\tau, \hat{q}(t_i) = \hat{Q}_{t_i}(\lambda, \mu)$. Note that the first two equations are identical to the standard instanton equations (24) and (25). The equation for $\hat{Q}(\lambda, \mu)$ along a characteristic simplifies to

$$\begin{aligned} -\frac{d}{dt} \hat{Q}_t(\tilde{u}(t), \tau \hat{h}(t)) \\ = [(2 - \dot{w}_t)\tilde{u}(t) + (1+a + \tau^{-1})] \hat{Q}_t(\tilde{u}(t), \tau \hat{h}(t)). \end{aligned} \quad (153)$$

Its solution is

$$\begin{aligned} \hat{Q}_{t_i}(\tilde{u}(t_i), \tau \hat{h}(t_i)) \\ = \exp \left\{ \int_{t_i}^{t_f} [(2 - \dot{w}_s)\tilde{u}(s) + (1+a + \tau^{-1})] ds \right\} \\ \times \hat{Q}_{t_f}(\tilde{u}(t_f), \tau \hat{h}(t_f)). \end{aligned} \quad (154)$$

The initial condition \hat{Q}_{t_f} depends on the observable we want to compute. For concreteness, let us think about the propagator \mathcal{P}_{abs} . There we have

$$\begin{aligned} Q_{t_f}(\dot{u}, h) &= \delta(\dot{u} - \dot{u}_f) \delta(h - h_f) \\ \Rightarrow \hat{Q}_{t_f}(\tilde{u}(t_f), \tau \hat{h}(t_f)) &= e^{\dot{u}_f \tilde{u}(t_f) + \tau h_f \hat{h}(t_f)}. \end{aligned} \quad (155)$$

The propagator \mathcal{P}_{abs} is given by inverting the Laplace transform

$$\begin{aligned} \int_0^\infty d\dot{u}_i \int_{-\infty}^\infty dh_i e^{\lambda\dot{u}_i + \mu h_i} \mathcal{P}_{\text{abs}}(\dot{u}_f, h_f; t_f | \dot{u}_i, h_i; t_i) \\ = \hat{Q}_{t_i}(\lambda, \mu) \\ = \exp \left\{ \int_{t_i}^{t_f} [(2 - \dot{w}_s)\tilde{u}(s) + (1+a + \tau^{-1})] ds \right. \\ \left. + \dot{u}_f \tilde{u}(t_f) + \tau h_f \hat{h}(t_f) \right\}. \end{aligned} \quad (156)$$

To summarize, one can say the following: The usual instanton equations (24) and (25) encode the solution of our model with a reflecting boundary at $\dot{u} = 0$. The backward instanton equations (150) and (151) encode the solution with an absorbing

physical quadrant $\dot{u} \geq 0, h \geq 0$, one cannot avoid a boundary term from $h = 0$, since $Q_t(\dot{u}, h = 0^+)$ does not vanish. Since there is no noise term in the evolution equation for h , the solution does not have to be continuous, and there is no contradiction to $Q_t(\dot{u}, h = 0) = 0$. One possibility to eliminate the boundary term is to add an extra diffusion term $\epsilon h \partial_h^2 Q_t$ on the right-hand side of (145), which leads to an additional term $\epsilon \mu^2 \partial_\mu \hat{Q}_t$ on the right-hand side of (149) and $\epsilon \hat{h}^2$ on the left-hand side of Eq. (151). Then Q_t vanishes at $h = 0$ and is continuous, and one can show that as $\epsilon \rightarrow 0$ it converges pointwise for any $h > 0$ to the (discontinuous) restriction to the quadrant of the presently considered solution in full space. We will, however, not need to further explore this method here but can work with h on the full real line.

boundary at $\dot{u} = 0$, assuming the absorbing boundary indeed satisfies $\mathcal{P}_{\text{abs}}(\dot{u}_f, h_f; t | \dot{u}_i = 0^+, h_i, t_i) = 0$.

It would be interesting to extend this approach to a general retardation kernel beyond the simple exponential. In that case, no local-in-time Fokker-Planck approach seems available. It is tempting to conjecture that the correct generalization of the backward instanton equation (150) is

$$-\partial_t \hat{u}_t + (1+a)\hat{u}_t + \hat{u}_t^2 + a \int_{-\infty}^t ds f'(t-s)\hat{u}_s = -\lambda_t, \quad (157)$$

corresponding to (18) after mapping $\tilde{u} \rightarrow -\hat{u}$. Note that (157) reduces to (150) and (151) for the exponential kernel (8) by setting

$$\hat{h}_t := \frac{a}{\tau} \int_{-\infty}^t e^{-(t-s)/\tau} \hat{u}_s ds, \quad (158)$$

as would be required.

E. Subavalanche durations with retardation

In order to compute subavalanche durations, we need to eliminate the h variable from (156). This is done by integrating over h_f and fixing a value of h_i .¹⁷ In Appendix F, we motivate the following generalization of (156) for this case,

$$\begin{aligned} & \int_{-\infty}^{\infty} dh_f \int_0^{\infty} d\dot{u}_i e^{\lambda \dot{u}_i} \mathcal{P}_{\text{abs}}(\dot{u}_f, h_f; t_f | \dot{u}_i, h_i; t_i) \\ &= \exp \left\{ \int_{t_i}^{t_f} [(2 - \dot{w}_s)\hat{u}_s + (1+a + \tau^{-1})] ds \right. \\ & \quad \left. + \dot{u}_f \hat{u}_{t_f} - \tau h_i \hat{h}_{t_i} \right\} \left[\partial_{\hat{h}(t_f)} \Big|_{\hat{h}(t_f)=0} \hat{h}(t_i) \right]. \end{aligned} \quad (159)$$

Now \hat{u} , \hat{h} are solutions of the backward instanton equations (150) and (151) with the boundary conditions

$$\hat{h}(t_f) = 0, \quad \hat{u}(t_i) = \lambda. \quad (160)$$

The effect of going from a fixed h_f to a fixed h_i is, thus, a change in boundary conditions for \hat{h} and the Jacobian factor in (159). To understand its importance, let us see how (159) reduces to the pure ABBM solution (132) in the case of $a = 0$. This is not trivial; for example, the exponential factors in (156), (159), and (132) differ markedly.

1. Recovering the pure ABBM model

For $a = 0$, we can solve Eq. (151) explicitly,

$$\hat{h}_f = \hat{h}_i e^{(t_f - t_i)/\tau}. \quad (161)$$

Thus, the Jacobian factor in (159) is

$$\partial_{\hat{h}(t_f)} \Big|_{\hat{h}(t_f)=0} \hat{h}(t_i) = e^{-(t_f - t_i)/\tau}.$$

¹⁷Or convoluting later with a normalized distribution of h_i . In any case, this is not the same as setting $\mu = 0$ in (156). The latter would be an integral over all h_i , which in general diverges. For example, in the pure ABBM model the subavalanche duration is independent of h_i .

Inserting this into (159) for $a = 0$ gives

$$\begin{aligned} & \int_{-\infty}^{\infty} dh_f \int_0^{\infty} d\dot{u}_i e^{\lambda \dot{u}_i} \mathcal{P}_{\text{abs}}(\dot{u}_f, h_f; t_f | \dot{u}_i, h_i; t_i) \\ &= \exp \left\{ \int_{t_i}^{t_f} [(2 - \dot{w}_s)\hat{u}_s + 1] ds + \dot{u}_f \hat{u}_{t_f} - \tau h_i \hat{h}_{t_i} \right\}, \end{aligned} \quad (162)$$

where now \hat{h} , \hat{u} are solutions of (150) and (151) with $a = 0$ and with the boundary conditions (160). Note that the Jacobian factor was necessary to cancel the term $(t_f - t_i)/\tau$ of the exponential. The solution (161) for \hat{h} with the boundary condition $\hat{h}_f = 0$ from (160) implies that $\hat{h}_t = 0$ for all t . Hence, (162) reduces to the pure ABBM solution (132), and the equation (150) for \hat{u} reduces to the pure ABBM instanton equation (131).

As expected, we obtain that in the limit $a = 0$

$$\int_{-\infty}^{\infty} dh_f \mathcal{P}_{\text{abs}}(\dot{u}_f, h_f; t_f | \dot{u}_i, h_i; t_i) = \mathcal{P}_{\text{abs}}(\dot{u}_f; t_f | \dot{u}_i; t_i)$$

is independent of h_i and reduces to the propagator of the standard ABBM model.

Now let us return to the more interesting case of the ABBM model with retardation. In the following section we will apply (159) to determine the correction to the duration distribution of the first subavalanche, for small a (weak relaxation) and $\tau = 1$. This is similar to the perturbation theory in a performed in Appendix C. We also attempted to analyze the backward instanton solution in the physically interesting limits of fast and slow relaxation, as done in Secs. V and VI for the forward (reflecting boundary) solution. However, we encountered technical difficulties and leave this for future work.

2. Weak-relaxation limit

Let us consider the solution of (150) and (151) with boundary condition

$$\hat{h}(t_f) = \mu, \quad \hat{u}(t_i) = \lambda. \quad (163)$$

We will be interested in the limit of small μ (required for computing the Jacobian factor in (159); the rest can be computed at $\mu = 0$). To this end we expand the instanton to order a, μ as

$$\begin{aligned} \hat{u}_t &= \hat{u}_t^{(00)} + \mu \hat{u}_t^{(10)} + a \hat{u}_t^{(01)} + O(a\mu, a^2, \mu^2) \\ \hat{h}_t &= \mu \hat{h}_t^{(10)} + a \hat{h}_t^{(01)} + a\mu \hat{h}_t^{(11)} + O(a^2, \mu^2). \end{aligned} \quad (164)$$

The correction of order a to P_{surv} , i.e., the cumulative distribution function for the avalanche durations, is obtained

from (159) as

$$\begin{aligned}
 \hat{P}_{\text{surv}}(\lambda, h_i) &:= \int_0^\infty d\dot{u}_i e^{\lambda \dot{u}_i} P_{\text{surv}}(t_f | \dot{u}_i, h_i; t_i) := \int_0^\infty d\dot{u}_i e^{\lambda \dot{u}_i} \int_0^\infty d\dot{u}_f \int_{-\infty}^\infty dh_f \mathcal{P}_{\text{abs}}(\dot{u}_f, h_f; t_f | \dot{u}_i, h_i; t_i) \\
 &= \exp \left\{ \int_{t_i}^{t_f} [(2 - \dot{w}_s) \hat{u}_s + (1 + a + \tau^{-1})] ds - \tau h_i \hat{h}_{t_i} \right\} \left[-\frac{1}{\hat{u}(t_f)} \right] [\partial_{\hat{h}(t_f)} |_{\hat{h}(t_f)=0} \hat{h}(t_i)] \\
 &= \exp \left\{ \int_{t_i}^{t_f} [(2 - \dot{w}_s) (\hat{u}_s^{(00)} + a \hat{u}_s^{(01)}) + (1 + a + \tau^{-1})] ds - a \tau h_i \hat{h}_{t_i}^{(01)} \right\} \left[-\frac{1}{\hat{u}^{(00)}(t_f) + a \hat{u}^{(01)}(t_f)} \right] [\hat{h}_{t_i}^{(10)} + a \hat{h}_{t_i}^{(11)}] \\
 &= \hat{P}_{\text{surv}}^{a=0}(\lambda) \left\{ 1 + a \left[\int_{t_i}^{t_f} [(2 - \dot{w}_s) \hat{u}_s^{(01)} + 1] ds - \frac{\hat{u}_{t_f}^{(01)}}{\hat{u}_{t_f}^{(00)}} + \frac{\hat{h}_{t_i}^{(11)}}{\hat{h}_{t_i}^{(10)}} \right] \right\} \exp[-a \tau \hat{h}_{t_i}^{(01)} h_i]. \tag{165}
 \end{aligned}$$

The pure ABBM result $\hat{P}_{\text{surv}}^{a=0}(\lambda)$ is given by (138). By time translation invariance, this expression only depends on $T := t_f - t_i$. In Appendix D we perform the perturbative calculation and determine explicitly the functions appearing in the expansion (164) for the case $\tau = 1$. In Fig. 15 we show the form of the resulting backward instantons, obtained from the perturbative expansion and a numerical solution. The case of general τ is more complicated and left for future research.

The survival probability P_{surv} is the probability of having a first-passage time to $\dot{u} = 0$ of $T \geq t_f - t_i$. The (normalized) probability distribution of first-passage times at $\dot{u} = 0$, starting from \dot{u}_i is, thus,

$$P_{\text{first}}(T | \dot{u}_i, h_i) = \partial_{t_f} |_{t_f=t_i+T} P_{\text{surv}}(t_f | \dot{u}_i, h_i; t_i). \tag{166}$$

By time-translation invariance, this is independent of t_i . For the pure ABBM model, we computed P_{first} in (140). The (unnormalized) density of avalanche durations $\rho(T)$ at a fixed value of h_i is the leading order of $P_{\text{first}}(\dot{u}_i, h_i)$ as $\dot{u}_i \rightarrow 0$, in our case,

$$\rho(T) := \lim_{\dot{u}_i \rightarrow 0} \dot{u}_i^{ah_i+v-1} P_{\text{first}}(T | \dot{u}_i, h_i).$$

We then can express $\rho(T)$ as the leading order of \hat{P}_{surv} , as $\lambda \rightarrow -\infty$,

$$\begin{aligned}
 \int_T^\infty \rho(T') dT' &= \lim_{\lambda \rightarrow -\infty} \hat{P}(\lambda, 0) (-\lambda)^{-2+v+ah_i} \\
 &= \frac{e^{-ah_i T}}{(e^T - 1)^{1-v-ah_i}} \left\{ 1 + a \frac{e^T [-2(v-1)\text{Li}_2(1-e^T) - (T^2+1)v + T^2 + T - 1] + (2-v)T + v + 1}{2(e^T - 1)} + \mathcal{O}(a^2) \right\}. \tag{167}
 \end{aligned}$$

This further simplifies for the case of a vanishing driving velocity, $v \rightarrow 0$. There we obtain

$$\int_T^\infty \rho(T') dT' = \frac{1}{(e^T - 1)^{1-ah_i}} \left[1 + a \frac{e^T (T^2 + 2\text{Li}_2(1-e^T) + T - 1) + 2T + 1}{2(e^T - 1)} + \mathcal{O}(a^2) \right].$$

On the other hand, expanding (167) for small T we get

$$\rho(T) = T^{-2+v+ah_i} \left[ah_i + v - 1 + \frac{1}{2}(ah_i + v)(1+a) \left(v - 1 - \frac{ah_i}{1+a} \right) T + \mathcal{O}(T^2) \right]. \tag{168}$$

We observe that the power-law behavior near $T = 0$, $\rho(T) \sim T^{-2+v}$, is not modified for the first subavalanche ($h_i = 0$) but is modified for later ones to

$$\rho(T) \sim T^{-2+v+ah_i} \tag{169}$$

to leading order in a . This is natural, since for small avalanches h remains essentially unchanged and replaces in (19) $v \rightarrow v + ah_i$. In order to obtain the subavalanche-duration distribution for stationary driving, one would need to average over all h_i taken from the stationary distribution $P(h_i | \dot{u}_i = 0)$. Presumably, this would replace the correction ah_i to the exponent in (169) by a velocity-dependent correction. We leave the details for further research.

In Figs. 9 and 10, we compare the result (167) to numerical simulations of the original model. One observes good agreement for small a but larger deviations starting around $a \approx 0.5$. In Fig. 11 we verify numerically the result (169) for the sub-avalanche-duration exponent as a function of h_i . The agreement is very good, even for $a = 1$.

3. Numerical results

Since the analytical results we obtained above for sub-avalanche sizes and durations are rather limited, we also give a few qualitative numerical results. In this section we neglect the difference between densities and probability distributions and use P instead of ρ everywhere.

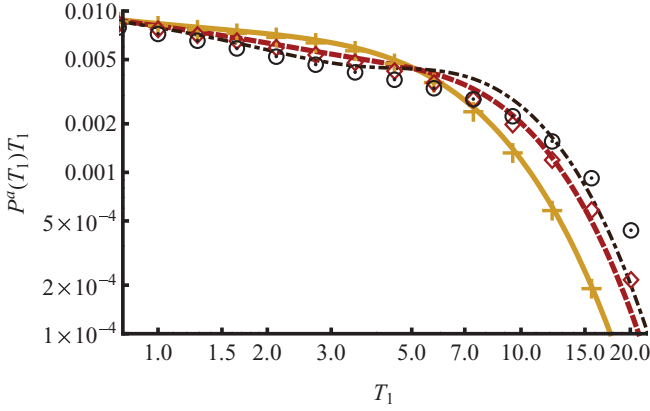


FIG. 9. (Color online) Duration distribution of an avalanche starting at $\dot{u} = 0, h = 0$ and $\tau = 1, v = 0.6$. Crosses, diamonds, and circles: Results from numerical integration of (19) for $a = 0, a = 0.3, a = 0.5$ with time step $dt = 10^{-5}$ (for details, see Appendix H). Lines: Expansion in a , (167). Yellow (thick) line: Pure ABBM model, $a = 0$. Red (dashed) line: $a = 0.3$. Black (dotted) line: $a = 0.5$.

(1) Subavalanches at fixed initial $\dot{u}_i, h_i = 0$ and $v = 0$. In (168), we derived that the ABBM power-law $P(T) \propto T^{-2}$ for small T [see (143)] remains unchanged in this case, at least for $\tau = 1$ and small a . In Fig. 12 we consider the subavalanche sizes and durations for general values of a, τ . We see that the mean-field zero-velocity power laws $P(S) \sim S^{-3/2}, P(T) \sim T^{-2}$ are clearly visible even when varying a, τ . For large a and small τ , there is an interesting crossover in the shape of the distributions, showing a similar power law but with different amplitudes, depending on a, τ . The case of large τ is equivalent to a modification of the mass, i.e., of the large-avalanche cutoff, as discussed in Sec. II A.

(2) Subavalanches at fixed \dot{u}_i , and h_i taken from the stationary distribution at the driving velocity. We observe in Fig. 13 that this leads to a modification of the ABBM power-law exponent. However, the variation in the exponent due to retardation becomes smaller as the driving velocity

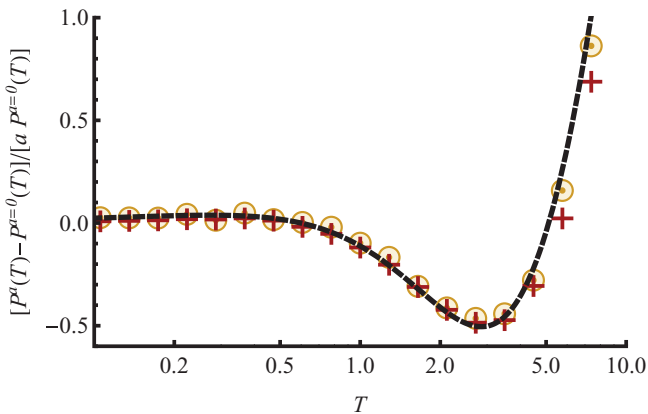


FIG. 10. (Color online) Correction to the duration distribution of an avalanche starting at $\dot{u} = 0, h = 0$ due to retardation, $[P^a(T) - P^{a=0}(T)]/[a P^{a=0}(T)]$. $\tau = 1, v = 0.6$. (Yellow) Circles, (red) squares: Results from numerical integration of (19) for $a = 0.1, a = 0.3$ with time step $dt = 10^{-4}$ (for details, see Appendix H). Dashed line: (167).

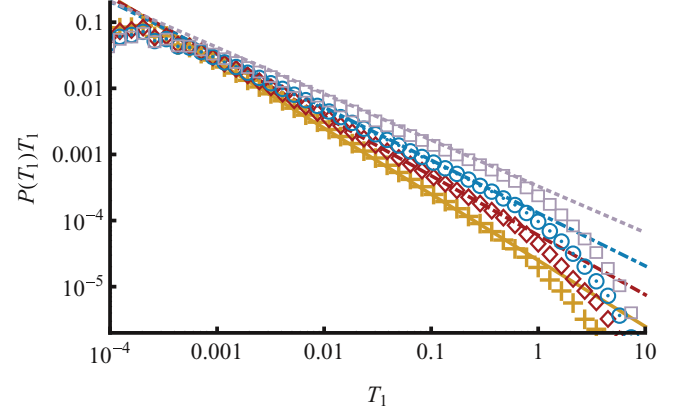


FIG. 11. (Color online) Duration distribution of the first subavalanche as a function of h_i . $\tau = 1, a = 1, v = 0$. (Yellow) Crosses, (red) diamonds, (blue) circles, and (gray) squares correspond to numerical simulations of (19) for $h_i = 0, h_i = 0.1, h_i = 0.2$, and $h_i = 0.3$ with time step $dt = 10^{-5}$ (for details, see Appendix H). Solid, dashed, dot-dashed, and dotted lines correspond to power laws $P(T_1) \sim T_1^{-2}, T_1^{-1.9}, T_1^{-1.8}, T_1^{-1.7}$.

decreases. This is expected from (169), since the typical value of h_i (and, hence, the correction to the exponent) decreases as $v \rightarrow 0$.

From these numerical results we conjecture that subavalanche durations in the ABBM model with retardation, at constant driving, satisfy

$$P(T) \sim T^{-2+v(1+c_T)}, \quad P(S) \sim S^{-3/2+v/2(1+c_S)}.$$

Here c_T, c_S depend on a, τ , and vanish as $a \rightarrow 0$ and/or $\tau \rightarrow 0$. In other words, we conjecture that the zero-velocity exponents are unchanged, and only the driving-velocity-dependent part is modified. This is also consistent with our analytical results in Secs. V and VI for the velocity distribution $P(\dot{u})$. Verifying these conjectures in more detail, numerically or analytically, would be an interesting task for the future.

IX. CONCLUSION AND OUTLOOK

In this article we have analyzed in detail a general ABBM model with retardation. We showed that it satisfies the Middleton property (monotonicity of the dynamics). Using this, and the Brownian nature of the ABBM disorder, we have been able to reduce the calculation of the expectation value of a general observable in the presence of monotonous driving to the problem of solving retarded nonlinear instanton equations. These equations can be implemented numerically for arbitrary retardation kernels and are much simpler than the original model with quenched disorder. To obtain analytical results, we focused on a model with exponential relaxation, which reduces to two coupled “instanton” equations, local in time. We have derived explicit forms for a number of observables at stationary and nonstationary driving. We mostly focused on the two limits of fast relaxation (describing eddy current effects in magnetic Barkhausen noise) and slow relaxation (of interest for earthquake models).

In the limit of slow relaxation, the main physics is the splitting of a single avalanche of size S of the standard

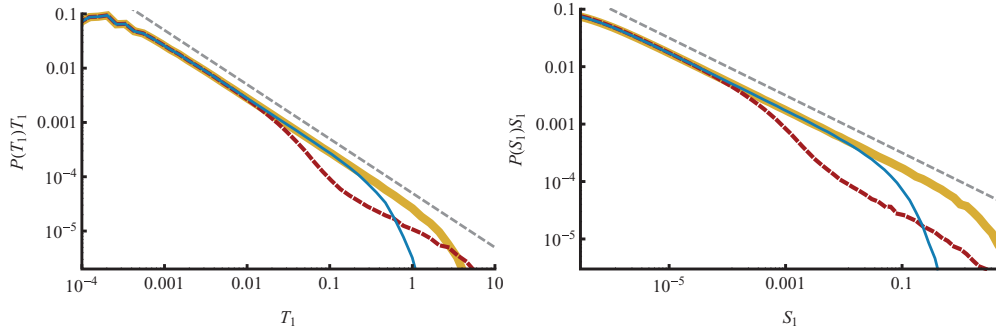


FIG. 12. (Color online) First subavalanche sizes (right) and durations (left) from numerical simulation of the ABBM model with retardation, starting from $\dot{u}_i = 0, h_i = 0$, at $v = 0$ (for details, see Appendix H). Gray (dashed) lines: power laws $P(S) \sim S^{-3/2}$, $P(T) \sim T^{-2}$. Yellow (thick) line: pure ABBM model $a = 0$. Red (dashed) line: $a = 60, \tau = 0.05$. Blue (thin) line: $a = 5, \tau = 10$.

ABBM model into a “cluster of aftershocks” of the *same* total size $S = \sum_{\alpha} S_{\alpha}$ but of much longer duration (strictly infinite for an exponential retardation kernel). This splitting is sharp in the limit of quasistatic driving and strong time-scale separation. Although we have been able to quantify some of these ideas, a more detailed analysis of the statistics of these subavalanches remains an important challenge for future work. In particular, if these ideas are to be extended to realistic earthquake dynamics, one needs to investigate power-law retardation kernels motivated by the Omori law of decay of activity. Still, it is of great interest to have found a tractable model with aftershocks, given that the standard ABBM model, which also models interfaces within mean-field theory (at the upper critical dimension), yields independent avalanches following a Levy process [17,18,29].¹⁸ Another recent study on the effects of slow relaxation processes on avalanche statistics [62] shows that these can lead to quasiperiodic avalanche bursts, such as also observed in crystal plasticity [62] and earthquakes in certain seismogenic regions [63,64]. This so-called *avalanche oscillator* [62] approaches criticality when no large avalanches occur and departs from criticality after a large avalanche, leading to stick-slip behavior. It would be interesting to see what minimal ingredients need to be added to the ABBM model with retardation discussed here, in order to observe similar quasiperiodic behavior (and whether this can be done preserving its useful analytical properties, such as monotonicity).

In the context of magnetic systems, the retardation describes the influence of eddy currents on the statistics of Barkhausen noise pulses. Experimentally, the time scale of eddy current relaxation is much shorter than that of the domain-wall motion, motivating our study of the fast-relaxation limit. In this limit, the effects of retardation are perturbative and vanish when the eddy-current relaxation-time tends to zero. We have obtained the leading corrections to the stationary velocity distribution, as well as the decay following a kick in the driving velocity.

In both the slow-relaxation and the fast-relaxation limit, the influence of retardation turned out to be most pronounced in nonstationary observables. For example, we computed explicitly the tail of the avalanche shape at fixed size. While it is Gaussian in the standard ABBM model, in the ABBM model with retardation it decays exponentially. Furthermore, we showed that, formally, the avalanche activity following a kick in the driving velocity never stops (even if, in the fast-relaxation limit, all significant avalanche activity still ceases), also in strong contrast to the pure ABBM model.

One important direction for future theoretical investigations is the role of the internal dimension of the interface. Here we reduce the description of the magnetic domain wall, which is a two-dimensional elastic interface in a three-dimensional medium, to a single degree of freedom (its center of mass). This mean-field description has been argued [32] and recently shown in detail [18,25] to be accurate for the center of mass of the interface above a critical internal dimension d_c . For certain soft magnets, due to long-range elastic forces, one has $d_c = 2$ [24,32]. Hence, some realistic domain walls have just the critical internal dimension. In that situation the internal degrees of freedom of the interface contribute only logarithmic corrections to the mean-field behavior as described in detail in Ref. [18]. Other ferromagnets are known to be in a non-mean-field universality class [31]. There, correctly describing the details of Barkhausen noise requires combining the eddy current modifications discussed in this article with a treatment of the spatial degrees of freedom, for example, using the functional renormalization group as in Refs. [18,25,65].

Another important avenue for further work is a detailed comparison of the analytical results discussed here with experiments on real magnetic domain walls. Considering the above results, nonstationary observables seem most promising. For example, the avalanche shape discussed in Sec. VII B shows a clear qualitative difference to the result of the standard ABBM model. As recognized in Refs. [19,22] this is an inertial effect due to an effective negative domain-wall mass. However, inertia can be modelled in different ways—for example, the retarded ABBM model considered here and in Ref. [22], the ABBM model with second-order dynamics considered in Ref. [49], and the mean-field model with stress overshoots considered in Ref. [40]. We believe the avalanche shape allows identifying not just the existence and the sign of inertial effects

¹⁸While this work was completed we learned of an independent work by Jagla and Rosso [61]. These authors consider several variants of earthquake models, and one of them is similar to the retarded model considered here.

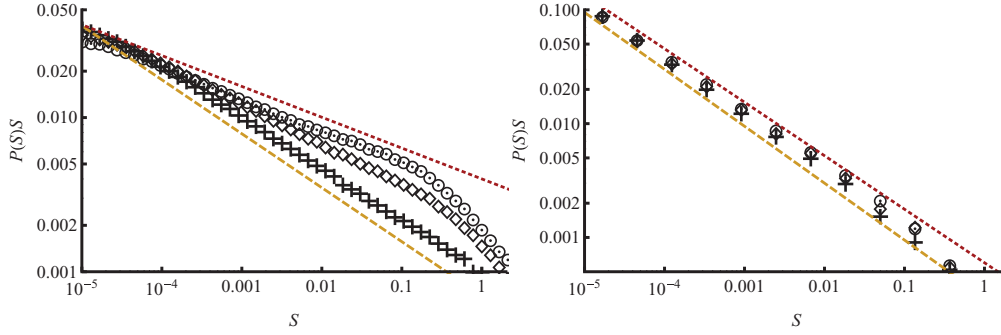


FIG. 13. (Color online) Subavalanche sizes from numerical simulation of the ABBM model with retardation, in a steady state with $v = 0.3$ (left) and $v = 0.02$ (right). For details, see Appendix H. Yellow (dashed) lines: power laws $P(S) \sim S^{-(3-v)/2}$; left: $S^{-1.35}$, right: $S^{-1.49}$. Red (dotted) lines: power laws; left: $S^{-1.2}$, right: $S^{-1.47}$. Crosses: pure ABBM model $a = 0$. Diamonds: $a = 1$, Circles: $a = 2$. In all cases, $\tau = 1$.

but their *precise form*. To this end, more precise analytical and experimental results (which go beyond a single “skewness” quantity and consider the entire shape) are necessary.

ACKNOWLEDGMENTS

We thank Yanjiun Chen, Gianfranco Durin, Aleksandra Petkovic, and Andrei Fedorenko for useful discussions. We are particularly grateful to Aleksandra Petkovic for bringing to our attention Ref. [22]. We also thank Alberto Rosso and Eduardo Jagla for bringing to our attention their independent work [61] and for discussions. This work was supported by ANR Grant No. 09-BLAN-0097-01/2 and by the CNRS through a doctoral fellowship for A.D.

APPENDIX A: MONOTONICITY OF THE DOMAIN-WALL MOTION IN THE RETARDED ABBM MODEL

The model defined in (5) satisfies Middleton’s theorem [44]: If the driving is monotonous, $w_t \geq w_s$ for $t \geq s$, then so is the motion of the domain wall.¹⁹

To prove this, note, first, that the velocity \dot{u}_t is continuous. Hence, before any negative velocities can occur, there would be an instant $t > 0$, where \dot{u}_t becomes zero for the first time. Then, using (5), we get

$$\begin{aligned} \eta \partial_t \dot{u}_t &= \dot{u}_t F'(u_t) + m^2 [\dot{w}(t) - \dot{u}(t)] - a \dot{u}(t) \\ &\quad - a \int_{-\infty}^t ds f'(t-s) \dot{u}(s) \\ &= m^2 \dot{w}(t) - a \int_{-\infty}^t ds f'(t-s) \dot{u}(s) > 0. \end{aligned}$$

The first term is $\dot{w}(t) \geq 0$ by monotonicity of the driving w . The second term is ≥ 0 , since $a > 0$, $f'(t-s) \leq 0$, and $\dot{u}_s > 0$ for all $s < t$. Similarly, one checks that if $\ddot{u}_t = 0$, then $\partial_t \ddot{u}_t \geq 0$. In other words, at any time where $\dot{u}_t = 0$, the first nonvanishing derivative of \dot{u}_t is positive. Thus, the domain-wall motion is monotonous.

¹⁹Note this is not true for models where domain-wall inertia is included by adding a second-order derivative in the ABBM equation of motion [49]. This makes the retarded ABBM model considered here quite special.

Note that the vanishing of $\dot{u} F'(u)$ for $\dot{u} = 0$ is ensured if $F(u)$ is smooth. In the case of the ABBM Brownian landscape, $F'(u)$ is a white noise. One can then consider a version smoothed at short scale and take the continuum limit. Alternatively, one sees on the formulation $\dot{u} F'(u) \leftrightarrow \sqrt{\tilde{u}} \xi(t)$ in (20) that this is not a problem.

When an inertial term, i.e., a second-order derivative is included in (5), this monotonicity property no longer holds. In particular, near the end of an avalanche the trajectory converges to a shallow minimum (metastable state) by oscillating around it indefinitely, with decreasing amplitude [49] [in contrast to (5), where it approaches the minimum monotonously from one side]. Furthermore, Middleton’s *no-passing theorem* [44] fails: two trajectories $u^{(1)}$, $u^{(2)}$ starting from initial points $u_{t_i}^{(1)} \leq u_{t_i}^{(2)}$ and subject to the same disorder and the same driving, in the presence of inertia, do *not* necessarily satisfy $u_t^{(1)} \leq u_t^{(2)}$ for all $t \geq t_i$. This is since the trajectory which was initially on the left can gain sufficient kinetic energy by rolling down from a large potential “hill” to overtake the trajectory which was initially on the right. In particular, the domain wall can overshoot a metastable state. The state reached asymptotically at long times for a fixed value of w , even for monotonous driving, depends on the history of the motion and not just on the final value of w .

APPENDIX B: POSITION DIFFERENCES IN THE SMALL-DISSIPATION LIMIT

As discussed in Sec. V C, instantaneous velocities \dot{u}_t are almost surely 0 in the small-dissipation limit $\eta = 0$. However, the distribution of position differences $u_T - u_0$ has a finite limit. The generating function of position differences at constant driving velocity v is given by (26),

$$\overline{e^{\lambda(u_T - u_0)}} = \overline{e^{\int_0^T dt \lambda \dot{u}_t}} = e^{vz(\lambda, T)}, \quad (\text{B1})$$

where $z(\lambda, T) = \int_0^T \tilde{u}_t$. \tilde{u}_t is given by the instanton equations (24) and (25) with sources $\lambda(t) = \lambda \theta(t) \theta(T-t)$, $\mu(t) = 0$. In the dissipation-less limit $\eta = 0$, (25) and (24) give an instanton equation similar to (41),

$$(1 + a - 2\tilde{u}_t) \partial_t \tilde{u}_t = \tilde{u}_t - \tilde{u}_t^2 + \lambda'_t - \lambda_t. \quad (\text{B2})$$

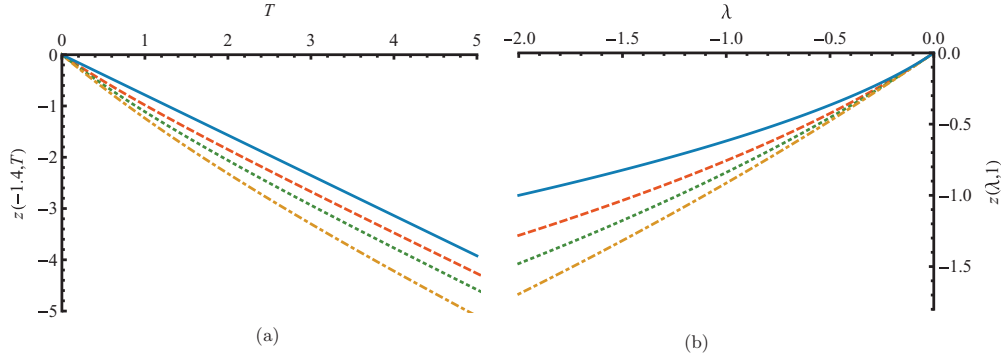


FIG. 14. (Color online) (a) z at $\lambda = -1.4$, as a function of T . Solid blue line: standard ABBM model (B6). Red (dashed), green (dotted), yellow (dot-dashed) lines: ABBM model with retardation for $a = 1, 2.3, 5.3$. (b) z at $T = 1$, as a function of λ . Dashed blue line: standard ABBM model (B6). Solid blue line: standard ABBM model (B6). Red (dashed), green (dotted), yellow (dot-dashed) lines: ABBM model with retardation for $a = 1, 2.3, 5.3$. Generating function for position differences $z(\lambda, T)$ as defined in (B1).

Here we thus work in the limit $\tau_m \ll \tau, \tau_v (=S_m/v)$, i.e., we set $\eta = 0$. We express all times in units of τ , i.e., our variable t is the variable s in Sec. V A. In other words, we set $\tau = 1$, while space units remain such that $S_m = 1$. For $t < 0$, the sources vanish and the solution is identical to that in Sec. V A. Thus, the integral over \tilde{u} in that region has the closed form (43),

$$\int_{-\infty}^0 \tilde{u}_t dt = 2\tilde{u}_{0^-} + (1-a) \ln(1 - \tilde{u}_{0^-}). \quad (\text{B3})$$

Similarly, the integral over \tilde{u} in the region $0 < t < T$ is

$$\begin{aligned} \int_0^T \tilde{u}_t dt &= \int_{\tilde{u}_{0^+}}^{\tilde{u}_{T^-}} \frac{1+a-2\tilde{u}}{\tilde{u}-\tilde{u}^2-\lambda} \tilde{u} d\tilde{u} \\ &= \left[-\frac{1}{2}(a-1) \ln(\lambda + (\tilde{u}-1)\tilde{u}) \right. \\ &\quad \left. + \frac{(a+4\lambda-1) \tanh^{-1}\left(\frac{2\tilde{u}-1}{\sqrt{1-4\lambda}}\right)}{\sqrt{1-4\lambda}} + 2\tilde{u} \right]_{0^+}^{T^-}. \end{aligned} \quad (\text{B4})$$

The relationship between \tilde{u}_{0^+} and \tilde{u}_{T^-} is given implicitly by

$$\begin{aligned} T &= \int_0^T ds = \int_{\tilde{u}_{0^+}}^{\tilde{u}_{T^-}} \frac{1+a-2\tilde{u}}{\tilde{u}-\tilde{u}^2-\lambda} d\tilde{u} \\ &= \left[\frac{2a \tanh^{-1}\left(\frac{2\tilde{u}-1}{\sqrt{1-4\lambda}}\right)}{\sqrt{1-4\lambda}} + \ln(\lambda + (\tilde{u}-1)\tilde{u}) \right]_{0^+}^{T^-}. \end{aligned} \quad (\text{B5})$$

The relationship between \tilde{u}_{0^+} and \tilde{u}_{0^-} , as well as between \tilde{u}_{T^-} and $\tilde{u}_{T^+} = 0$, is given by the matching conditions

$$\begin{aligned} [(1+a)\tilde{u}_{0^+} - \tilde{u}_{0^+}^2] - [(1+a)\tilde{u}_{0^-} - \tilde{u}_{0^-}^2] &= \lambda \\ -[(1+a)\tilde{u}_{T^-} - \tilde{u}_{T^-}^2] &= -\lambda. \end{aligned}$$

Altogether, this gives a complete (albeit implicit) solution for $\int_t \tilde{u}_t$ in terms of T, λ . This allows us to plot the generating function (B1), Fig. 14. It can also be compared to the result of the standard ABBM model,

$$z_0(\lambda, T) = \frac{T}{2}(1 - \sqrt{1-4\lambda}). \quad (\text{B6})$$

While the result (B6) holds in the small-dissipation (equivalently large-time) limit $\tau_m \ll T$, a more general result was obtained in Ref. [18] (Sec. II F) for the standard ABBM model in the case where τ_m and T are comparable.

In Fig. 14(b) one observes that the slope $\partial_\lambda|_{\lambda=0} z(T, \lambda) = T$ is independent of the value of a . This is also seen from the explicit solution above: The instanton equation (B2), to linear order in λ (equivalently to linear order in \tilde{u}), simplifies to

$$(1+a)\partial_t \tilde{u}_t = \tilde{u}_t + \lambda'_t - \lambda_t. \quad (\text{B7})$$

Its solution is

$$\tilde{u}_t = \frac{1}{1+a} \int_t^\infty ds e^{-(s-t)/(1+a)} (\lambda'_s - \lambda_s), \quad (\text{B8})$$

and its integral is

$$\int_{-\infty}^\infty dt \tilde{u}_t = \int_{-\infty}^\infty ds (\lambda'_s - \lambda_s) = \lambda T. \quad (\text{B9})$$

Thus, $z(T, \lambda) = \lambda T + O(\lambda)^2$. This means that the average displacement, $(u_T - u_0) = v \partial_\lambda|_{\lambda=0} z(T, \lambda) = vT$. Of course, this is consistent with the fact that the mean velocity of the domain wall is fixed by the harmonic well $m^2(u_t - vt)$.

On the other hand, from Fig. 14(b) one also sees that the curvature $\partial_\lambda^2|_{\lambda=0} z(T, \lambda)$ decreases with increasing a . Thus, the fluctuations $(u_T - u_0)^2$ are *decreased* by retardation effects. This is in agreement with the intuition of eddy currents slowing the domain wall down when it is moving fast and pushing it forward when it is moving slowly.

APPENDIX C: DIRECT PERTURBATION THEORY IN a

Instead of looking at the slow-relaxation limit $\tau \gg \tau_m$ or fast-relaxation limit $\tau \ll \tau_m$ discussed in Secs. V and VI, one may attempt to determine the corrections to the stationary velocity distribution for $a \ll 1$ through a direct perturbation expansion in a . For this, we need to solve the instanton equations (24) and (25) for $\lambda(t) = \lambda \delta(t)$, $\mu(t) = 0$. We take τ fixed but $a \ll 1$ and work, as in most of the article, in the

units where $\tau_m = 1$, $S_m = 1$. We set

$$\tilde{u}(t) = \tilde{u}_0(t) + a\tilde{u}_1(t) + O(a)^2, \quad \tilde{h}(t) = a\tilde{h}_1(t) + O(a)^2, \quad (\text{C1})$$

where $\tilde{u}_0(t)$ is the known instanton for the standard ABBM model [25],

$$\tilde{u}_0(t) = \frac{\lambda}{(1-\lambda)e^{-t} + \lambda} \theta(-t).$$

$\tilde{h}_1(t)$ for $t < 0$ is then determined by (25),

$$\tilde{h}_1(t) = \frac{1}{\tau} \int_t^0 ds e^{-(s-t)} \tilde{u}_0(s)$$

$$= {}_2F_1\left(1, \tau^{-1}; \tau^{-1} + 1; e^{-t/\tau} \left(1 - \frac{1}{\lambda}\right)\right) - e^{t/\tau} {}_2F_1\left(1, \tau^{-1}; \tau^{-1} + 1; 1 - \frac{1}{\lambda}\right).$$

To obtain $\tilde{u}_1(t)$ for $t < 0$, we need to solve the linear equation

$$\tilde{u}'_1(t) - \tilde{u}_1(t) - \tilde{u}_0(t) + 2\tilde{u}_1(t)\tilde{u}_0(t) + \tilde{h}_1(t) = 0, \quad (\text{C2})$$

with $\tilde{u}_1(0) = 0$. One simple case is $\tau = 1$, where

$$\tilde{h}_1(t) = \frac{\lambda}{1-\lambda} e^t \ln(\lambda + e^{-t}(1-\lambda)) \quad (\text{C3})$$

and

$$\begin{aligned} \tilde{u}_1(t) = & \frac{\lambda e^t}{2(\lambda-1)[\lambda(e^t-1)+1]^2} \left[2(\lambda-1)^2 \text{Li}_2\left(\frac{\lambda}{\lambda-1}\right) + (\lambda-1) \left\{ -\lambda - 2(\lambda-1) \text{Li}_2\left(\frac{e^t \lambda}{\lambda-1}\right) + (\lambda-1)(t-2t) \right. \right. \\ & + 3(\lambda-1) \ln(\lambda(e^t-1)+1) + 2t \ln\left(\frac{e^t}{1-\lambda}\right) + 2\lambda t \ln(e^{-t}(1-\lambda)) \left. \right\} \\ & \left. + \lambda^2 e^{2t} \ln(\lambda - (\lambda-1)e^{-t}) - \lambda(\lambda-1)e^t(4 \ln(\lambda - (\lambda-1)e^{-t}) - 1) \right]. \end{aligned}$$

This solution has the asymptotics

$$\lim_{\lambda \rightarrow -\infty} \tilde{u}_1(t) = \frac{e^t(2t - 4e^t + e^{2t} + 3)}{2(e^t - 1)^2} \ln(-\lambda).$$

We see that $\tilde{u}_1(t) \rightarrow -\infty$ as $\lambda \rightarrow -\infty$ for any fixed $t < 0$. Consistent with the discussion in Secs. VC and VD, we recover the result that there is no $\delta(\dot{u})$ contribution, $p_{\dot{u}=0} = 0$ following a kick, and avalanches never end.

Instead of the stationary velocity distribution, one can also consider the stationary distribution of eddy-current pressure as in Sec. VA. In contrast to (C1), the contribution $\tilde{h}_0(t)$ of order $O(a)^0$ to \tilde{h} does not vanish. To order $O(a)^0$ the expressions (24) and (25) in dimensionless units reduce to

$$\begin{aligned} \partial_t \tilde{u}_0 - \tilde{u}_0 + \tilde{u}_0^2 + \tilde{h} &= 0 \\ \tau \partial_t \tilde{h}_0 - \tilde{h}_0 &= -\mu \delta(t). \end{aligned}$$

Thus,

$$\tilde{h}_0(t) = \frac{\mu}{\tau} e^{t/\tau} \theta(-t),$$

and the equation for \tilde{u}_0 becomes

$$\partial_t \tilde{u}_0 - \tilde{u}_0 + \tilde{u}_0^2 = -\frac{\mu}{\tau} e^{t/\tau} \theta(-t). \quad (\text{C4})$$

It is the instanton equation for the standard ABBM model ($a = 0$), but with a time-dependent source $\lambda_t = \frac{\mu}{\tau} e^{t/\tau} \theta(-t)$. This is natural, stating that to $O(a)^0$, the distribution of $\mu h(t = 0)$ is the distribution of the observable $\int_t^0 \lambda_t \dot{u}_t = \frac{\mu}{\tau} \int_{-\infty}^0 dt e^{t/\tau} \dot{u}_t$ in the pure ABBM model.

The solution of (C4) is $\tilde{u}_0(t) = \frac{\psi'(t)}{\psi(t)}$, where

$$\begin{aligned} 0 &= \tau \psi''(t) - \tau \psi'(t) + \mu e^{t/\tau} \psi(t) \\ \Rightarrow \psi(t) &= [c_1 J_{-\tau}(2e^{t/(2\tau)} \sqrt{\mu\tau}) \\ &+ c_2 J_{\tau}(2e^{t/(2\tau)} \sqrt{\mu\tau})] e^{t/2}. \end{aligned}$$

Fixing c_1/c_2 using the boundary condition $\tilde{u}_0(t = 0) = 0$, we obtain

$$\int dt \tilde{u}_0(t) = \ln \frac{\psi(0)}{\psi(-\infty)} = -\ln {}_0F_1(\tau, -\mu\tau).$$

Thus, the generating function of the stationary distribution of h is

$$\overline{e^{\mu h}} = [{}_0F_1(\tau, -\mu\tau)]^{-v} [1 + O(a)]. \quad (\text{C5})$$

We can now make contact with the result of Sec. VA. Defining $\mu := \tau\mu_r$, $v_r := v\tau$ and using that

$$\begin{aligned} \lim_{\tau \rightarrow \infty} \frac{1}{\tau} \ln {}_0F_1(\tau, -\mu_r \tau^2) &= -1 + \sqrt{1 - 4\mu_r} \\ &- \ln \frac{1}{2} (1 + \sqrt{1 - 4\mu_r}), \end{aligned}$$

Equation (C5) in the limit $\tau \rightarrow \infty$ reduces to the $a = 0$ limit of (44). Its Laplace inverse is given by (45) for $a = 0$. However, computing the Laplace inverse of (C5) for general τ, v seems to be doable only numerically. Likewise, we did not manage to obtain simple expressions for \tilde{u}_1, \tilde{h}_1 at the next-to-leading order, $O(a)$.

In the limit $v \rightarrow 0^+$ one defines the density $\rho(h) = \partial_v P(h)|_{v=0^+}$ and one finds

$$h\rho(h) = -\text{LT}_{s \rightarrow h}^{-1} \frac{\partial_s [{}_0F_1(\tau, s\tau)]}{{}_0F_1(\tau, s\tau)}, \quad (\text{C6})$$

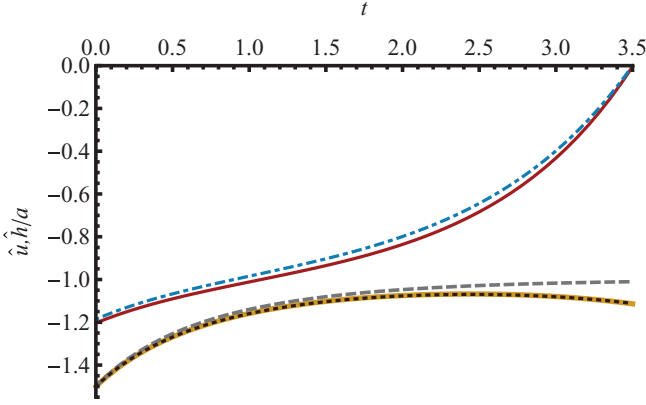


FIG. 15. (Color online) Numerical solution and perturbative expansion of (150) and (151) for $a = 0.2$, $\tau = 1$. Boundary conditions are (160) with $t_i = 0$, $t_f = 3.5$, $\mu = 0$, $\lambda = -1.5$. Thick (yellow) line: \hat{u}_t from numerical solution. Thin (red) line: \hat{h}_t/a from numerical solution. Gray (dashed) line: Pure ABBM instanton $\hat{u}_t^{(00)}$, given by (134). Blue (dot-dashed) line: $\hat{h}_t^{(01)}$ given by (D11). Black (dotted) line: $\hat{u}_t^{(00)} + a\hat{u}_t^{(01)}$ given by (134) and (D12).

where we defined $s := -\mu$; for the following suppose $s > 0$. For half-integer values of τ (C6) can be expressed in terms of elementary functions, for instance, for $\tau = 1/2$,

$$\begin{aligned} h\rho(h) &= \text{LT}_{s \rightarrow h}^{-1} \frac{\tanh(\sqrt{2s})}{\sqrt{2s}} = \sum_{k=1}^{\infty} \text{LT}_{s \rightarrow h}^{-1} \frac{1}{\frac{\pi^2(2k-1)^2}{8} + s} \\ &= \sum_{k=1}^{\infty} e^{-\pi^2(2k-1)^2 h/8} = \frac{1}{2} \theta_2(0; e^{-h\pi^2/2}), \end{aligned}$$

$$\begin{aligned} \hat{u}_t^{(10)} &= - \int_{t_i}^t ds_1 \exp \left\{ \int_{s_1}^t ds_2 [1 + 2\hat{u}_{s_2}^{(00)}] \right\} e^{-(t-s_1)/\tau} \\ &= \frac{\tau e^{-\frac{t}{\tau}}}{(\tau^2 - 1) [\lambda e^t - (\lambda + 1)e^{t_i}]^2} \left\{ -\lambda^2(\tau - 1)e^{t(\frac{1}{\tau}+2)} + 2(\lambda + 1)\lambda(\tau^2 - 1)e^{\frac{t}{\tau}+t+t_i} \right. \\ &\quad \left. - [2\lambda(\lambda + 1)\tau^2 + 2\lambda\tau + \tau + 1]e^{t+\frac{t_i}{\tau}+t_i} + (\lambda + 1)^2(\tau + 1)e^{\frac{t}{\tau}+2t_i} \right\}. \end{aligned} \quad (\text{D8})$$

On the other hand, $\hat{h}_t^{(01)}$ is obtained by solving (D4) with the boundary condition $\hat{h}_{t_f}^{(01)} = 0$. The solution reads

$$\begin{aligned} \hat{h}_t^{(01)} &= -\frac{1}{\tau} \int_{t_f}^t ds_1 e^{(t-s_1)/\tau} \frac{\lambda}{e^{t_i-s_1}(\lambda + 1) - \lambda} \\ &= \frac{\lambda e^{\frac{t}{\tau}-t_i}}{(\lambda + 1)(\tau - 1)} \left[e^{\frac{(\tau-1)t_f}{\tau}} {}_2F_1 \left(1, \frac{\tau-1}{\tau}; 2 - \frac{1}{\tau}; \frac{e^{t_f-t_i}\lambda}{\lambda + 1} \right) - e^{\frac{t(\tau-1)}{\tau}} {}_2F_1 \left(1, \frac{\tau-1}{\tau}; 2 - \frac{1}{\tau}; \frac{e^{t-t_i}\lambda}{\lambda + 1} \right) \right]. \end{aligned} \quad (\text{D9})$$

Obtaining the higher-order terms for arbitrary $\tau > 0$ is now complicated, due to the appearance of hypergeometric functions. However, the latter simplify significantly in the limit $\tau \rightarrow 1$. From now on, we will consider this limit only. We then have

$$\hat{u}_t^{(10)} = \frac{e^{t-t_i}}{2[\lambda e^t - (\lambda + 1)e^{t_i}]^2} \{-\lambda^2 e^{2t} + 4(\lambda + 1)\lambda e^{t+t_i} + e^{2t_i}\lambda[-3\lambda - 2(\lambda + 2)t + 2(\lambda + 2)t_i - 4] - 2e^{2t_i}(t - t_i)\}, \quad (\text{D10})$$

$$\hat{h}_t^{(01)} = \frac{\lambda e^{t-t_i}}{\lambda + 1} \left[t_f - t + \ln \frac{(\lambda + 1)e^{t_i} - \lambda e^t}{(\lambda + 1)e^{t_i} - \lambda e^{t_f}} \right]. \quad (\text{D11})$$

where θ_2 is the Jacobi θ function. For small h it diverges as $\rho(h) \simeq \frac{1}{\sqrt{2\pi}} h^{-3/2}$, similarly to the result (47) found in the limit of large τ and fixed (not necessarily small) a .

APPENDIX D: PERTURBATION THEORY IN a FOR THE BACKWARD EQUATION

In this section, we compute the six functions $\hat{u}_t^{(00)}, \hat{u}_t^{(10)}, \hat{u}_t^{(01)}$ and $\hat{h}_t^{(10)}, \hat{h}_t^{(01)}, \hat{h}_t^{(11)}$ used in the perturbative expansion (164) for subavalanche durations. Expanding (150) and (151) in a and μ , and inserting the ansatz (164), we obtain the following set of equations:

$$-\partial_t \hat{u}_t^{(00)} + \hat{u}_t^{(00)} + (\hat{u}_t^{(00)})^2 = -\lambda \delta(t - t_i), \quad (\text{D1})$$

$$-\tau \partial_t \hat{h}_t^{(10)} + \hat{h}_t^{(10)} = \delta(t - t_f), \quad (\text{D2})$$

$$[-\partial_t + 1 + 2\hat{u}_t^{(00)}] \hat{u}_t^{(10)} - \hat{h}_t^{(10)} = 0, \quad (\text{D3})$$

$$-\tau \partial_t \hat{h}_t^{(01)} + \hat{h}_t^{(01)} - \hat{u}_t^{(00)} = 0, \quad (\text{D4})$$

$$[-\partial_t + 1 + 2\hat{u}_t^{(00)}] \hat{u}_t^{(01)} + \hat{u}_t^{(00)} - \hat{h}_t^{(01)} = 0, \quad (\text{D5})$$

$$-\tau \partial_t \hat{h}_t^{(11)} + \hat{h}_t^{(11)} - \hat{u}_t^{(10)} = 0. \quad (\text{D6})$$

Some numerical solutions, and their comparison to this perturbative expansion, can be seen in Fig. 15.

Equation (D1) shows that $\hat{u}_t^{(00)}$ is given by the pure ABBM solution (134). Similarly, (D2) shows that $\hat{h}_t^{(10)}$ is also given by the expression from the pure ABBM model (161),

$$\hat{h}_t^{(10)} = e^{-(t_f-t)/\tau}. \quad (\text{D7})$$

The term $\hat{u}_t^{(10)}$ can still be computed at order a^0 by solving (D3) with the boundary condition $\hat{u}_{t_i}^{(10)} = 0$. The solution reads

To obtain $\hat{u}_t^{(01)}$, we need to solve (D5) with the boundary condition $\hat{u}_{t_i}^{(01)} = 0$. The solution reads

$$\hat{u}_t^{(01)} = \int_{t_i}^t ds_1 \exp \left\{ \int_{s_1}^t ds_2 [1 + 2\hat{u}_{s_2}^{(00)}] \right\} (\hat{u}_{s_1}^{(00)} - \hat{h}_{s_1}^{(01)}). \quad (\text{D12})$$

This integral can be evaluated in closed form and gives a lengthy expression in terms of logarithms and dilogarithms. However, the expression (165) for the avalanche duration only depends on $\int_{t_i}^{t_f} dt \hat{u}_t^{(01)}$ and on $\hat{u}_{t_f}^{(01)}$. These two terms depend only on $T := t_f - t_i$ and are simpler,

$$\begin{aligned} \hat{u}_{t_f}^{(01)} &= \int_{t_i}^{t_f} ds_1 \exp \left\{ \int_{s_1}^{t_f} ds_2 [1 + 2\hat{u}_{s_2}^{(00)}] \right\} (\hat{u}_{s_1}^{(00)} - \hat{h}_{s_1}^{(01)}) \\ &= \frac{e^T \lambda}{2(\lambda + 1)(-e^T \lambda + \lambda + 1)^2} \left[-T^2(\lambda + 1)^2 - T(\lambda^2 - 2) - (e^T - 1)\lambda(\lambda + 1) + (2T - 3)(\lambda + 1)^2 \ln \left(1 - \frac{e^T \lambda}{\lambda + 1} \right) \right. \\ &\quad \left. + \lambda(3\lambda + 4) \ln(-e^T \lambda + \lambda + 1) + 2(\lambda + 1)^2 \text{Li}_2 \left(\frac{e^T \lambda}{\lambda + 1} \right) + 3(\lambda + 1)^2 \ln \left(\frac{1}{\lambda + 1} \right) - 2(\lambda + 1)^2 \text{Li}_2 \left(\frac{\lambda}{\lambda + 1} \right) \right], \end{aligned} \quad (\text{D13})$$

$$\begin{aligned} \int_{t_i}^{t_f} dt \hat{u}_t^{(01)} &= \frac{1}{2(\lambda + 1)[(e^T - 1)\lambda - 1]} \left\{ \lambda [T\lambda + e^T(T(T\lambda + T - 2) + \lambda + 1) + 2T - \lambda - 1] \right. \\ &\quad \left. + [2e^T \lambda((\lambda + 1) \ln(\lambda) - (\lambda + 1) \ln(\lambda + 1) + 1) + 1] \ln[-e^T \lambda + \lambda + 1] \right. \\ &\quad \left. - 2e^T \lambda(\lambda + 1) \left[\text{Li}_2 \left(\frac{1}{\lambda + 1} \right) - \text{Li}_2 \left(1 - \frac{e^T \lambda}{\lambda + 1} \right) \right] \right\}. \end{aligned} \quad (\text{D14})$$

To obtain $\hat{h}_t^{(11)}$, we need to solve (D6) with the boundary condition $\hat{h}_{t_f}^{(11)} = 0$. Note that the formula (165) for the avalanche duration only contains $\hat{h}_{t_i}^{(11)}$. The result for this value again only depends on $T := t_f - t_i$,

$$\begin{aligned} \hat{h}_{t_i}^{(11)} &= \frac{1}{2} e^{-T} \left[\frac{T^2(\lambda + 1)^2((e^T - 1)\lambda - 1) + T\lambda(e^T(\lambda^2 - 2) - (\lambda + 1)(3\lambda + 4)) + (e^T - 1)\lambda(2\lambda + 3)(\lambda + 1)}{(\lambda + 1)^2(-e^T \lambda + \lambda + 1)} \right. \\ &\quad \left. - \frac{(2\lambda + 3) \ln(-e^T \lambda + \lambda + 1)}{(\lambda + 1)^2} + 2T \ln \left(1 - \frac{e^T \lambda}{\lambda + 1} \right) + 2\text{Li}_2 \left(\frac{e^T \lambda}{\lambda + 1} \right) - 2\text{Li}_2 \left(\frac{\lambda}{\lambda + 1} \right) \right]. \end{aligned} \quad (\text{D15})$$

Finally, $\hat{h}_i^{(01)}$ is obtained from (D11) as

$$\hat{h}_i^{(01)} = \frac{\lambda}{1 + \lambda} [T - \ln(1 + \lambda - \lambda e^T)]. \quad (\text{D16})$$

In Fig. 15, we show that these perturbative expressions compare well to a direct numerical solution of the backward-instanton equations.

In order to apply (165) we need to compute the leading behavior as $\lambda \rightarrow -\infty$. We get

$$\lim_{\lambda \rightarrow -\infty} \hat{h}_{t_i}^{(11)} = \frac{T}{e^T - 1} - \frac{1}{2} e^{-T} [2\text{Li}_2(1 - e^T) + (T + 1)(T + 2)], \quad (\text{D17})$$

$$\lim_{\lambda \rightarrow -\infty} \int_{t_i}^{t_f} dt \hat{u}_t^{(01)} = \frac{e^T T^2 + 2e^T \text{Li}_2(1 - e^T) + T + e^T - 1}{2(e^T - 1)}, \quad (\text{D18})$$

$$\lim_{\lambda \rightarrow -\infty} \hat{u}_{t_f}^{(01)} = -\frac{e^T}{2(e^T - 1)^2} [T^2 + 2\text{Li}_2(1 - e^T) + T + e^T - 1], \quad (\text{D19})$$

$$\lim_{\lambda \rightarrow -\infty} (-\lambda)^{ah_i} \exp(-ah_i \hat{h}_i^{(01)}) = (1 - e^{-T})^{-ah_i}. \quad (\text{D20})$$

Inserting these results into (165), we obtain (167).

APPENDIX E: AVALANCHE SIZES AT FINITE DRIVING VELOCITY v IN THE STANDARD ABBM MODEL

Similarly to the computation of avalanche durations in the standard ABBM model at finite driving velocity in Sec. VIII A2, we can also compute the avalanche sizes. The discussion follows closely Ref. [45] where some explicit expressions were obtained in the small- m limit (at fixed $x = v/v_m$). Let us now consider the stochastic process $\dot{u}(u)$, i.e., the domain-wall velocity as a function of its position. Its first-passage distribution was derived in Ref. [45] [equivalent to formula (E30) there]²⁰ and later in Ref. [59],

$$\begin{aligned} &\int_0^\infty du e^{\lambda u} P_{\dot{u}}(u | \dot{u}_0) \\ &= e^{-\frac{1}{2}(1 - \sqrt{1 - 4\lambda})(\dot{u}_0 - \dot{u})} \frac{U\left[\frac{v}{2}\left(1 - \frac{1}{\sqrt{1 - 4\lambda}}\right), v, \sqrt{1 - 4\lambda}\dot{u}_0\right]}{U\left[\frac{v}{2}\left(1 - \frac{1}{\sqrt{1 - 4\lambda}}\right), v, \sqrt{1 - 4\lambda}\dot{u}\right]}. \end{aligned} \quad (\text{E1})$$

²⁰ \mathbf{v} and \mathbf{v}' must be replaced by v in the first argument of the hypergeometric function there.

As $\dot{u} \rightarrow 0$, this has a finite limit for $v < 1$ (the first-passage distribution at $\dot{u} = 0$),

$$\int_0^\infty du e^{\lambda u} P_0(u|\dot{u}_0) = e^{-\frac{\dot{u}_0}{2}(1-\sqrt{1-4\lambda})} \frac{U\left[\frac{v}{2}\left(1-\frac{1}{\sqrt{1-4\lambda}}\right), v, \sqrt{1-4\lambda}\dot{u}_0\right]}{\Gamma(1-v)/\Gamma\left[1-\frac{v}{2}\left(1+\frac{1}{\sqrt{1-4\lambda}}\right)\right]}.$$

Integrating this over the stationary distribution for $\dot{u}_0(u)$, $P(\dot{u}_0) = \frac{1}{\Gamma(v+1)}\dot{u}_0^v e^{-\dot{u}_0}$, we get the Laplace-transformed cumulative distribution of avalanche sizes in the form

$$\int_0^\infty e^{\lambda u} \frac{P(S \geq u)}{\int_0^\infty dS' S' P(S')} du = -\frac{(1-4\lambda)^{\frac{1-v}{2}}}{\lambda v B\left[1-v, \frac{v}{2}\left(1-\frac{1}{\sqrt{1-4\lambda}}\right)\right]}.$$
(E2)

Here, $B(x, y)$ is the usual Beta function. (E2) is valid since the probability that $u = 0$ belongs to an avalanche of size S is $SP(S)/\int_0^\infty dS' S' P(S')$ and the conditional distribution of u is then $P(u|S) = \theta(S-u)/S$. Putting this together produces (E2). One can check that, taking the large- λ limit and Laplace inverting, one recovers exactly the formula below (E28) in Ref. [45], valid in the small- m limit (at fixed $x = v/v_m$).

The Laplace transform of the avalanche density $\rho(S) = P(S)/[\int_0^\infty dS' S' P(S')]$ is obtained by integration by part of (E2),

$$\int_0^\infty dS (e^{\lambda S} - 1) \rho(S) = -\frac{(1-4\lambda)^{\frac{1-v}{2}}}{v B\left[1-v, \frac{v}{2}\left(1-\frac{1}{\sqrt{1-4\lambda}}\right)\right]}.$$
(E3)

A nontrivial check of (E3) is that it satisfies the normalization condition $\int dS S \rho(S) = 1$ automatically.

Using standard relations for the Beta function [54], one can rewrite (E3) as

$$\int_0^\infty dS (e^{\lambda S} - 1) \rho(S) = \frac{\sin \pi v}{2\pi} (1-4\lambda)^{-\frac{v}{2}} (1+\sqrt{1-4\lambda}) \times B\left[v, -\frac{v}{2}\left(1+\frac{1}{\sqrt{1-4\lambda}}\right)\right].$$
(E4)

Using the substitution $r := 1 + \sqrt{1-4\lambda}$, we can write the inverse Laplace transform in the compact form

$$\rho(S) = \int_{r_0-i\infty}^{r_0+i\infty} \frac{dr}{2\pi i} \frac{\sin(\pi v)}{4\pi} \times r e^{\frac{1}{4}(r-2)rS} (r-1)^{1-v} B\left(v, \frac{rv}{2-2r}\right),$$

where $r_0 > 1$.

For the case $v = 0$, (E3) reduces to the known expression [17,18]

$$\int_0^\infty dS (e^{\lambda S} - 1) \rho(S) = \frac{1}{2} (1 - \sqrt{1-4\lambda}),$$

which leads to the standard ABBM avalanche-size density $\rho(S) = \frac{1}{2\sqrt{\pi} S^{3/2}} e^{-S/4}$.

For any $0 < v < 1$, we can obtain the behavior of $\rho(S)$ at small S from the $\lambda \rightarrow -\infty$ limit of (E4). In this limit, the Beta function tends to a constant and we obtain

$$\int_0^\infty dS (e^{\lambda S} - 1) \rho(S) = \frac{\sin \pi v}{2\pi} (-4\lambda)^{\frac{1-v}{2}} [1 + O(|\lambda|^{-1/2})] B\left(v, -\frac{v}{2}\right).$$

Inverting the Laplace transform, we see that near $S = 0$

$$\rho(S) = S^{-(3-v)/2} \left[\frac{(v-1)\Gamma(-v/2)\sin(\pi v)}{4\pi^{3/2}} + O(S)^{1/2} \right].$$
(E5)

This is in agreement with previous results [24,45,55] and extends them by giving the prefactor of the power law.

APPENDIX F: FIXING INITIAL CONDITIONS INSTEAD OF FINAL CONDITIONS

In this section, we discuss how to transform (156), a formula with a fixed value of h_f and a Laplace transform taken with respect to h_i , into (159), a formula with a fixed value of h_i and a Laplace transform taken with respect to h_f .

We start by integrating (156) over h_f ,

$$\int_{-\infty}^\infty dh_f \int_0^\infty d\dot{u}_i \int_{-\infty}^\infty dh_i e^{\lambda \dot{u}_i + \mu h_i} \mathcal{P}_{\text{abs}}(\dot{u}_f, h_f; t_f | \dot{u}_i, h_i; t_i) = \exp \left\{ \int_{t_i}^{t_f} [(2 - \dot{w}_s) \hat{u}_s + (1 + a + \tau^{-1})] ds + \dot{u}_f \hat{u}_{t_f} \right\} (2\pi) \delta[i \tau \hat{h}(t_f)].$$
(F1)

We now invert the Laplace transform from $\mu = \tau \hat{h}(t_i)$ to h_i using a complex integral,

$$\begin{aligned} & \int_{-\infty}^\infty dh_f \int_0^\infty d\dot{u}_i e^{\lambda \dot{u}_i} \mathcal{P}_{\text{abs}}(\dot{u}_f, h_f; t_f | \dot{u}_i, h_i; t_i) \\ &= \int_{-i\infty}^{i\infty} d\mu \exp \left\{ \int_{t_i}^{t_f} [(2 - \dot{w}_s) \hat{u}_s + (1 + a + \tau^{-1})] ds + \dot{u}_f \hat{u}_{t_f} \right\} \delta(\hat{h}_{t_f}) \exp(-\tau \hat{h}_{t_f} h_i) \\ &= \exp \left\{ \int_{t_i}^{t_f} [(2 - \dot{w}_s) \hat{u}_s + (1 + a + \tau^{-1})] ds + \dot{u}_f \hat{u}_{t_f} - \tau h_i \hat{h}_{t_f} \right\} [\partial_{\hat{h}(t_f)} |_{\hat{h}(t_f)=0} \hat{h}(t_f)]. \end{aligned}$$

This now is Eq. (159). Due to the δ function, the only value of $\hat{h}(t_f)$ that contributes is the one which leads to $\hat{h}(t_f) = 0$. So, the effect of going from a fixed h_f to a fixed h_i in the propagator is a change in the boundary conditions for the pair of backward instanton equations (150) and (151). When integrating over all h_f , we have to impose the boundary conditions (160)

$$\hat{h}(t_f) = 0, \quad \hat{u}(t_f) = \lambda.$$

In addition, we get the ‘‘Jacobian’’ factor in (159). In the pure ABBM case $a = 0$, as discussed in Sec. VIII E1, it just cancels the $(t_f - t_i)/\tau$ factor in the exponential. For $a > 0$ it is more complicated.

APPENDIX G: SOME EXACT RELATIONS FOR THE PROPAGATOR

Finding general solutions to the forward instanton equations (24) and (25) and the backward instanton equations (150) and (151) is difficult. However, simple particular solutions exist, where the instanton is constant in time. These imply exact relations on particular observables in the ABBM model with retardation, which we discuss below.

1. Forward instanton

A particular solution of (24) and (25) is

$$\begin{aligned} \lambda_t &= \delta(t - t_f), & \mu_t &= a\tau\delta(t - t_f), \\ \tilde{u}_t &= \theta(t_f - t), & \tilde{h}_t &= a\theta(t_f - t). \end{aligned} \quad (\text{G1})$$

To see the significance of this solution, consider starting at fixed \dot{u}_i, h_i at $t = 0$, and driving with a constant velocity $\dot{w}_t = v$ for $0 < t < t_f$. Using (26), and accounting for the initial condition as in Ref. [46], Eq. (4), we get

$$\overline{e^{\dot{u}(t_f) + a\tau h(t_f)}} = e^{\dot{u}_i \tilde{u}_0 + \tau h_i \tilde{h}_0 + \int_0^{t_f} dt \dot{w}_t \tilde{u}_t} = e^{\dot{u}_i + a\tau h_i + vt_f}. \quad (\text{G2})$$

This implies the following exact relation on the propagator of the ABBM model with retardation at constant driving velocity v ,

$$\int_0^\infty d\dot{u}_f \int_0^\infty dh_f e^{\dot{u}_f + a\tau h_f} \mathcal{P}(\dot{u}_f, h_f; t_f | \dot{u}_i, h_i; 0) = e^{\dot{u}_i + a\tau h_i + vt_f}. \quad (\text{G3})$$

For the case $a = 0$ (pure ABBM model), this relation can be checked explicitly using the formula for the ABBM propagator, Eq. (19) in Ref. [46]. It generalizes similarly to the case of arbitrary driving \dot{w} .

2. Backward instanton

Now let us apply the same idea to the backward instanton, used in Sec. VIII, in order to perform calculations with an absorbing boundary at $\dot{u} = 0$. A particular solution of (150) and (151) is

$$\begin{aligned} \lambda_t &= -\delta(t - t_f), & \mu_t &= -a\tau\delta(t - t_f), \\ \hat{u}_t &= -\theta(t_f - t), & \hat{h}_t &= -a\theta(t_f - t). \end{aligned} \quad (\text{G4})$$

To see the significance of this solution, consider the density to arrive at \dot{u}_f, h_f at $t = t_f$, while driving with a constant velocity $\dot{w}_t = v$ for $0 < t < t_f$, as a function of the initial condition at $t = 0$. Using (154), we get

$$\begin{aligned} \overline{e^{-\dot{u}(0) - a\tau h(0)}} &= e^{\dot{u}_f \hat{u}_t + \tau h_f \hat{h}_t + \int_0^{t_f} dt (2 - \dot{w}_t) \hat{u}_t + (1 + a + \tau^{-1})} \\ &= e^{-\dot{u}_f - a\tau h_f + (v - 1 + a + \tau^{-1})t_f}. \end{aligned} \quad (\text{G5})$$

This implies the following exact relation on the propagator of the ABBM model with retardation at constant driving velocity v , with an absorbing boundary at $\dot{u} = 0$:

$$\int_0^\infty d\dot{u}_i \int_{-\infty}^\infty dh_i e^{-\dot{u}_i - ah_i} \mathcal{P}_{\text{abs}}(\dot{u}_f, h_f, t_f | \dot{u}_i, h_i, 0) = e^{-\dot{u}_i - ah_i + (v - 1 + a)t_f}. \quad (\text{G6})$$

Again, for the pure ABBM model $a = 0$, this relation can easily be checked using the expression (136) for the propagator with an absorbing boundary at $\dot{u} = 0$.

APPENDIX H: NUMERICAL METHODS

Here we give some details on the numerical simulations shown in Figs. 9–13. Since all these simulations concern the case of exponential relaxation, instead of the nonlocal SDE (19) we simulate the local SDEs (23). This is done using the simple Euler-Maruyama method with a sufficiently small time step. The time steps we used were $dt = 10^{-5}$ for Figs. 9, 11, 12 (left), and 13 (right); $dt = 10^{-4}$ for Figs. 10 and 12 (right); $dt = 10^{-3}$ for Fig. 13 (left).

For Figs. 9–12, we consider subavalanches with a fixed initial condition \dot{u}_i, h_i . In this case, after a subavalanche terminates (i.e., at the first time step where \dot{u} becomes ≤ 0), \dot{u} and h are reset to their initial values. For Fig. 13, we consider subavalanches at stationary driving with a fixed driving velocity v . In this case, after a subavalanche terminates, \dot{u} is reset to 0 but the value of h is kept. The subavalanche sizes for the histograms in Fig. 13 are collected after a sufficiently long transient (of order v^{-1}) in order to ensure that the stationary state is reached.

[1] H. Barkhausen, *Phys. Z.* **20**, 401 (1919).
 [2] J. Gauthier, T. Krause, and D. Atherton, *NDT&E Int.* **31**, 23 (1998).
 [3] D. Stewart, K. Stevens, and A. Kaiser, *Curr. Appl. Phys.* **4**, 308 (2004).
 [4] R. Ranjan, D. C. Jiles, O. Buck, and R. B. Thompson, *J. Appl. Phys.* **61**, 3199 (1987).

[5] S. Yamaura, Y. Furuya, and T. Watanabe, *Acta Mater.* **49**, 3019 (2001).
 [6] H. J. Herrman and S. Roux, *Statistical Models for the Fracture of Disordered Media* (North Holland, Amsterdam, 1990).
 [7] B. K. Chakrabarti and L. G. Benguigui, *Statistical Physics of Fracture and Breakdown in Disordered Systems* (Clarendon, Oxford, 1997).

- [8] K. J. Måløy, S. Santucci, J. Schmittbuhl, and R. Toussaint, *Phys. Rev. Lett.* **96**, 045501 (2006).
- [9] E. Rolley, C. Guthmann, R. Gombrowicz, and V. Repain, *Phys. Rev. Lett.* **80**, 2865 (1998).
- [10] S. Moulinet, C. Guthmann, and E. Rolley, *Eur. Phys. J. E* **8**, 437 (2002).
- [11] P. Le Doussal and K. J. Wiese, *Phys. Rev. E* **82**, 011108 (2010).
- [12] P. Le Doussal, K. J. Wiese, S. Moulinet, and E. Rolley, *Europhys. Lett.* **87**, 56001 (2009).
- [13] Y. Ben-Zion and J. Rice, *J. Geophys. Res.* **98**, 14109 (1993).
- [14] A. P. Mehta, K. A. Dahmen, and Y. Ben-Zion, *Phys. Rev. E* **73**, 056104 (2006).
- [15] D. S. Fisher, K. Dahmen, S. Ramanathan, and Y. Ben-Zion, *Phys. Rev. Lett.* **78**, 4885 (1997).
- [16] Y. Ben-Zion and J. Rice, *J. Geophys. Res.* **102**, 17 (1997).
- [17] P. Le Doussal and K. J. Wiese, *Phys. Rev. E* **85**, 061102 (2012).
- [18] P. Le Doussal and K. J. Wiese, *Phys. Rev. E* **88**, 022106 (2013).
- [19] J. P. Sethna, K. A. Dahmen, and C. R. Myers, *Nature* **410**, 242 (2001).
- [20] B. Alessandro, C. Beatrice, G. Bertotti, and A. Montorsi, *J. Appl. Phys.* **68**, 2901 (1990).
- [21] B. Alessandro, C. Beatrice, G. Bertotti, and A. Montorsi, *J. Appl. Phys.* **68**, 2908 (1990).
- [22] S. Zapperi, C. Castellano, F. Colaiori, and G. Durin, *Nat. Phys.* **1**, 46 (2005).
- [23] F. Colaiori, G. Durin, and S. Zapperi, *Phys. Rev. B* **76**, 224416 (2007).
- [24] F. Colaiori, *Adv. Phys.* **57**, 287 (2008).
- [25] P. Le Doussal and K. J. Wiese, *Europhys. Lett.* **97**, 46004 (2012).
- [26] T. Nattermann, S. Stepanow, L.-H. Tang, and H. Leschhorn, *J. Phys. II* **2**, 1483 (1992).
- [27] P. Chauve, P. Le Doussal, and K. J. Wiese, *Phys. Rev. Lett.* **86**, 1785 (2001).
- [28] P. Le Doussal, K. J. Wiese, and P. Chauve, *Phys. Rev. B* **66**, 174201 (2002).
- [29] P. Le Doussal and K. J. Wiese, *Phys. Rev. E* **79**, 051106 (2009).
- [30] K. P. O'Brien and M. B. Weissman, *Phys. Rev. E* **50**, 3446 (1994).
- [31] G. Durin and S. Zapperi, *Phys. Rev. Lett.* **84**, 4705 (2000).
- [32] P. Cizeau, S. Zapperi, G. Durin, and H. E. Stanley, *Phys. Rev. Lett.* **79**, 4669 (1997).
- [33] D. Spasojević, S. Bukvić, S. Milošević, and H. E. Stanley, *Phys. Rev. E* **54**, 2531 (1996).
- [34] M. C. Kuntz and J. P. Sethna, *Phys. Rev. B* **62**, 11699 (2000).
- [35] S. Papanikolaou, F. Bohn, R. L. Sommer, G. Durin, S. Zapperi, and J. P. Sethna, *Nat. Phys.* **7**, 316 (2011).
- [36] V. Lecomte, S. E. Barnes, J.-P. Eckmann, and T. Giamarchi, *Phys. Rev. B* **80**, 054413 (2009).
- [37] S. E. Barnes, J.-P. Eckmann, T. Giamarchi, and V. Lecomte, *Nonlinearity* **25**, 1427 (2012).
- [38] M. C. Marchetti, A. A. Middleton, and T. Prellberg, *Phys. Rev. Lett.* **85**, 1104 (2000).
- [39] M. C. Marchetti, *Pramana* **64**, 1097 (2005).
- [40] J. M. Schwarz and D. S. Fisher, *Phys. Rev. Lett.* **87**, 096107 (2001).
- [41] P. Le Doussal, M. C. Marchetti, and K. J. Wiese, *Phys. Rev. B* **78**, 224201 (2008).
- [42] J. E. L. Bishop, *J. Phys. D: Appl. Phys.* **13**, L15 (1980).
- [43] H. Houston, H. M. Benz, and J. E. Vidale, *J. Geophys. Res.* **103**, 29895 (1998).
- [44] A. A. Middleton, *Phys. Rev. Lett.* **68**, 670 (1992).
- [45] P. Le Doussal and K. J. Wiese, *Phys. Rev. E* **79**, 051105 (2009).
- [46] A. Dobrinevski, P. Le Doussal, and K. J. Wiese, *Phys. Rev. E* **85**, 031105 (2012).
- [47] P. Le Doussal, A. A. Middleton, and K. J. Wiese, *Phys. Rev. E* **79**, 050101 (2009).
- [48] A. Rosso, P. Le Doussal, and K. J. Wiese, *Phys. Rev. B* **80**, 144204 (2009).
- [49] P. Le Doussal, A. Petković, and K. J. Wiese, *Phys. Rev. E* **85**, 061116 (2012).
- [50] E. A. Jagla, *Phys. Rev. E* **81**, 046117 (2010).
- [51] E. A. Jagla and A. B. Kolton, *J. Geophys. Res.* **115**, B05312 (2010).
- [52] E. A. Jagla, *Europhys. Lett.* **93**, 19001 (2011).
- [53] C. H. Scholz, *Nature* **391**, 37 (1998).
- [54] M. Abramowitz and I. Stegun, *Handbook of Mathematical Functions: With Formulas, Graphs, and Mathematical Tables*, 1st ed. (Dover, New York, 1965).
- [55] G. Durin and S. Zapperi, in *The Science of Hysteresis*, edited by G. Bertotti and I. Mayergoyz (Academic Press, Amsterdam, 2006), p. 51.
- [56] F. Colaiori, S. Zapperi, and G. Durin, *J. Magn. Magn. Mater.* **272–276**, E533 (2004).
- [57] R. A. White and K. A. Dahmen, *Phys. Rev. Lett.* **91**, 085702 (2003).
- [58] M. LeBlanc, L. Angheluta, K. Dahmen, and N. Goldenfeld, *Phys. Rev. E* **87**, 022126 (2013).
- [59] J. Masoliver and J. Perelló, *Phys. Rev. E* **86**, 041116 (2012).
- [60] C. Gardiner, *Stochastic Methods: A Handbook for the Natural and Social Sciences*, 4th ed. (Springer, Berlin, 2009).
- [61] E. A. Jagla and A. Rosso (in preparation).
- [62] S. Papanikolaou, D. M. Dimiduk, W. Choi, J. P. Sethna, M. D. Uchic, C. F. Woodward, and S. Zapperi, *Nature* **490**, 517 (2012).
- [63] D. P. Schwartz and K. J. Coppersmith, *J. Geophys. Res.* **89**, 5681 (1984).
- [64] R. M. Nadeau, W. Foxall, and T. V. McEvilly, *Science (NY)* **267**, 503 (1995).
- [65] A. Dobrinevski, P. Le Doussal, and K. Wiese (in preparation).